



University of Kentucky
UKnowledge

Theses and Dissertations--Biomedical
Engineering

Biomedical Engineering


2017

SYNTHESIS AND CHARACTERIZATION OF POLY(SIMVASTATIN) - INCORPORATED COPOLYMERS AND BLENDS FOR BONE REGENERATION

Theodora Asafo-Adjei

University of Kentucky, theoa09@gmail.com

Author ORCID Identifier:

 <https://orcid.org/0000-0001-8124-9040>

Digital Object Identifier: <https://doi.org/10.13023/ETD.2017.362>

[Right click to open a feedback form in a new tab to let us know how this document benefits you.](#)

Recommended Citation

Asafo-Adjei, Theodora, "SYNTHESIS AND CHARACTERIZATION OF POLY(SIMVASTATIN) -
INCORPORATED COPOLYMERS AND BLENDS FOR BONE REGENERATION" (2017). *Theses and
Dissertations--Biomedical Engineering*. 46.
https://uknowledge.uky.edu/cbme_etds/46

This Doctoral Dissertation is brought to you for free and open access by the Biomedical Engineering at UKnowledge. It has been accepted for inclusion in Theses and Dissertations--Biomedical Engineering by an authorized administrator of UKnowledge. For more information, please contact UKnowledge@lsv.uky.edu.

STUDENT AGREEMENT:

I represent that my thesis or dissertation and abstract are my original work. Proper attribution has been given to all outside sources. I understand that I am solely responsible for obtaining any needed copyright permissions. I have obtained needed written permission statement(s) from the owner(s) of each third-party copyrighted matter to be included in my work, allowing electronic distribution (if such use is not permitted by the fair use doctrine) which will be submitted to UKnowledge as Additional File.

I hereby grant to The University of Kentucky and its agents the irrevocable, non-exclusive, and royalty-free license to archive and make accessible my work in whole or in part in all forms of media, now or hereafter known. I agree that the document mentioned above may be made available immediately for worldwide access unless an embargo applies.

I retain all other ownership rights to the copyright of my work. I also retain the right to use in future works (such as articles or books) all or part of my work. I understand that I am free to register the copyright to my work.

REVIEW, APPROVAL AND ACCEPTANCE

The document mentioned above has been reviewed and accepted by the student's advisor, on behalf of the advisory committee, and by the Director of Graduate Studies (DGS), on behalf of the program; we verify that this is the final, approved version of the student's thesis including all changes required by the advisory committee. The undersigned agree to abide by the statements above.

Theodora Asafo-Adjei, Student

Dr. David Puleo, Major Professor

Dr. Abhijit Patwardhan, Director of Graduate Studies

SYNTHESIS AND CHARACTERIZATION OF POLY(SIMVASTATIN) -
INCORPORATED COPOLYMERS AND BLENDS FOR BONE REGENERATION

DISSERTATION

A dissertation submitted in partial fulfillment of the
requirements for the degree of Doctor of Philosophy in the
College of Engineering
at the University of Kentucky

By

Theodora Atta Asafo-Adjei

Lexington, Kentucky

Advisor: Dr. David Puleo, Professor of Biomedical Engineering
Co-Advisor: Dr. Thomas Dziubla, Professor of Chemical and Materials Engineering

Lexington, Kentucky

Copyright © Theodora Atta Asafo-Adjei 2017

ABSTRACT OF DISSERTATION

SYNTHESIS AND CHARACTERIZATION OF POLY(SIMVASTATIN) - INCORPORATED COPOLYMERS AND BLENDS FOR BONE REGENERATION

Common biodegradable polyesters such as poly(lactic acid) (PLA), poly(lactic-co-glycolic acid) (PLGA) and poly(ϵ -caprolactone) (PCL) are used as drug delivery vehicles for tissue regenerative applications. However, they are typically bioinert, with drug loading limitations. Polymerizing the active agent or precursor into its respective biodegradable polymer would control drug loading via molar ratios of drug to initiator used for synthesis. Simvastatin was chosen due to its favorable anti-inflammatory, angiogenic, and osteogenic properties. In addition, its lactone ring lends itself to ring-opening polymerization and, consequently, the synthesis of poly(simvastatin) with controlled simvastatin release.

Simvastatin was first polymerized with a 5kDa methyl-terminated poly(ethylene glycol) (mPEG) initiator and catalyzed via stannous octoate to form poly(simvastatin)-*block*-poly(ethylene glycol). Molecular weights ranged from 9.5kDa, with a polydispersity index (PDI) of 1.1 at 150 °C, to 75kDa with a PDI of 6.9 at 250 °C. First-order propagation rates were seen. Infrared spectroscopy showed carboxylic and methyl ether stretches unique to simvastatin and mPEG in the copolymer, respectively. Slow degradation was seen in neutral and alkaline conditions, with simvastatin, simvastatin-incorporated macromolecules, and mPEG identified as degradation products.

Alternatively, triazabicyclodecene (TBD) was used to mediate simvastatin polymerization. A lower temperature of 150°C led to successful polymerization using 5kDa mPEG, compared to at least 200 °C via stannous octoate. TBD was also successful for reactions using 2 or 0.55kDa mPEG. The biodegradability of poly(simvastatin)-*block*-poly(ethylene glycol) via TBD improved, losing twice more mass in phosphate-buffered saline, pH 7.4, than the copolymer synthesized via stannous octoate. Release rates of three different copolymers synthesized demonstrated tunable simvastatin release.

To further modulate degradation, poly(simvastatin)-*block*-poly(ethylene glycol) was blended with 5, 2, or 0.55kDa mPEG-initiated PLA copolymers. The blends showed a compressive elastic modulus ranging from 26 to 44MPa, within the magnitude of trabecular bone (approximately 50MPa). Tunability in mass loss and release was also seen due to varied ratios of incorporated PLA copolymers.

Lastly, copolymer degradation byproducts inhibited HMG-CoA reductase and showed possible enhancement of osteoblastic activity *in vitro*. A pilot study using a rodent calvarial onlay model showed tolerability of the polymers and potential for long-term evaluations of bioactivity. Poly(simvastatin) may be useful in regenerative applications.

Keywords: poly(simvastatin), ring-opening polymerization, drug delivery, simvastatin, regenerative applications

Theodora Atta Asafo-Adjei
Student Signature

7/6/2017
Date

SYNTHESIS AND CHARACTERIZATION OF POLY(SIMVASTATIN) -
INCORPORATED COPOLYMERS AND BLENDS FOR BONE REGENERATION

By

Theodora Atta Asafo-Adjei

Dr. David Puleo
Advisor of Dissertation

Dr. Thomas Dziubla
Co-Advisor of Dissertation

Dr. Abhijit Patwardhan
Director of Graduate Studies

7/6/2017
Date

ACKNOWLEDGEMENTS

The number of friends and colleagues who have helped me push through during my time at UK are endless. I would like to thank my former labmates Matt Brown, Sharath Sundararaj, Amanda Rudd, Paul Fisher, Bryan Orellana, Sandeep Ramineni, Cheryl Jennings, Rohith Jaraham, Yuan Zou, Amir Najarzadeh, Michelle Fuentes, Matt Rudd, Nicholas Anderson, Nicholas Kohrs, Alexander Chen, Andrew Phan, Nandakumar Venkatesan, Thilanga Liyanage, Paritosh Wattamwar, David Cochran, Sundar Authimoolam, Prachi Gupta, Vinod Patil, Andrew Lakes, and Carolyn Jordan. There are many others, but always having you guys around to bounce ideas off of and help out in and out of lab was such a lifesaver for me.

I would like to thank my advisors Dr. Puleo, for your understanding in allowing me to find my voice while guiding me to ask the most relevant questions in designing experiments, and Dr. Dziubla, for pushing me to think past the question in front of me while providing insightful perspectives on ways to investigate them. You two provided the ideal balance in our meetings to realize what work it would take to answer the question at hand, and resolve experimental setbacks while providing the motivation needed to navigate through the project.

To my close friends, thank you for always checking up on me, being great cooks, giving me sound advice about life, and just being the occasional escape I needed to get away from the many obstacles I had in lab.

Last but not least, I'd like to thank my family. Thanks to my younger siblings,

Olivia and Miles, for being my rocks of support through these years, my dad who taught me that goals are always attainable with hard work, and mom who has instilled in me strength and resilience taught only by the actions of her own.

I am so grateful for how involved you all have been throughout my journey here. I've learned so much, as a result. Know that you will always be appreciated. It was a challenging, but fun experience!

Table of Contents

ACKNOWLEDGMENTS.....	iii
List of Tables	viii
List of Figures.....	ix
Ch. 1 Introduction.....	1
Ch. 2 Background and Significance.....	5
2.1 Bone Grafts and Substitutes.....	5
2.1.1 Autologous and Allogenic Bone Grafts.....	5
2.1.2 Calcium-Based Substitutes	6
2.2 Common Biodegradable Polymers.....	7
2.2.1 Poly(lactic acid) (PLA).....	7
2.2.2 Poly(lactic-co-glycolic acid) (PLGA).....	8
2.2.3 Poly(ϵ -caprolactone) (PCL).....	9
2.2.4 Poly(anhydrides).....	10
2.3 Polymer Synthesis.....	12
2.3.1 Radical Polymerization.....	12
2.3.2 Direct Condensation of Biodegradable Polymers	13
2.2.3 Ring-Opening Polymerization Polymerization of Poly(lactones).....	14
2.4 Tuning Polymer Degradation.....	15
2.4.1 Polymer Architecture.....	15
2.4.2 Poly(ethylene glycol) (PEG) Conjugation and Blending.....	16
2.5 Drug Encapsulation in Polymeric Systems.....	17
2.6 Polymer-Drug Conjugations.....	19
2.7 Osteogenic Bioactive Agents.....	21
2.7.1 Bone Morphogenetic Proteins (BMP)	21
2.7.2 Statins in Bone Repair.....	22
2.8 Significance and Objectives.....	23
2.9 Specific Aims.....	25
Ch. 3 Synthesis and characterization of a poly (ethylene glycol)– poly(simvastatin) diblock copolymer.....	27
3.1. Introduction	27
3.2. Experimental.....	30
3.2.1. Materials.....	30
3.2.2. Methods.....	30
3.2.2.1 Poly (ethylene glycol)-block-poly(simvastatin) synthesis.....	30
3.2.2.2 Gel permeation chromatography (GPC).....	33
3.2.2.3 Nuclear magnetic resonance (NMR) spectroscopy.....	33
3.2.2.4 Fourier transform infrared (FTIR) spectroscopy.....	33
3.2.2.5 In vitro degradation.....	34

3.2.2.6 Matrix-assisted laser desorption/ionization-time of flight mass spectrometry (MALDI-TOF MS).....	34
3.2.2.7 Statistical analysis.....	34
3.3 Results.....	35
3.4 Discussion.....	50
3.4.1. Copolymer Characteristics	50
3.4.2. Polymerization Mechanism.....	51
3.4.3. Kinetic Analysis.....	52
3.4.4. Polydispersity	55
3.4.5. NMR Analysis.....	56
3.4.6. Functional groups and bond formation.....	56
3.4.7. Degradation.....	57
3.5. Conclusions.....	59

Ch. 4 Synthesis of Poly(ethylene glycol)-block-poly(simvastatin) via Triazabicyclodecene.....	61
4.1 Introduction.....	61
4.2 Experimental.....	63
4.2.1 Materials.....	63
4.2.2 Methods.....	63
4.2.2.1 Poly(ethylene glycol)-block-poly(simvastatin) synthesis.....	63
4.2.2.2 Gel permeation chromatography (GPC).....	64
4.2.2.3 Nuclear magnetic resonance (NMR) spectroscopy.....	64
4.2.2.4 Matrix-assisted laser desorption/ionization-time of flight mass spectrometry (MALDI-TOF MS).....	65
4.2.2.5 In vitro Degradation.....	65
4.2.2.6 High Performance Liquid Chromatography (HPLC).....	65
4.2.2.7 Statistical Analysis.....	65
4.3 Results and Discussion.....	66
4.3.1 Polymerization Mechanism.....	66
4.3.2 Stannous Octoate vs. TBD Catalyst Mediated Reactions.....	67
4.3.3 NMR and mass spectrometry of PSIM-mPEG (5k) via TBD.....	71
4.3.4 Poly(simvastatin) Copolymer Synthesis using Different mPEGs.....	75
4.3.5 Kinetics.....	77
4.3.6 Crude vs Purified Polymers.....	83
4.3.7 Degradation.....	85
4.4 Conclusion	88

Ch. 5 Tuning Degradation and Mechanical Properties of Poly(ethylene glycol) – Poly(simvastatin)-based diblock copolymer blends.....	90
5.1 Introduction.....	90
5.2 Experimental.....	92
5.2.1 Materials.....	92
5.2.2 Methods.....	93
5.2.2.1 Poly(ethylene glycol)-block-poly(simvastatin) synthesis via TBD.....	93

5.2.2.2 Poly(ethylene glycol)-block-poly(lactic acid) synthesis via Stannous Octoate.....	93
5.2.2.3 Purification.....	93
5.2.2.4 Gel Permeation Chromatography (GPC).....	94
5.2.2.5 Film Formulation.....	94
5.2.2.6 In vitro Degradation.....	94
5.2.2.7 High Performance Liquid Chromatography (HPLC).....	95
5.2.2.8 Mechanical Testing.....	95
5.2.2.9 X – Ray Diffraction (XRD).....	95
5.2.2.10 Biochemical Activity of Degradation Products.....	96
5.2.2.11 Statistical Analysis.....	96
5.3 Results.....	96
5.4 Discussion.....	106
5.4.1 Degradation.....	106
5.4.2 Mechanical and crystalline properties.....	110
5.4.3 Biochemical activity of degradation products.....	114
5.5 Conclusion.....	114
Ch. 6 <i>In vitro</i> and <i>In vivo</i> bioactivity of poly(simvastatin) – poly(ethylene glycol) diblock copolymer for bone therapeutic applications.....	116
6.1 Introduction.....	116
6.2 Experimental.....	118
6.2.1 Materials.....	118
6.2.2 Methods.....	118
6.2.2.1 Copolymer synthesis.....	118
6.2.2.2 Degradation Products.....	119
6.2.2.3 Cell culture.....	119
6.2.2.4 Cytotoxicity.....	119
6.2.2.5 Alkaline Phosphatase (AP) Activity.....	120
6.2.2.6 Myotube Staining.....	120
6.2.2.7 Copolymer Disk Formulation.....	121
6.2.2.8 Pilot Animal Study.....	121
6.2.2.9 Statistical Analysis.....	122
6.3 Results.....	122
6.4 Discussion.....	131
6.5 Conclusion.....	134
Ch. 7 Summary and Conclusions.....	135
References.....	137
Curriculum Vita.....	149

List of Tables

Table 3.1 Summary of the highest M_w obtained, derived rate equation, and percentage in the crude product at each temperature at 24 hr.....	37
Table 3.2 Summary of product M_w distributions from purification, measured via GPC..	42
Table 4.1 GPC measurement of simvastatin and mPEG composition in copolymer.....	77
Table 5.1 Comparing simvastatin released from PSIM and blends in PBS and 0.1 wt% esterase in PBS.....	100
Table 6.1 <i>In vivo</i> experimental design.....	122

List of Figures

- Figure 3.1** a) Tin alkoxide complex formation and proposed mechanism of ROP reaction to form poly(ethylene glycol)-*block*-poly(simvastatin). b) Proposed mechanism of hydrolytic degradation of the copolymer.....32
- Figure 3.2** M_w of copolymer during ROP at increasing temperatures. Simvastatin and mPEG (5 kDa) were mixed at a 100 to 1 molar ratio for each reaction. The 0 hr time point represents the M_w of mPEG before poly(simvastatin) chain growth. The GPC molecular weight of mPEG registered higher than its theoretical value due to differences in chemistry between mPEG and the polystyrene standards used. Data are mean \pm standard deviation (n=3).....36
- Figure 3.3** GPC chromatogram showing monomer (simvastatin) attachment to the mPEG block to form copolymer at 250 °C. Chromatograms were normalized to the copolymer peak. The 1 hr mPEG and simvastatin peaks are excluded from normalization due to the monomer peak registering at a high intensity (6.4).....38
- Figure 3.4** Changes in PDI at different temperatures of 24 hr ROP reactions. The PDI at 0 hr represents solely the mPEG block, and the subsequent points reflect addition of simvastatin monomers. Data are mean \pm standard deviation (n=3).....39
- Figure 3.5** GPC chromatogram of separated products after purification of the crude copolymer.....41
- Figure 3.6** H-NMR spectra in $CDCl_3$ (7.25 ppm) of: a) simvastatin and mPEG mixed at a 100:1 molar ratio and b) poly(ethylene glycol)-*block*-poly(simvastatin).....43
- Figure 3.7** FTIR spectra of: a) mPEG, b) simvastatin, c) simvastatin and mPEG blended at the same molar ratio used for the reaction (100:1), and d) poly(ethylene glycol)-*block*-poly(simvastatin).....46

Figure 3.8 Degradation and drug release during incubation of samples in PBS or 1 M NaOH. a) Wet mass loss, b) dry mass loss, and c) drug release. Data are mean \pm standard deviation.....	47
Figure 3.9 Mass spectra of a) simvastatin, b) mPEG (5 kDa), c) low molecular weight degradation products, and d) high molecular weight degradation products.....	49
Figure 4.1 ROP mechanism using TBD catalyst via hydrogen bonding.....	67
Figure 4.2 Compared GPC measurements of the percent composition of PSim-mPEG(5k) synthesized via TBD or stannous octoate, intermediates, and simvastatin monomer in the melt during the reaction.....	68
Figure 4.3 Mass spectrometry of PSim-mPEG(5k) degradation products synthesized via TBD.....	69
Figure 4.4 H-NMR spectroscopy of the PSim-mPEG(5k) copolymer synthesized via TBD in CDCl ₃ (7.25 ppm).....	72
Figure 4.5 GPC chromatograms of poly(simvastatin) synthesized via TBD using 3 different Mw mPEG initiators compared with reactants.....	74
Figure 4.6 PSIM-mPEG 24 hr rxns comparing the Mw growth kinetics of (a) the PSIM copolymer with different mPEG MWs with 1 wt% TBD, (b) different molar ratios of sim to mPEG (550 Da), and (c) two different catalyst wt %s at two different molar weight ratios.....	76
Figure 4.7 GPC chromatograms of the PSIM copolymer before and after purification with respective MW and PDI.....	81
Figure 4.8 a) Final mass remaining and b) simvastatin release from 5kDa mPEG, 2kDa mPEG, and 550 Da mPEG initiated PSIM diblock copolymers.....	84
Figure 4.9 Stannous octoate and TBD catalysts used in the ROP of poly(simvastatin)...	86

Figure 5.1 Degradation of PSIM and PLA copolymers and their blends in PBS, pH 7.4, showing a) mass loss and b) drug release profiles.....	99
Figure 5.2. Cylindrical mechanical testing samples of PSIM copolymers and blends. From <i>left to right</i> : mPEG (5kDa), mPEG (2kDa), PLA(5k), PLA(2k), PLA(550), PSIM(5k), 80:20 PSIM(5k):PLA(5k), and 60:40 PSIM:PLA.....	101
Figure 5.3 Mechanical properties of PSIM and PLA copolymers and blended samples: a) compressive strength and b) modulus. *p<0.05,**p<0.01, ***p<0.001, ****p<0.0001.....	102
Figure 5.4 X-ray diffractograms of mPEG block components, simvastatin and D,L-lactide monomer components, PLA-mPEG copolymers, the PSIM-mPEG(5k) copolymer, and PSIM:PLA blends.....	104
Figure 5.5. Inhibition of HMG-CoA reductase activity in the presence of simvastatin, lactide, and PSIM and PLA degradation products at different concentrations. (n = 3) *p<0.05, **p<0.01.....	105
Figure 6.1 Cytocompatibility of simvastatin and lactide monomers and poly(simvastatin) and poly(lactide) degradation products at different concentrations in C2C12 myoblast cell cultures. $\Delta p < 0.001$	123
Figure 6.2 Alkaline phosphatase expression by C2C12 myoblast cells in the presence of poly(simvastatin) and poly(lactide) degradation products, simvastatin, D,L-lactide, BMP-2, and untreated controls a) without and b) with phenamil. *p<0.05, #p<0.01, $\Delta p < 0.001$	125
Figure 6.3 a) Relative myotube thickness normalized to PBS control at 7 d and b) cell images comparing myotube formation between groups. BMP-2 was excluded from the plot since myotubes did not form with treatment. n=10, *p<0.05, $\Delta p < 0.001$	128
Figure 6.4 Images of fragmented and intact poly(simvastatin) disk samples at wk 1...	129

Figure 6.5 a) Photographs of harvested calvaria with disks intact at 3 and 4 wks. b)
MicroCT images of calvaria of the same specimens.....130

Ch. 1 Introduction

The development of biodegradable polydrugs is an emerging and rapidly growing area in drug delivery as they serve to significantly increase the weight percent of the bioactive agent in the biomaterial, allowing the biomaterial to be comprised almost entirely of the drug, while providing controlled release upon degradation. Polyactives, termed by Uhrich's group,¹ encompass a broad range of therapeutic agents that are used as monomers which are ultimately polymerized into their homopolymers or into a polymer backbone. These systems have been investigated in response to drawbacks seen in more common poly(lactic acid) (PLA)- and poly(lactic-co-glycolic acid) (PLGA)-based drug eluting systems where the percentage of drug encapsulated or bound to the polymer backbone can be limited. Different polyactives have been developed incorporating well known therapeutic drugs into polymerized forms. However, little investigation has been done that has taken advantage of lactonized structures found in prodrugs or active agents to utilize ROP in effectively polymerizing their respective resorbable polymers, specifically for tissue regenerative therapeutics. Ahead, the synthesis of a copolymerized form of simvastatin, a commercially available and lactonized prodrug, and characterization of the degradable biomaterial is discussed for bone regenerative applications.

Chapter 2 gives an overview of current treatments for bone repair and the chemical and physical properties of common biodegradable polyesters utilized for bone and soft tissue therapeutic applications. The chapter further delves into different polymerization mechanisms which occur during polyester synthesis, most often

determined by the catalyst used, and secondary monomeric or polymeric components incorporated into the polyester by copolymerization or blending to help in tuning degradation rates. The evolution of different methods used to incorporate bioactive agents or drugs into the polymer matrix or backbone are also discussed, with a stronger emphasis on osteogenic active agents. The discussion then leads into intended treatment applications which include maxillofacial bone defects or fractures and periodontitis. The chapter concludes with the specific aims of the project.

Chapter 3 addresses the different reaction conditions attempted to synthesize a novel poly(simvastatin)-*block*-poly(ethylene glycol) copolymer using tin (II) ethylhexanoate (stannous octoate) as the catalyst. Quantitative analysis of copolymer growth throughout the reactions, followed by copolymer degradation in different pH conditions, was primarily discussed. Further qualitative characterization of the resulting copolymer and degradation products via chromatography and spectroscopy methods was another focus to demonstrate success in forming a polymeric biomaterial.

Chapter 4 alternatively elaborates on the synthesis of poly(simvastatin)-mPEG diblock copolymer using triazabicyclodecene (TBD) as a catalyst, and touches on the differing ring-opening polymerization mechanism it governs from stannous octoate. A comparison between the two catalysts focuses on the reaction conditions, capability of using different block components for copolymerization, and quality of the resulting copolymer expressed by the biodegradability of the resulting copolymer. The comparison demonstrates the advantages of using TBD over stannous octoate in

synthesizing poly(simvastatin) and in synthesizing poly(simvastatin) copolymers with different drug release rates.

Chapter 5 focuses on blending the most hydrophilic poly(simvastatin) copolymer synthesized with different poly(lactide)-*block*-poly(ethylene glycol) copolymers at two different weight ratios. Mass loss and resulting simvastatin amounts released in neutral and enzymatic conditions were quantified to demonstrate the effect of blending on the degradation rate of poly(simvastatin). Mechanical and crystalline properties were also quantified to show the effect of blending on the physical properties of the resulting blends.

Chapter 6 primarily looks at the bioactivity of the poly(simvastatin) copolymer degradation products via alkaline phosphatase expression and degree of myotube formation in a muscle cell line. Biocompatibility of the copolymer was also observed in a pilot in vivo study. Comparisons between the activities of degraded poly(simvastatin) and poly(D,L-lactide) copolymers against the monomer and general controls demonstrates the potential of tunable poly(simvastatin)-incorporated polymer biomaterials for bone regeneration.

Overall, this dissertation focuses on the repurposing of simvastatin, well-known for cholesterol-regulation, for regenerative applications by polymerizing the drug into a biodegradable biomaterial for controlled simvastatin release. ROP was investigated as a mechanism, novel in polymerizing simvastatin. The continued investigation of polyactives, including poly(simvastatin), can extend to other lactonized active agents

which advantageously use ROP as another method to create more effectively controlled drug delivery systems for therapeutic applications.

Copyright © Theodora Atta Asafo-Adjei 2017

Ch. 2 Background and Significance

2.1 Bone Grafts and Substitutes

The high incidence of bone defects results from a range of causes including injury, infection, tumor resection, and abnormalities to bone and vascular diseases from osteoporosis to various forms of necrosis.²⁻⁴ In many instances, these complications are so extensive that natural bone repair becomes impaired and is no longer capable of completely healing the wound. This hindered process leaves remaining fractures, voids, and non-unions in need of external clinical intervention. Approximately 500,000 to 600,000 bone grafting procedures are performed annually in the US.⁵ Autografts, as well as allografts, are used in approximately 2.2 million orthopaedic surgeries each year, worldwide.⁶ Investigations that are being done to improve upon the disadvantages of current treatment focus on multiple forms of biological and synthetic bone substitutes which incorporate the desirable characteristics of synthetic polymers. Some of these devices may administer drugs to enhance efficacy of the biomaterial. The development of these materials aims towards developing the ideal material that eliminates the risk of disease transmission and rejection, improves biocompatibility, and provides an easily available, inexpensive, and abundance necessary for bone defect-related procedures.

2.1.1 Autologous and Allogenic Bone Grafts

Autografts are used as the primary bone graft of choice, or the “golden standard,” because their use diminishes the possibility of rejection and infectious disease transmission due to its harvest from the iliac or pelvic crest of the same patient in need of

the implant.⁷ They also possess four main properties needed for successful bone grafting: osteoconduction, osteoinduction, osteogenesis and osteointegration.⁶ Osteoconduction is the stimulation of bone tissue growth within the graft. Osteoinduction involves the differentiation of mesenchymal stem cells into osteoblasts, leading to bone growth. Osteogenesis stems from osteoprogenitor cells remaining in grafts that further proliferate and differentiate into characteristic bone cells which adhere within the graft. Osteointegration is the integrative bonding of the graft to surrounding bone tissue. Even though the autograft seems ideal by possessing these primary characteristics, it requires additional surgery to harvest the bone needed for the graft which increases the risk of complication.³ In fact, 8 to 20% of complications arise from harvesting host bone.⁶ Allografts, harvested from cadavers or another host of the same species, are also used but have an increased chance of rejection due to being foreign to the host along with increased chances of transmitting infection or disease.^{3, 7, 8}

2.1.2 Calcium-Based Substitutes

Ceramics used as synthetic bone substitutes are developed from calcium sulfate (CaS), calcium phosphate (CaP), or bioactive glass derivatives.^{9, 10} Due to chemical structure of CaP, which include hydroxyapatite (HA), ceramics being found in the inorganic components of bone, these scaffolds are found to be favorably biocompatible, and have been a focus alongside bone grafts to minimize the risk of infection otherwise seen with bone grafts.¹¹ Their biocompatibility is defined by bioactive ceramic surfaces being able to form hydroxyl carbonate apatite (HCA) which bonds with surrounding tissues at the implant interface.¹² This characteristic enhances osteointegration, and its

porosity gives it osteoconductive properties as well, for bone tissue growth. However, they are brittle leading to inadequate structural support.⁹ Also, while they are capable of being resorbed, the resorption rate of some HA-incorporated implants can be extensively slow.¹³ Shindo *et al.* showed that approximately half the amount of their porous hydroxyapatite cement implants were resorbed in bone within 9 and 18 months.¹⁴ Biodegradable polymers have instead been combined with these ceramics to improve their mechanical and resorptive properties, and have also emerged on the forefront of biomaterials being investigated for tissue repair and regeneration.

2.2 Common Biodegradable Polymers

Biodegradable polymers are increasingly being used for biomedical therapeutic applications. This is due to their desirable characteristics which include tunable degradation, mechanical properties, and relative biocompatibility in the body. Their ability to degrade allows for the avoidance of revision surgery to remove the implant, as opposed to some fixation devices, after therapeutic treatment is done. This capability is due to the hydrolytically labile bonds present within the polymer backbone of these resorbable materials. Specific characteristics of each of the more common biodegradable polymers make each very unique and the most favorable for their specific use.

2.2.1 Poly(lactic acid) (PLA)

Lactic acid, the monomer of PLA was first isolated in 1780 and commercialized in 1880.¹⁵ PLA was then first developed into synthetic biodegradable sutures in 1969 before being considered for many other biomedical and drug delivery applications.¹⁶

Good mechanical properties, thermoplasticity, and a thermal degradation temperature of

200 °C makes PLA a very suitable candidate for widescale processing (while within a narrow temperature range of 185 to 190 °C).¹⁵ At desirably processable molecular weights over 100 kDa, a high tensile strength and modulus around 61 MPa and 2.2 GPa, respectively, are reached, which can be modified based on the ratio of lactide isomers used in synthesis, making it adaptable for its intended application.¹⁷ The ratio of D to L-lactide isomers also determines how amorphous or crystalline the polymer will be allowing its degradation rate and glass transition temperature, normally around 55 °C, to be slightly altered as well.¹⁵ Poly(D,L-lactic acid) is known to be the amorphous polymer because of the randomized configuration of methyl groups in the polymer backbone, creating more incoherent polymer matrix regions. Poly(L-lactic acid) has a uniform backbone resulting in a rigid uniform matrix that water is less likely to penetrate. Upon degradation, when PLA degrades into lactic acid, the simplest of its degradation products via hydrolysis, it is recognized as a product developed in the body, and is later metabolized into carbon dioxide and water via the Krebs cycle.¹⁸ PLA has been copolymerized with poly(ethylene glycol) (PEG) and combined with hydroxyapatite to develop different types of fabrications for bone regeneration.^{19, 20} It has also been formulated into micro- and nanoparticles to release various classes of drugs for bone and soft tissue healing, along with cancer therapies.

2.2.2 Poly(lactic-co-glycolic acid) (PLGA)

Like PLA, PLGA possesses many similar mechanical and degradation characteristics making it amendable to processing for biomedical applications. The incorporation of glycolic acid and its properties into the polymer backbone does

introduce a broader range of adaptable changes in mechanical and degradation tunability. With its lack of a methyl group, glycolic acid is more hydrophilic than lactic acid, allowing PLGA to become a more hydrophilic and generally faster degrading polymer or vice versa depending on the lactic acid to glycolic acid molar ratio in the polymer backbone. However, the structural state of the polymer matrix plays the most influence in its degradation at a 50:50 molar ratio which has been found to have the fastest degradation rate compared to a greater incorporation of either monomer in the backbone.²¹ This characteristic is most likely due to an increasing amorphous nature as the incorporation of either lactide or glycolide monomer increases up to 50% as the amorphous regions allows easier access of water into the polymer matrix allowing for faster degradation. Each of the homopolymers of the L-lactide stereo-isomer and glycolide are known to be semi-crystalline, at 37 and 45-55%, respectively.^{22, 23} The T_g range for PLGA can range from 44 to 55 °C, increasing in T_g as the lactide content and/or MW increases.^{24, 25} Like lactide, glycolide is also metabolized in the body or excreted by the kidneys. Different localized formulations for bone, such as microparticle-sintered scaffolds for growth plate regeneration and other micro- and nanoparticle systems have been developed for drug delivery.^{26, 27}

2.2.3 Poly(ϵ -caprolactone) (PCL)

PCL has previously been used in microelectronics, as an adhesive, and as an ecological biodegradable plastic.^{28, 29} Originally viewed as a biodegradable ecological plastic that degraded into non-toxic products via various microorganisms within the natural environment, PCL soon began being used for medical applications due to its

mechanical properties being similar to that of non-biodegradable polymers and for its ability to degrade in the body.²⁸ Due to its lack of functional groups attached to the 5-carbon portion of the aliphatic chain, PCL is very hydrophobic and degrades very slow compared to PLA and PLGA. Additionally, the lack of bulky side groups permits PCL to form a semi-crystalline structure, with a $-60\text{ }^{\circ}\text{C}$ T_g , which becomes increasingly crystalline as it degrades in its amorphous regions, allowing degradation to take up to years via hydrolysis. Its degradation properties, in combination with faster degrading polymers, has led to the synthesis of PCL block copolymers for sutures, such as Monocryl®, and bioglass composites formulated into fixation screws, among other devices for biomedical applications.^{23, 30} Compost microorganisms including *Aspergillus* spp. and *Penicillium funiculosum* are able to enzymatically degrade PCL into succinic acid, butyric acid, valeric acid, and hexanoic acid.²⁸ However, within the physiological environment of the body, studies have shown it incapable of degrading enzymatically.^{31, 32} Thus, solely hydrolysis at its ester linkages allows the polymer to degrade into its degradation products of 6-hydroxyhexanoic acid, its ϵ -caprolactone monomer, and the cyclic dimer and trimer of the monomer.²⁸ PCL has now been repeatedly utilized in bone regeneration and other biomedical applications due to its degradation and mechanical properties. PCL/hydroxyapatite composites and scaffolds have been developed as a result.^{33, 34}

2.2.4 Poly(anhydrides)

The unique chemistry of poly(anhydrides) sets them apart from other biodegradable polymers, allowing multiple subclasses of the polymer to be synthesized

which can ultimately degrade by surface erosion, instead of the bulk erosion experienced by polyesters like PLA, PLGA, and PCL. Aliphatic poly(anhydrides) were originally synthesized and extruded into fibers in 1932 by Carothers and Hill³⁵ and was eventually used in textiles, but was later discarded from the industry because of its hydrolytic instability. Langer and his group later took advantage of the polymer's degrading properties for therapeutic controlled drug delivery in 1980.³⁶ Since then, the polymer's desirable bioerodible qualities have been used in more localized drug release therapies for malignant tumors, thrombosis and restenosis, infection, but moreso for glaucoma, retinal, and neurological disorders.^{37, 38} For example, poly(anhydrides) have been fashioned into disks and injectable microparticles releasing 5-fluorouridine to extend the reduction of intraocular pressure after glaucoma filtration surgery.^{39, 40} An FDA approved poly(anhydride), known as Gliadel[®], has been formulated into wafers releasing carmustin, a chemotherapeutic, for treating brain tumors.³⁷ Cylinders of the polymer have also been made to locally deliver anesthetic to the sciatic nerve for pain.⁴¹ Bioerodible poly(anhydrides) in medicine are generally synthesized with diacids resulting in the labile anhydride group embedded within the polymer chain capable of degrading within weeks. In non-degradable poly(anhydrides), the anhydride is instead a side group. They are crystalline, opaque polymers with melting points between 50 °C and 120 °C dependent on the manipulation of their polymer chemistry. Altering their chemistry has led to the development of poly(ester-anhydrides)⁴², aromatic, aliphatic-aromatic, unsaturated, branched, and crosslinked poly(anhydrides) among many others, for different applications.³⁷

2.3 Polymer Synthesis

Different types of polyester synthesis are utilized to achieve a desired polymeric architecture. The mechanisms by which these architectures are constructed may be dictated by the catalyst and is confined to the chemistry of the monomers and initiators being used. A combination of these different forms of polymerization can be used sequentially in order to develop the desired biomaterial.

2.3.1 Radical Polymerization

In radical polymerization, a free radical, or possible cation or anion, acts as the initiator by cleaving a pi-bond within the monomer and forming a new reactive species that continues chain propagation, repeating the process. One form of radical polymerization is photopolymerization.⁴³ It is generally used to achieve a desired gelation or crosslinking of polymer chains to form hydrogels in various drug delivery applications and to cure non-amalgam restorative dental applications.⁴⁴⁻⁴⁶ The degree of crosslinking directly relates to the amount of swelling the hydrogel is capable of undergoing in order to release entrapped drug. The method and reaction of photopolymerization is usually very simple and quick, requiring an accessible ultraviolet (UV) light source and photoinitiator within the macromer acrylate mixture. Afterwards, the gel is washed in an aqueous medium to remove any residual macromer and initiator. UV light bombards light susceptible photoinitiators, cleaving C-C, C-Cl, C-O, or C-S bonds in double bonds to form radicals and initiate propagation. The UV light may also promote hydrogen atom transfer from a H donor to the photoinitiator forming hydrogen and ketal radicals for polymerization, also known as hydrogen abstraction. Sawhney *et al.* developed acrylate-

terminated PEG-block-oligo(lactide) and PEG-block-oligo(glycolide) macromers which were made into crosslinkable gels via photopolymerization.⁴⁷

2.3.2 Direct Condensation of Biodegradable Polymers

Poly(α -hydroxy acids) like PLA and PLGA can be synthesized by direct condensation when the simplest reactant units of the polymer, lactic acid and glycolic acid, are chosen for synthesis. In this form of step polymerization, the hydroxyl and carboxylic terminal end-groups of these monomers allows them to undergo an intermolecular reaction with like monomers. This results in the formation of dimers, trimers, and oligomers of varying lengths, along with the loss of a water molecule driven by the high temperature conditions of the reaction. At times a coupling agent, such as zinc compounds, carbodiimide or a phosgene compound,⁴⁸ is used to enhance the efficiency of polymerization, but otherwise the aid of a catalyst is not needed.⁴⁹ While the methodology for direct condensation is fairly simple, the process generally forms oligomeric low molecular weight (MW) polymer chains. The mechanically unstable and quickly degrading formulations these polymers would make are not ideal for biomedical therapeutics. The increasing difficulty of distilled water removal with increased melt viscosity, followed by the equilibrium between water and acid reactants limit the progression of polymer chain growth.¹⁷

In other instances, the monomers can be bifunctional, such as diols or diacids. This characteristic only allows one type of monomer to react with a different monomer type within the mixture.⁵⁰ However, some exceptions to this to this concept have been

reported by Uhrich *et al.* which includes the melt condensation of dicarboxylic acid monomers to develop salicylic acid-based poly(ester-anhydrides).^{42, 51}

2.2.3 Ring-Opening Polymerization of Poly(α -hydroxyacids) or Poly(lactones)

Ring-opening polymerization (ROP) requires the use of cyclic monomers, such as the lactone or cyclic dimer structures of lactic and glycolic acid, otherwise known as lactide and glycolide. An initiator and catalyst are usually necessary for the reaction to begin and to further mediate the type of ROP mechanism that occurs. The main mechanisms of ROP that exist are coordination-insertion or pseudo-anionic, anionic, cationic and monomer activated ROP.²⁹ Coordination-insertion involves an alkoxide nucleophilic initiator which coordinates with the lactone ring moiety of the monomer, then inserts the monomer into its metal-oxygen bond while cleaving the ring open at the acyl-oxygen bond to propagate the polymer chain. The metal remains at the end of the chain to continue propagation, otherwise known as a living polymerization.^{29, 52} It is the most common form with an array of metal and metal alkoxide catalysts that mediate this mechanism, which include tin (II) octoate, tin triflate, and lanthanum, aluminum, and yttrium isopropoxide.²⁹ Anionic ROP also has a nucleophilic initiator which acts on the carbon atom of the carbonyl group of the lactone, which in turn drives open the ring at the acyl-oxygen bond. Catalysts that mediate anionic ROP mechanisms include small oxides like potassium methoxide,⁵³ to organocatalysts such as 1,3-dimesitylimidazol-2-ylidene (IMes), diazabicycloundecene (DBU), and triazabicyclodecene (TBD).^{54, 55} In cationic ROP, the oxygen in the carbonyl group of the lactone acts on the cationic catalyst to initiate ring opening of the lactone. Various acid cosystems can be used as the

catalyst for this mechanism, such as hydrochloric acid in diethyl ether.⁵⁶ Lastly, the monomer can act as an activated catalyst that continuously adds to the end of the polymer chain. In all instances, ROP reactions lead to the synthesis of high MW polymers with relatively low polydispersity and is considered one of the more preferred methods of polyester synthesis.

2.4 Tuning Polymer Degradation

The mechanisms and properties influencing polymer are invaluable to understand in their development for specific drug delivery applications. Depending on whether the therapy is intended for bone tissue healing, which may require longer times of treatment, to fibrotic tissue prevention, requiring relatively shorter treatment periods, the rate of degradation will have to accommodate the recovery time of the specific type of injured tissue in question.

2.4.1 Polymer Architecture

The architecture of the polymer chain may influence how the resulting polymeric biomaterial degrades. Polyesters, such as PLA, PLGA, and PCL undergo bulk erosion which creates an increasingly acidic environment within the bulk as more ester bonds cleave within polymer chains, exposing carboxylic end groups. An accelerated form of degradation results from this occurrence, known as autocatalysis, which is represented by a first-order rate with respect to the copolymer, water, and autocatalytic acid products.^{57,}

⁵⁸ Polymers like poly(anhydrides) generally undergo surface erosion due to a combination of high hydrophobicity and highly water-labile bonds, impeding water penetration into the polymer matrix while easily cleaving linkages on the surface of the

bulk sample. This process is represented by zero-order degradation kinetics and near zero-order drug release from the matrix.^{1, 59} However, when the linear chains of some of these polymers have been chemically manipulated to incorporate branched members of the polymer chain or branched linkers, the rate of polymer degradation may be affected. An increased degradation rate was seen in star-branched PLGA and PLA copolymers with multi-arm poly(ethylene glycol) (PEG) initiators compared to their linear block copolymer counterparts due to the extended retention of multifunctional PEG in the microparticle polymer matrix.⁶⁰ Biphasic forms of degradation, presented in terms of decreasing molecular weight, was discovered of hyperbranched poly(silyl-esters) compared to its linear polymer counterpart, showing a more linear decrease in MW with time.⁶¹ Many other graft, comb, and dendritic types of branched polymers have been explored as potential biomaterials for drug delivery due to some of their unique degradation properties.^{62, 63}

2.4.2 Poly(ethylene glycol) (PEG) Conjugation and Blending

PEG is a hydrophilic polymer synthesized from ethylene oxide via ring opening polymerization.⁶⁴ It has repeatedly been coated on, copolymerized and covalently bonded with aliphatic polyesters that have been formulated into micro- and nanoparticle systems for targeted drug delivery.⁶⁵ PEG's common use stems from its protective qualities that prolong circulation throughout the body, extending the drug release and therapeutic treatment of these particles, and ultimately increasing their biocompatibility. The terminal-end hydroxyl groups and ether linkages throughout the backbone solubilize PEG in water. Its hydrophilic nature combined with an absence of functional groups

allows for PEG incorporated surfaces to become more nonionic, minimizing protein adsorption, and further masking the immunogenicity of the system and its bioactive agents, systemically and locally.⁶⁵⁻⁶⁷ More specifically, the polymer and agents are shielded from premature and proteolytic degradation from phagocytic cells before reaching targeted tumors or the blood-brain barrier for treatment.⁶⁸

While PEGs are useful for creating relatively bioinert biomaterials, they also serve as avenues to tune the degradation rate and crystallinity of aliphatic polyester-based materials as a plasticizer, blend, or via copolymerization. Hydrophobic polymers like PLA, PLGA, and PCL which can be slow to degrade, can be made more hydrophilic via copolymerization, enhancing water uptake of the polymer. As the MW of PEG increases, the more hydrophilic the copolymer becomes. While the T_g of PEG remains at $-60\text{ }^\circ\text{C}$ as MW increases,⁶⁹ crystallinity increases up to a point which may contribute to better toughness of the resulting polymeric biomaterial. Li *et al.* found that at 10 wt% of PEG in PLA/PEG blends, crystallinity and impact strength decreased as PEG MW increased up to 6000 Da. Crystallinity and impact strength increased as PEG MW increased from 6000 Da to 20 kDa.⁷⁰ However, as seen with Li *et al.*'s study, the weight percent and MW of PEG chosen can also impede specific mechanical properties. Sungsanit *et al.* found that blending PLA with 1000 Da PEG increased impact strength, crystallinity, and elongation-at-break and decreased the modulus and tensile strength with increasing PEG wt%.⁷¹

2.5 Drug Encapsulation in Polymeric Systems

Encapsulating drugs or bioactive molecules was first explored in the early 1930s as a method of protection before the technique was adapted to drug delivery concepts

utilizing biodegradable polyesters (i.e. PLA and PLGA) in the 1970s, and has since become the most common and well-known method for drug incorporation.⁷² The most common and simplistic forms of drug encapsulation in micro- and nanoparticle systems include oil-water (o/w) and water-oil-water (w/o/w) emulsions which entrap the drug to be released. Bioactive agents significantly soluble in organic solvents undergo the o/w technique where the polymer and drug are dissolved in an organic solvent, such as dichloromethane or acetone, before adding to an aqueous solution with an incorporated surfactant, such as poly(vinyl alcohol) or Pluronic F-68, to obtain polymeric spherical particles with entrapped drug after the solvent is evaporated. For agents more soluble in water, an additional water phase is added (i.e, w/o/w). Parameters that affect the rate of release include polymer composition, polymer molecular weight, polymer-to-drug interactions and ratios. Proteins are known to adsorb onto PLGA matrices which can cause slow dissolution rates or lead to incomplete cumulative release in drug delivery systems.⁷³

Lax or vague consideration of the volume ratios of dispersed to continuous phases, the organic solvents and aqueous solutions chosen in relation to drug solubility, or the partitioning characteristics of the drug between organic and aqueous phases, may result in low encapsulation efficiencies. For example, using an o/w method for encapsulating a hydrophobic drug like hydrocortisone, also partially soluble in aqueous phases, would lead to expected low drug loading. As a result, emulsion techniques such as oil-in-oil (o/o) and solid-in oil-in water (s/o/w) exist, along with other method variations.⁷²

In fluorescein isothiocyanate (FITC)-dextran and FITC-immunoglobulin G (IgG) loaded PLGA/PEG blended microparticles, developed by Cleek *et al.*, the percent encapsulation efficiencies increased from 67 to 77% as the PEG content decreased with dextran incorporation, and increased from 85 to 92% as the PEG content also increased with IgG.⁷⁴ These percentages lead to total drug loading weight percents ranging from 0.67 to 0.92 which are close to the theoretical loading of 1 wt%. Weight percents reported in the study represent a normal range for some polymeric microparticle systems, and while others have attained higher loading percentages, the formulation exposes a limitation or predictable cap to the drug payload, despite their effectiveness. Polymeric microparticle systems in the market include Decapeptyl® Depot, Vivitrol®, and Lupron Depot® formulated using coacervation (water-in-oil), o/w, and w/o/w methods, respectively, to entrap peptides and proteins for cancer, disease, and substance dependency therapies.⁷²

2.6 Polymer-Drug Conjugations

Most of the previously described polymeric systems have bioactive agents dispersed throughout the polymer matrix, which may have limitations in drug loading capacity or premature burst drug release due to the structure of the polymer matrix. To better control release, various forms of polymer-drug conjugations have been formulated.¹ Ringsdorf first introduced the concept of polymeric drugs in 1975 by proposing a model which included a polymer backbone, targeting moiety, and linker molecule from the polymer backbone which covalently linked to the bioactive agent.^{75, 76} Since then, many different types of non-degradable polymeric drug formulations have been synthesized, utilizing PEG, poly(lysine), poly(glutamic acid), poly(phosphazene),

and crosslinked hydroxypropyl methacrylate (HPMA) polymers, bound to antioxidant, anticancer, and anti-inflammatory drugs such as peroxidase, doxorubicin, and methotrexate, respectively.^{66, 76} A couple of PEG-drug conjugated systems in the market are Oncaspar[®], and Macugen[®] for leukemia and macular degeneration, respectively.

The field has continued to grow with the development of biodegradable polymeric active systems. Systems where the drug still remains as a side group, but bound to a hydrolytically labile polymer backbone, include the synthesis of linear PEG, sebacic acid, and glycerol comprised polyesters with ketoprofen side groups, developed by Wang et al.¹ Novel polyesters with ibuprofen and naproxen side groups have also been synthesized by Uhrich's group.¹ Antioxidant and anti-microbial phenols such as curcumin and quercetin have also served as active pendant groups conjugated into poly(β -amino ester) backbones.^{77, 78} Biodegradable polydrugs or polyactives have also been developed where the bioactive structure is either chemically incorporated into the polymer backbone or serves as the monomer to its respective homopolymer. Different examples of this class of polyactives include the novel synthesis of salicylic-based poly(ester-anhydride)s, poly(trolox-ester) and poly(peroxalate-ester) polymers, along with polymers comprised of antibiotic, analgesic and antiseptic monomers for bone, anti-inflammatory, and antioxidant therapeutics.¹ Before polymerization, the bioactive molecules are most likely activated or further synthesized into a diol or diacid monomer precursor, either by reacting with a cyclic anhydride, acyl chloride, or other linker component, before typically undergoing a solution polymerization via a step mechanism using a coupling agent. The advantage of polyactives over more common encapsulation

methods is that the drug weight percent within the polymer system is significantly increased while controlled release rates are still maintained.

2.7 Osteogenic Bioactive Agents

Different bioactive factors are commonly incorporated into biodegradable polymeric systems to enhance bioactivity, more specifically, osteogenic and osteoinductive agents for bone. Osteogenic agents include families of growth factors such as insulin-like growth factor (IGF-1) and transforming growth factor (TGF) β , which includes bone morphogenetic proteins (BMPs) [4-7]. Statins are also recognized for their osteogenic properties which have been taken advantage of in drug delivery systems for bone regenerative applications.⁷⁹⁻⁸⁴

2.7.1 Bone Morphogenetic Proteins (BMP)

BMPs are a class of osteoinductive proteins that belong to the TGF- β superfamily. More specifically, they are known as differentiation factors since they induce vascularization, proliferation, and maturing of mesenchymal cells into bone and cartilage cells.⁸⁵ They differentiate cells by binding to surface cell receptors which initiate the Smad transduction pathway, and causes the expression of an osteoblastic phenotype. BMPs initiate osteoblastic phenotypic expression in cells not related to bone, such as fat and muscle cells.⁸⁶ In the 1970s, Urist found that these BMP amino acid sequences responsible for osteoinductive activity could be isolated and extracted from the mineral component of bone. Since then, more than 20 different types of proteins related to BMPs have been discovered.⁸⁷ BMP-2 and BMP-7 have been FDA approved and extensively investigated in literature for bone regeneration, since both have similar sequences and

mechanistic pathways, activity in vivo, and induce osteoinduction at lower concentrations compared to other BMPs.^{85, 87} Among other BMP-2-incorporated polymer systems,^{88, 89} Laurencin *et al.* also constructed a system using PLGA/hydroxyapatite composites with seeded BMP-2 expressed cells.⁹⁰ Alveolar and mandibular bone formation was also seen in surgically made defects using collagenous and demineralized bone matrices with BMP-2.⁸⁷ Currently, BMPs are produced by either transfecting BMP DNA coding into mammalian cells which express and amplify the sequence and is later removed from the cells (recombinant BMP) or by purifying the protein from the bone extract using chromatography.⁸⁵ However, reproducing the protein has very high costs due to low recovered yields from its expression in mammalian systems.^{91, 92} Ectopic bone formation leading to a delayed onset of nerve compression has also been seen with its use in lumbar spinal fusion treatments, which adds to its disadvantages in bone repairing applications.⁹³

2.7.2 Statins in Bone Repair

Statins are most well known as lipid-regulating agents by inhibiting 3-hydroxy-3-methyl-glutaryl coenzyme A (HMG CoA) reductase in the mevalonate pathway.⁹⁴ The inhibition of the committed step, occurring early in the pathway, subsequently inhibits geranyl and farnesyl pyrophosphate isoprenoid precursors, which lead to the prenylation of Ras and Rho proteins involved in multiple cell signaling pathways influencing cell proliferation and differentiation.^{94, 95} As a result, statins are also attributed pleiotropic properties which can be utilized for tissue repair. Agents within the statin family include lovastatin, simvastatin, mevastatin and pravastatin, directly and indirectly derived from the fungus *Aspergillus terreus*, along with synthetic statins: atorvastatin, cerivastatin,

fluvastatin, pitavastatin and rosuvastatin.⁹⁶ Their slight differences in structural chemistry allow for some, mainly pravastatin and rosuvastatin, to be hydrophilic molecules, while the others remain lipophilic, more capable of crossing cellular membranes by passive diffusion and being metabolized hepatically by P450 cytochrome enzymes, excluding pitavastatin.⁹⁶ Expressed activity levels also differ between statins. Mundy *et al.* tested lovastatin, among many other natural products, with an assay measuring the BMP-2 expression, a strong promoter of osteoblastic proliferation and differentiation.⁹⁷ The group found the statin to be the only product from their collection to upregulate BMP-2, and subsequently tested other statins for comparable osteogenic activity. Simvastatin, at an oral 5 to 50 mg/kg/day dose, caused a 25 to 94% increase in trabecular bone volume in ovariectomized rats after 35 d. Since this investigation, simvastatin has been extensively studied for bone formation and has been utilized in many polymeric drug delivery devices for bone repair in maxillofacial and periodontal therapeutics. For example, alveolar bone growth was seen in mandibular tooth sockets after the implantation of a simvastatin-loaded PLA-PGA copolymer system.⁹⁵ Yazawa *et al.* also found that simvastatin enhanced cell proliferation and alkaline phosphatase activity in periodontal ligament cells.⁹⁸ However, statins have been seen to induce myositis, rhabdomyolysis, and hepatotoxicity at high doses,⁹⁹ which is why local instead of systemic delivery may be a better avenue for treating bone.

2.8 Significance

A reported 66-87% of bone fractures seen in trauma centers in the US and Puerto Rico are head injury related.¹⁰⁰ Other cranio-maxillofacial bone defects include cleft

palate, and alveolar to calvarial deformations left from trauma, disease, and genetic events requiring complex treatment. The World Health Organization reported 1/2000 births with cleft palate in the world's western populations and 1/1600 newborns affected with other craniofacial anomalies.² In adults, periodontitis is a common disease causing bone loss in the alveolar region from severe stages of chronic gingival infection. The disease is prevalent in 42.7% of adults in the US and 70.1% of adults 65 yr and older.¹⁰¹ Bone defects caused by these factors often lead to repeated surgeries involving graft implantation. Autologous bone grafting has continued to be the standard for treatment for osseous defects but has also contributed to post-operative complications.

Bioresorbable polymeric biomaterials have been included in a host of bone substitutes investigated to improve upon the drawbacks of current treatment. They serve to degrade and release bioactive agents to promote bone growth, while also preventing the need for revision surgery. However, some of these polymeric biomaterials come with their own disadvantages, such as a limited loading capacity of active agents which may not be sufficient for sustained delivery or localized tissue repair. Synthesizing a degradable osteogenic polymerized prodrug would serve to combat these issues for bone tissue regeneration. Simvastatin was chosen for investigation due to ample amounts of existing literature investigating its osteogenic properties, its chemical structure being amendable to polymerization, multiple properties benefiting the healing and growth of supporting vascular tissue, relatively inexpensive cost, and ease in accessibility. Synthesizing poly(simvastatin)-block-poly(ethylene glycol) would prolong simvastatin release while increasing the simvastatin loading capacity to weight percentages not

characteristically seen in current polymeric systems, making the biomaterial more efficient for localized treatment.

2.9 Specific Aims

Aim 1: Synthesize and characterize a degradable mPEG-poly(simvastatin) diblock copolymer. The molecular structure of simvastatin possesses a lactone moiety amendable to ring opening polymerization (ROP). Reaction conditions were determined for polymerizing simvastatin. The synthesized product was analyzed using various separation and spectroscopy techniques to determine bond formation, composition and quality. The copolymer was then degraded to characterize its degradation products.

Aim 2: Assess the tunability of the mechanical and degradation properties of poly(simvastatin)-block-poly(ethylene glycol) and poly(simvastatin)-based biomaterials. Poly(ethylene glycol)s of different MWs can alter the rate of water uptake, and thus degradation, of the resulting copolymer when copolymerized with a more hydrophobic polymeric block. Blending poly(simvastatin)-block-poly(ethylene glycol) with another aliphatic polyester with different degrading and physical properties will influence the degradation and simvastatin release rate of the poly(simvastatin) component of the blend, along with altering mechanical properties. PLA copolymers initiated with three different MW PEGs were blended with poly(simvastatin)-block-poly(ethylene glycol) (5 kDa mPEG) at 2 different weight percentages to examine effects on mechanical strength and degradation.

Aim 3. Test the bioactivity of its degradation products biochemically and *in vitro* and *in vivo*. Degradation products of the implant will remain active and furthermore

promote osteogenic effects on surrounding tissue to restore natural bone. Cytotoxicity of poly(simvastatin)-block-poly(ethylene glycol) and its degradation products were investigated. The copolymer and degradation products were then tested biochemically and *in vitro* for osteogenic activity. Biocompatibility was also observed *in vivo*.

Copyright © Theodora Atta Asafo-Adjei 2017

Ch. 3 Synthesis and Characterization of a Poly(ethylene glycol)- Poly(simvastatin) Diblock Copolymer

This chapter was reproduced from a published manuscript, “Asafo-Adjei T.A., T.D. Dziubla, D.A. Puleo, Synthesis and characterization of a poly (ethylene glycol)–poly (simvastatin) diblock copolymer. RSC Advances. 2014;4(102):58287-98.”

3.1 Introduction

The use of biodegradable polymers in therapeutic applications has grown due to their favorable characteristics, which include biocompatibility, tailorable degradation, and the ability for some polymer degradation products to be metabolized.^{23, 102} Poly(glycolic acid) (PGA), poly(lactic acid) (PLA), and poly(lactic-co-glycolic acid) (PLGA) are among the earliest biodegradable polyesters to be investigated. Unlike the degradation products of some polyesters, such as poly(ϵ -caprolactone), glycolic and lactic acid are fully metabolized in the body.¹⁰³ Commercial products based on these polymers include PGA/PLA sutures, approved by the FDA in 1971, to PLGA-collagen and PLA meshes and devices on the market for clinical regenerative treatments.¹⁰⁴ These degradable biomaterials can also encapsulate active agents within their matrices or in reservoirs, but polymers have also carried covalently conjugated drugs.¹⁰⁵ Polymer-drug conjugates have been a prevalent method of drug delivery since their conceptual development in 1975 to many different conjugates currently used.^{106, 107} These systems have used synthetic polymers, such as poly(lysine), poly(glutamic acid), and poly(phosphazene), to bind anti-cancer and anti-inflammatory drugs along their backbone via cleavable hydrazine bond linkers.^{108, 109}

While several characteristics of polyesters are advantageous, promoting their recurrent use in drug delivery, these biomaterials can have a limited capacity to entrap

drug.^{110, 111} Also, if structural or mechanical loading-induced defects exist in coated or drug repository devices, dose-dumping could lead to concentrations high enough for toxic effects to occur.¹¹²⁻¹¹⁴ Drug conjugation to the polymer backbone can prevent this issue, and it can preserve activity by shielding drugs from degradation as well as prolong drug circulation.¹⁰⁷ However, this system also has the disadvantage of limited linkages available for drug loading.¹⁰⁹

Incorporation of drug into the polymeric backbone, such as the degradable aspirin-derivatized poly(anhydride ester)¹¹⁵ and poly(trolox ester) polymers¹¹⁶ developed for anti-inflammatory and antioxidant therapeutic applications, respectively, circumvents limited drug loading. In these polymers, the weight percentage of drug is increased to nearly 100% as a result of these active molecules essentially being linked to each other to form a macromolecule. The step growth and esterification polymerization mechanisms used to synthesize polydrugs such as the ones mentioned can require multiple reaction steps, however. Little literature exists on utilizing the molecular chemistry of a therapeutic agent to create the backbone of its homopolymer or copolymer via ring-opening polymerization (ROP), such as the polymerization of lactonized ricinoleic acid.¹¹⁷

ROP has been utilized to polymerize lactones, among many types of cyclic monomers, into their respective polymers. Lactide and glycolide are examples of lactone monomers used to synthesize PLA, PGA, and PLGA via ROP, which can be initiated by metal or organic catalysts to obtain high molecular weight macromolecules.¹¹⁸ Potential drawbacks that exist in the mechanism include competing depolymerization reactions and other side reactions that can influence the yield and quality of the resulting polymer.¹¹⁹

However, ROP is versatile in using a range of hydroxyl-containing macromolecules and alcohols to initiate polymerization and alter polymer properties, and minimal steps are usually necessary to develop the polymer. ROP also has the ability to develop high molecular weight chains depending on the type of catalyst and molar ratios chosen for synthesis, which control the number of monomeric units attached. These advantages reveal the usefulness of ROP to create a unique polyprodrug as a biomaterial for drug delivery.

The therapeutic prodrug simvastatin contains a 6-membered lactone ring that is theoretically capable of being opened and reacted to form a polymer via ROP, much like monomers of PLA and PGA. Simvastatin is well known as the active ingredient in Zocor, an oral medication for treating hypercholesterolemia. However, the drug also exhibits anti-atherosclerotic, anti-inflammatory, angiogenic, and osteogenic properties in its active hydroxyacid form.¹²⁰⁻¹²³ Different polymeric devices have already explored encapsulation and release of simvastatin for bone regenerative applications.^{79, 124, 125} Simvastatin is readily metabolized, ensuring removal from the body.¹²⁶ Oral administration of statins can cause adverse muscular and hepatic effects¹²⁷ that likely are related to the high frequency of large doses needed to overcome first-pass metabolism. Polymerizing simvastatin addresses the issue of dose dumping, removes the need for a bioinert polymeric carrier, and provides the option of increasing the loaded amount of simvastatin while prolonging release at therapeutic concentrations.

The objective of the present studies was to investigate the polymerization of simvastatin using ROP. Reactions were conducted at different temperatures to evaluate

the effects of temperature via kinetic analysis. The copolymer was also subjected to alkaline conditions to test degradation via hydrolysis.

3.2 Experimental

3.2.1 Materials

Simvastatin was purchased from Haouri Pharma-Chem (Edison, NJ). Tin (II) ethylhexanoate (stannous octoate), monomethyl ether poly(ethylene glycol) (mPEG), anhydrous toluene, anhydrous diethyl ether, dichloromethane (DCM), and deuterated chloroform (CDCl_3) were purchased from Sigma-Aldrich (St. Louis, MO). Tetrahydrofuran (THF) stabilized with 3,5-di-tert-butyl 4-hydroxytoluene (BHT) was purchased from Fisher Scientific (Pittsburgh, PA).

3.2.2 Methods

3.2.2.1 Poly(ethylene glycol)-*block*-Poly(simvastatin) Synthesis. Approximately 400 mg microscale reactions of simvastatin (400 mg, 0.956 mmol) and mPEG (47.8 mg, 9.56 μmol) were performed to assess reaction kinetics using a procedure adapted from the literature.¹²⁸ All reactions were performed at 150 to 250 °C in a silica sand bath for improved temperature control. Internal solution temperatures were found to be 10 to 20 °C lower than the sand bath temperatures. The reactant components were dried at 130 °C in a nitrogen atmosphere for 1 hr followed by the reaction temperature for an additional hour. Samples for the initial time point were taken after the reactants melted into a homogenous bulk mixture and before catalyst addition. After the drying period, 1 wt% of stannous octoate dissolved in toluene was added to the melt by syringe. Each reaction ran for 24 hr, with three samples taken at each of 0, 1, 4, 8, 12, 18, and 24 hr. The theorized reaction scheme is shown in Figure 3.1a.

A macroscale synthesis of the diblock copolymer (2.5 g) was performed at 230 °C for 24 hr with the same reaction conditions described in the preceding paragraph. The crude product was purified by vacuum filtration after obtaining the precipitate using DCM as the solvent and cold diethyl ether in excess as the anti-solvent to further remove any residual monomer. Simvastatin (0.4 g) with and without catalyst addition was heated at 240 °C for 24 hr to assess the effect of temperature on its molecular weight.

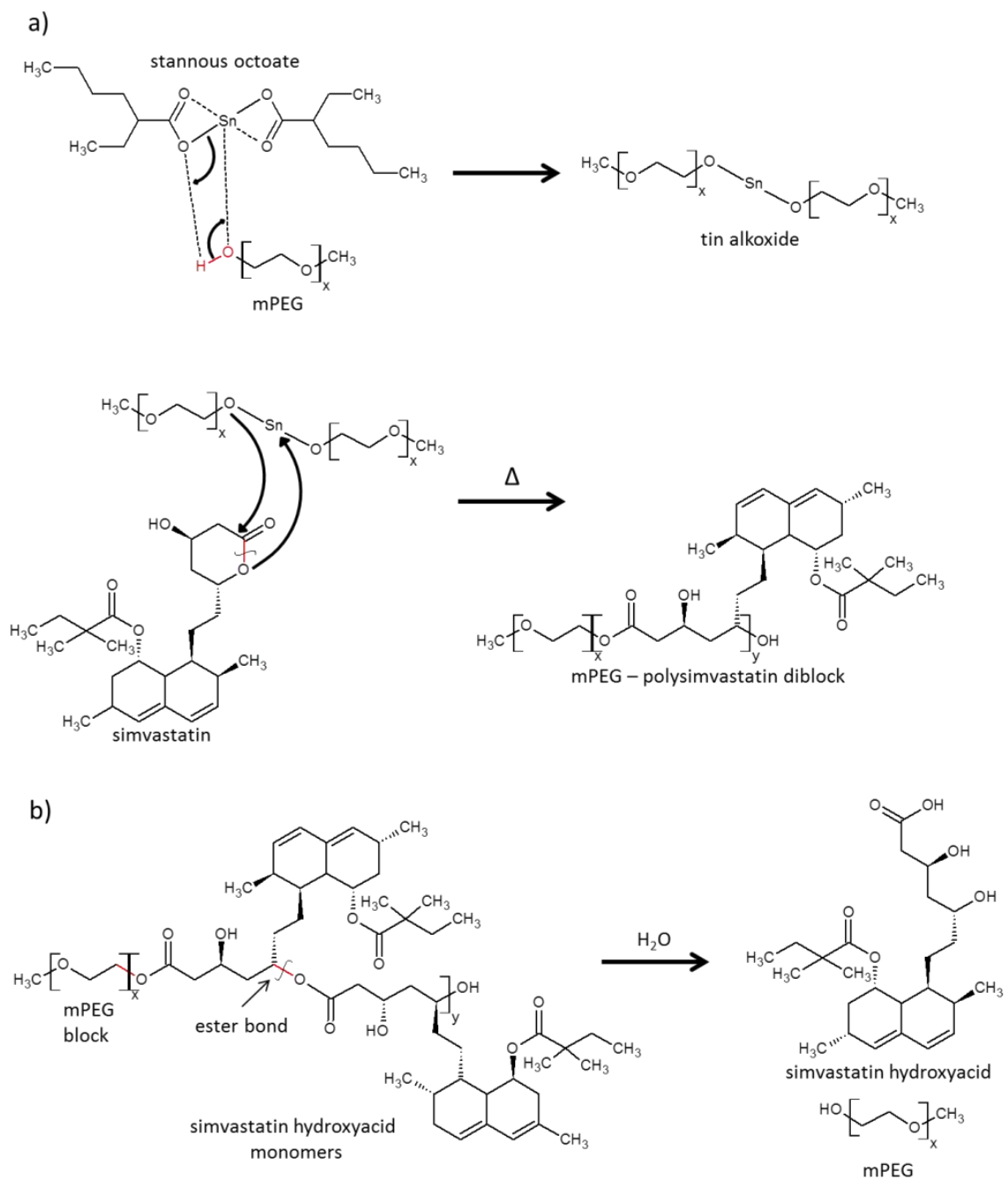


Figure 3.1 a) Tin alkoxide complex formation and proposed mechanism of ROP reaction to form poly(ethylene glycol)-*block*-poly(simvastatin). b) Proposed mechanism of hydrolytic degradation of the copolymer.

3.2.2.2 Gel Permeation Chromatography (GPC). Molecular weight was measured using a Shimadzu Prominence LC-20 AB HPLC system with a Waters 2410 refractive index detector. Two 300 x 7.5 mm, 3 μm particle size ResiPore columns (Agilent Technologies) in series were used for sample separation. Samples were injected using THF as the eluent at a 1.0 ml/min flow rate. Standard curves were prepared using polystyrene standards ranging from 160 Da to 370 kDa. Shimadzu Lab Solutions software was used to calculate weight- (M_w) and number-average molecular weight (M_n) and the polydispersity index (PDI, M_w/M_n). Simvastatin monomer conversion (*i.e.*, molecular weight growth of the poly(simvastatin) block) was determined as a function of time.

3.2.2.3 Nuclear Magnetic Resonance (NMR) Spectroscopy. H-NMR spectra were developed from Varian Gemini NMR 400 MHz spectrometers connected to a VnmrJ software interface. Samples of the copolymer and a melted mixture of simvastatin and mPEG (100:1 molar ratio) weighing 5 to 7 mgs each were dissolved in 1ml of CDCl_3 , transferred into NMR sample vials and analyzed for additional structure characterization.

3.2.2.4 Fourier Transform Infrared (FTIR) Spectroscopy. Spectra were obtained using a Varian FTS-7000e FTIR spectrophotometer with a 0.25 cm^{-1} resolution. Samples weighing 3 to 5 mg were placed directly onto a germanium attenuated total reflectance crystal and compressed for analysis. The functional groups of the copolymer (synthesized at $230\text{ }^\circ\text{C}$) were compared to those found in a melted mixture control of simvastatin and mPEG, as well as the components individually. Peak locations and heights of stretches characteristic of simvastatin and mPEG were identified in the copolymer and its control. Comparisons of peak location and height were assessed.

3.2.2.5 In Vitro Degradation. Small 16 to 18 mg disks were made by dissolving in dichloromethane (60 wt%) and pipetting the polymer solution onto a Teflon plate to evaporate the solvent overnight. Disks were placed in 3 ml of 1 M NaOH (aq) or phosphate-buffered saline, pH 7.4 (PBS). Disks were weighed and medium was completely replaced at each time interval. Total dry weight of the disks was measured at 2 and 6 weeks. Aliquots were retrieved at intervals and analyzed for absorbance at 240 nm using a PowerWave HT Microplate Spectrophotometer with a Gen5 analysis software interface. The theorized mechanism of degradation is shown in Figure 3.1b.

3.2.2.6 Matrix-Assisted Laser Desorption/Ionization – Time of Flight Mass Spectrometry (MALDI–TOF MS). Degradation supernatants were analyzed for product identification, relative abundance of different products, and molecular weight distribution using a Bruker Ultraflex extreme MALDI-TOFMS in positive ion mode. This instrument provides a smartbeam-II solid state laserbeam (355 nm) focus as low as 10 μm for quality spatial resolution, speed of up to 2 kHz, and a detector with a resolving power and mass accuracy of 40,000 and 1 ppm, respectively. Samples of simvastatin, mPEG, and degraded products in PBS were lyophilized and then solubilized in THF. The sample solutions were then centrifuged at 2500 rpm for 3 min to remove the undissolved salts. The remaining supernatants containing the dissolved compounds were syringe filtered (0.45 μm) before analysis. Approximately 1 μL of each sample solution was analyzed on a stainless steel target. Alpha-cyano-4-hydroxycinnamic acid (CHCA) was used as the matrix.

3.2.2.7 Statistical Analysis. Two-way ANOVA with a Bonferroni post-test was performed on the kinetic data to test the effects of reaction time and temperature on the

molecular weight growth of the copolymer and the effects of degradation time and pH on simvastatin release from the copolymer. An unpaired student t-test was conducted to test for differences between means of mass lost. Values of $p < 0.05$ were deemed statistically significant. Data were plotted as mean and standard deviation.

3.3 Results

Synthesizing poly(ethylene glycol)-*block*-poly(simvastatin) at 150 °C and above generated crude copolymers that increased in M_w with time (Figure 3.2). At 150 °C, a minimal M_w of 9.5 kDa was observed, which correlated to approximately two simvastatin monomers in each chain. However, as the temperature of reaction increased above 200 °C, polymer growth increased significantly, reaching poly(simvastatin) chain lengths of 19 to approximately 260 monomeric units attached to an mPEG block. The latter corresponded to a M_w of 74 kDa formed at 250 °C. The kinetics of the temperature-dependent reactions fitted best to a first-order rate model,

$$MW_t = MW_o e^{-kt} \quad (1)$$

where MW_t is molecular weight at time t , MW_o is initial molecular weight, and k is the rate constant (Table 1). Reactions run at 150 and 200 °C showed significantly lower rates of M_w growth, with constants of 0.0033 and 0.0169 hr^{-1} (Figure 3.2). First-order kinetics became more evident as the temperatures of 215, 230, 240, and 250 °C led to higher rate constants of 0.0052, 0.0042, 0.0782, and 0.0806 hr^{-1} , respectively. Regardless of the molecular weight values obtained at each temperature, the M_n values for the crude products did not exceed 13 kDa (Table 1).

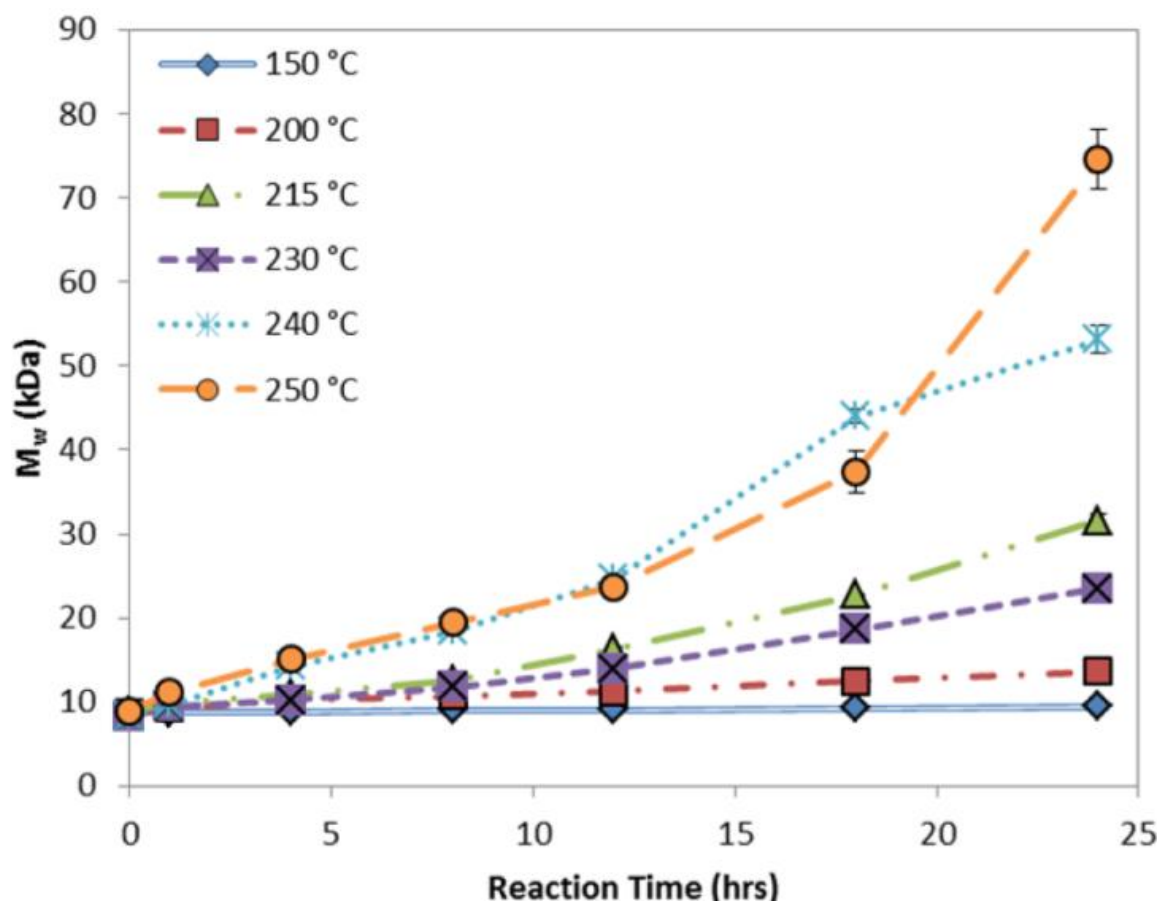


Figure 3.2. M_w of copolymer during ROP at increasing temperatures. Simvastatin and mPEG (5 kDa) were mixed at a 100 to 1 molar ratio for each reaction. The 0 hr time point represents the M_w of mPEG before poly(simvastatin) chain growth. The GPC molecular weight of mPEG registered higher than its theoretical value due to differences in chemistry between mPEG and the polystyrene standards used. Data are mean \pm standard deviation (n=3).

Table 3.1 Summary of the highest M_w obtained, derived rate equation, and percentage in the crude product at each temperature at 24 hr.

Temperature (°C)	Rate equation	Rate constant (hr ⁻¹)	M_w at 24 hr (kDa)	M_n at 24 hr (kDa)	% in crude product
150	$y = 8.74e^{0.0033t}$	0.0033	9.5	9.1	8.5
200	$y = 9.20e^{0.017t}$	0.017	13.6	10.7	38
215	$y = 8.88e^{0.052t}$	0.052	31.6	13.1	64
230	$y = 8.57e^{0.042t}$	0.042	23.5	12.2	60
240	$y = 9.40e^{0.078t}$	0.078	53.2	11.1	69
250	$y = 9.81e^{0.081t}$	0.081	74.6	10.9	75

Figure 3.3 shows a chromatogram depicting the conversion of monomers (i.e., simvastatin, represented by the peak at 22 min) to a larger M_w product at 250 °C. A marked decrease in the monomer peak area represented rapid consumption to form intermediate simvastatin-conjugates (17.5 to 21 min). The formation of product with a M_w higher than that of mPEG followed. The extended M_w growth of the copolymer was represented by a slight leftward shift from the peak of mPEG (17 min) and a broadened shoulder, beginning at 10 min, to the maximum peak height at 16.5 min.

The PDIs corresponding to the M_w kinetics are shown in Figure 3.4. At 150 °C, where minimal molecular weight growth was seen, the PDI remained at 1.05 after 24 hr. However, at 200 and 230 °C, the values increased up to 1.3 and 1.9, respectively. PDIs reached 4.8 and 6.9 at the highest temperatures of 240 and 250 °C, respectively.

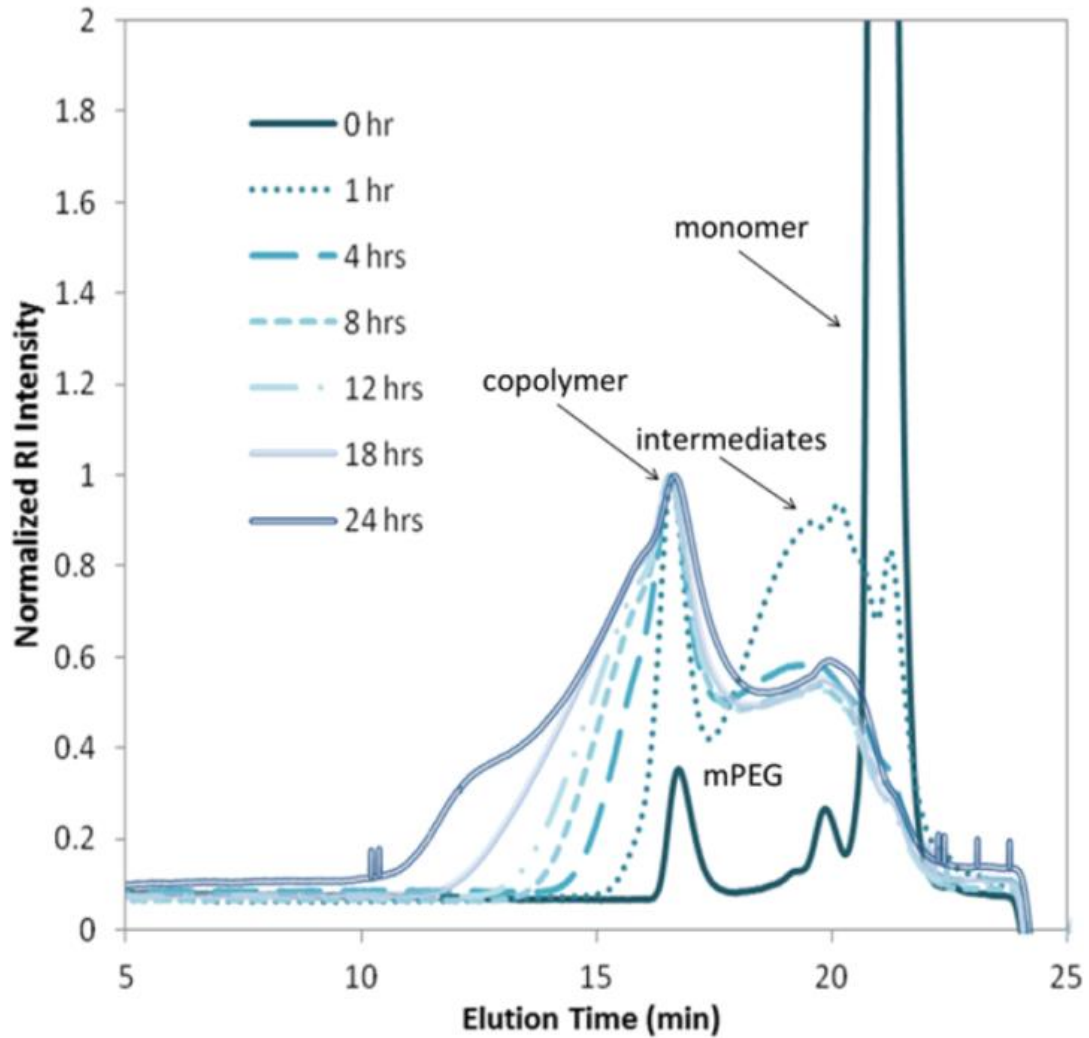


Figure 3.3 GPC chromatogram showing monomer (simvastatin) attachment to the mPEG block to form copolymer at 250 °C. Chromatograms were normalized to the copolymer peak. The 1 hr mPEG and simvastatin peaks are excluded from normalization due to the monomer peak registering at a high intensity (6.4).

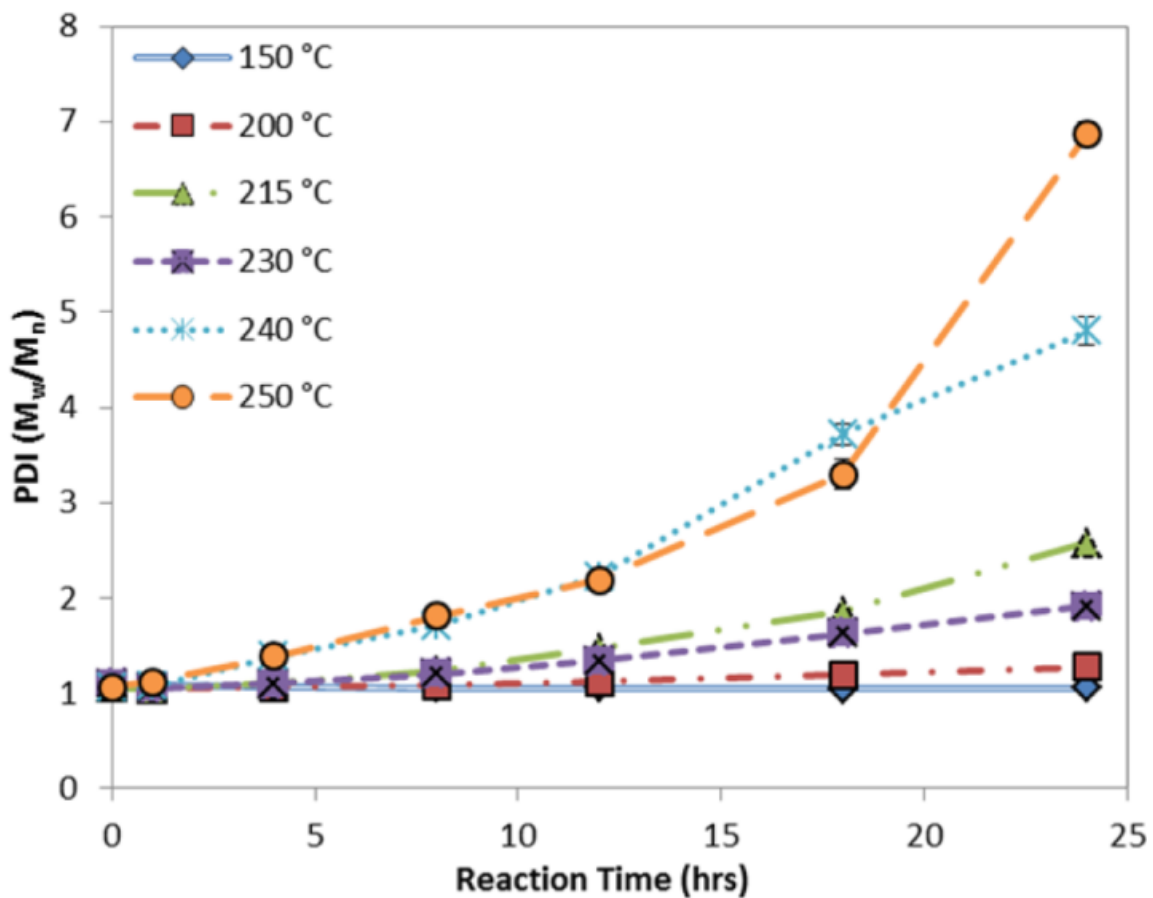


Figure 3.4 Changes in PDI at different temperatures of 24 hr ROP reactions. The PDI at 0 hr represents solely the mPEG block, and the subsequent points reflect addition of simvastatin monomers. Data are mean \pm standard deviation (n=3).

Further characterization of copolymer purification is shown by a GPC analysis of the crude product and the resulting retentate (desired copolymer) and filtrate (lower molecular weight products) (Figure 3.5). The copolymer peak after separation was seen at an elution time of 16.5 min. Intermediate products and unreacted simvastatin, represented by the elution time range of 18 to 22 min in Figure 3.3, were removed from the crude copolymer by subsequent vacuum filtration. The vacuum filtration step isolated the purified copolymer product in the retentate.

Analyzing the rate of propagation and the process by which the simvastatin monomer converted to copolymer at high temperatures led to heating the monomer, with and without the catalyst, at 240 °C to assess effects in the absence of mPEG as the initiator. Interestingly, heating simvastatin alone and simvastatin with catalyst produced molecular weights of 10 ± 4.7 kDa and 14 ± 11 kDa with PDIs of 2.3 ± 1.5 and 4.7 ± 2.5 , respectively. Both products still had lower M_w values than the product obtained in the high temperature copolymer reaction at 240 °C, which was 53 kDa with a PDI of 4.8. The majority of the conjugation produced was represented by the intermediate simvastatin product peaks, shown in Figure 3.3, most of which did not appear after purification (Figure 3.5, Table 3.2).

NMR spectra of the monomer and copolymer synthesized at 230 °C are shown in Figure 3.6. Integration measurements showed approximately 38 simvastatin monomers attached within the poly(simvastatin) block in the sample. Simvastatin has a molecular weight value of 418.57 Da, which led to a calculated M_w of 21 kDa, similar to the M_w seen in the kinetics analysis at 230 °C.

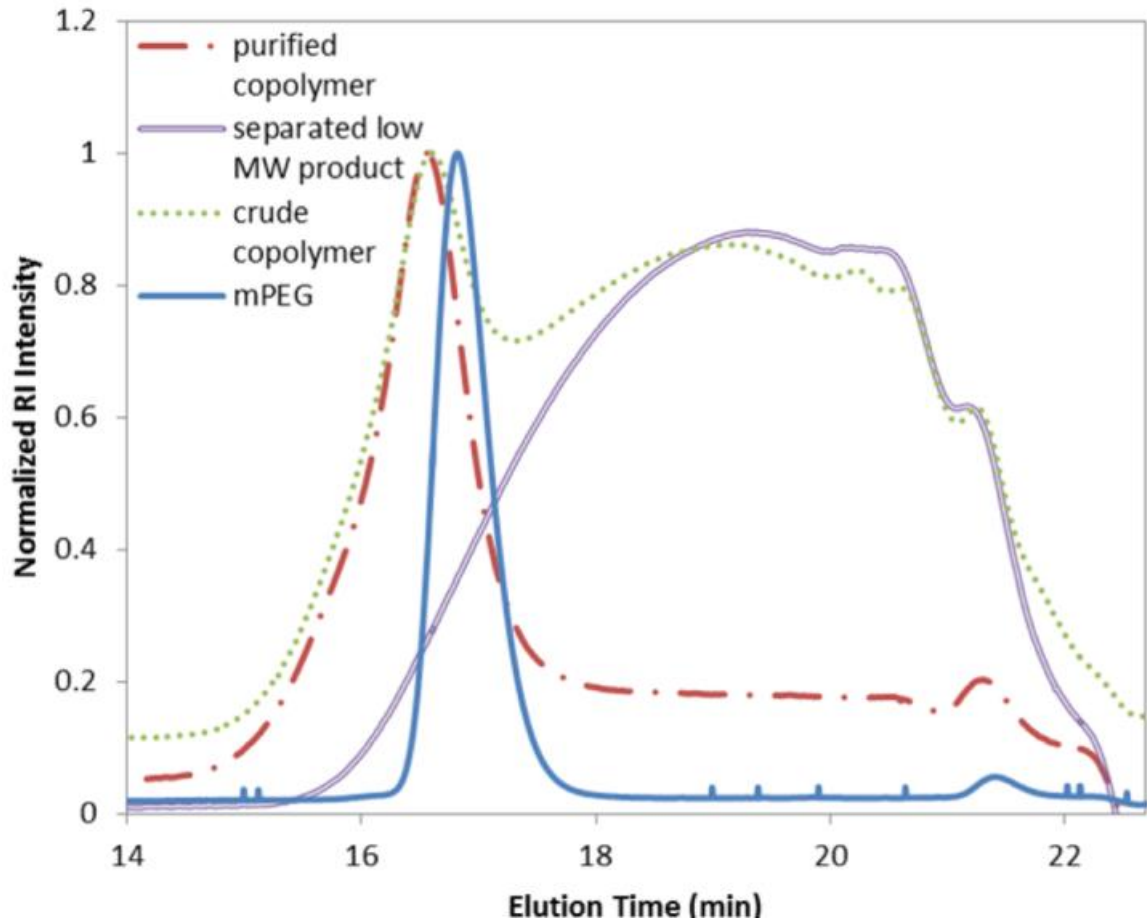


Figure 3.5 GPC chromatogram of separated products after purification of the crude copolymer.

Table 3.2. Summary of product M_w distributions from purification, measured via GPC.

Sample	Component	M_w (kDa)	Composition (%)	Yield (%)
Crude copolymer	highest M_w	11.5	28	-
	intermediates	2.1	48	-
	monomer	0.3	24	-
Purified copolymer	highest M_w	10.2	87	18
	intermediates	0.4	6.2	
	monomer	0.2 ^{a)}	6.8	
Separated low M_w weight product	intermediates	3.2	66	-
	monomer	0.3	34	-

^{a)} The GPC calibration curve has greater error for molecules with theoretical molecular weight values below 0.5 kDa, which may explain why the value for simvastatin monomer is not consistent in the table and why the value registers lower than the molecular weight value of 418.57 Da.

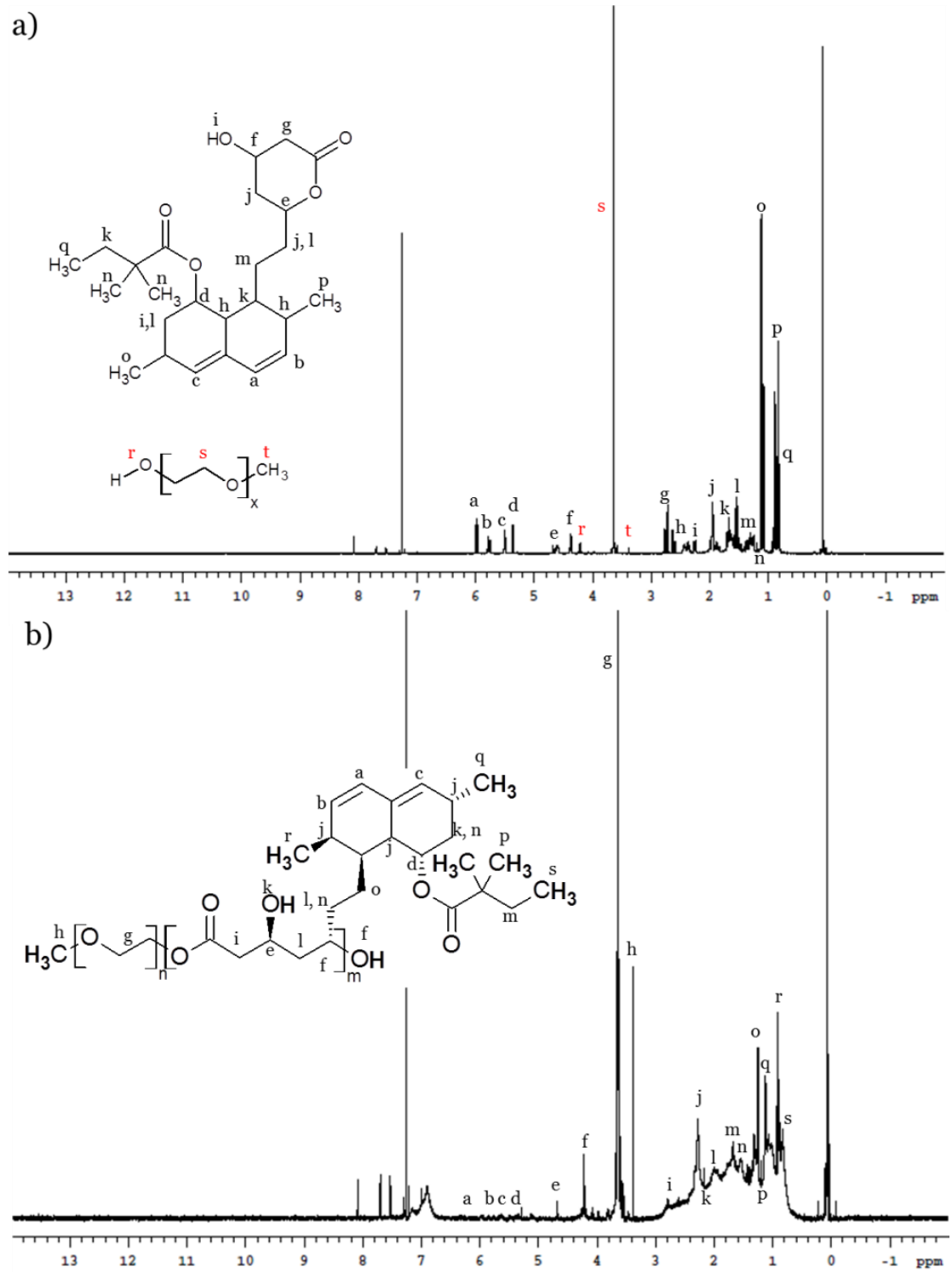


Figure 3.6 $^1\text{H-NMR}$ spectra in CDCl_3 (7.25 ppm) of: a) simvastatin and mPEG mixed at a 100:1 molar ratio and b) poly(ethylene glycol)-*block*-poly(simvastatin).

FTIR analysis of the functional groups of the synthesized copolymer is shown in Figure 3.7. Comparing the copolymer spectrum to the spectra of simvastatin and a mixture of simvastatin and mPEG revealed a carbonyl (-C=O) band shift from 1704 cm^{-1} to 1722 cm^{-1} . An increase in the band intensity ratio of the -CH-CH- peak ($2900\text{-}3000\text{ cm}^{-1}$) to -C=O band was seen in the copolymer spectrum compared to the control mixture. The copolymer spectrum also exhibited stretches characteristic of both simvastatin and mPEG, with the carbonyl band at 1722 cm^{-1} and the methyl ether band of mPEG at 1096 cm^{-1} .^{129, 130}

Mass loss and drug release of the disks in PBS and 1 M NaOH are shown in Figure 3.8. Over the first two weeks, water uptake by the samples led to an average maximum mass four and three times the initial mass for incubation in PBS and NaOH, respectively. The dry weights decreased 11 and 14% in the PBS and NaOH, respectively, during this time. At 6 weeks, the wet masses were 102 and 68% of the initial mass for PBS and NaOH, respectively, and the dry masses were 13 and 21% lower. The dry mass loss for the NaOH group had a larger mean decrease compared to samples in PBS, but the difference was not significant. The cumulative drug amounts released were 108 and 266 μg in PBS and NaOH, respectively. After an initial burst of 59 μg in 24 hr, a zero-order release rate was observed in NaOH with a constant of $7.4\ \mu\text{g}\cdot\text{hr}^{-1}$ between 1 and 10 days. A first-order release rate followed with a constant of $21\ \text{d}^{-1}$ for the remainder of the degradation period. In PBS, after an initial burst of 37 μg in 24 hr, only 2.5 μg was released during the following 8 days. A zero-order release constant of $2.1\ \mu\text{g}\cdot\text{d}^{-1}$ was determined for the remainder of the degradation period. The amounts of simvastatin

released in PBS and NaOH were significantly different at day 2 ($p<0.05$), day 3 ($p<0.01$), day 4 ($p<0.001$), and days 5 to 44 ($p<0.0001$).

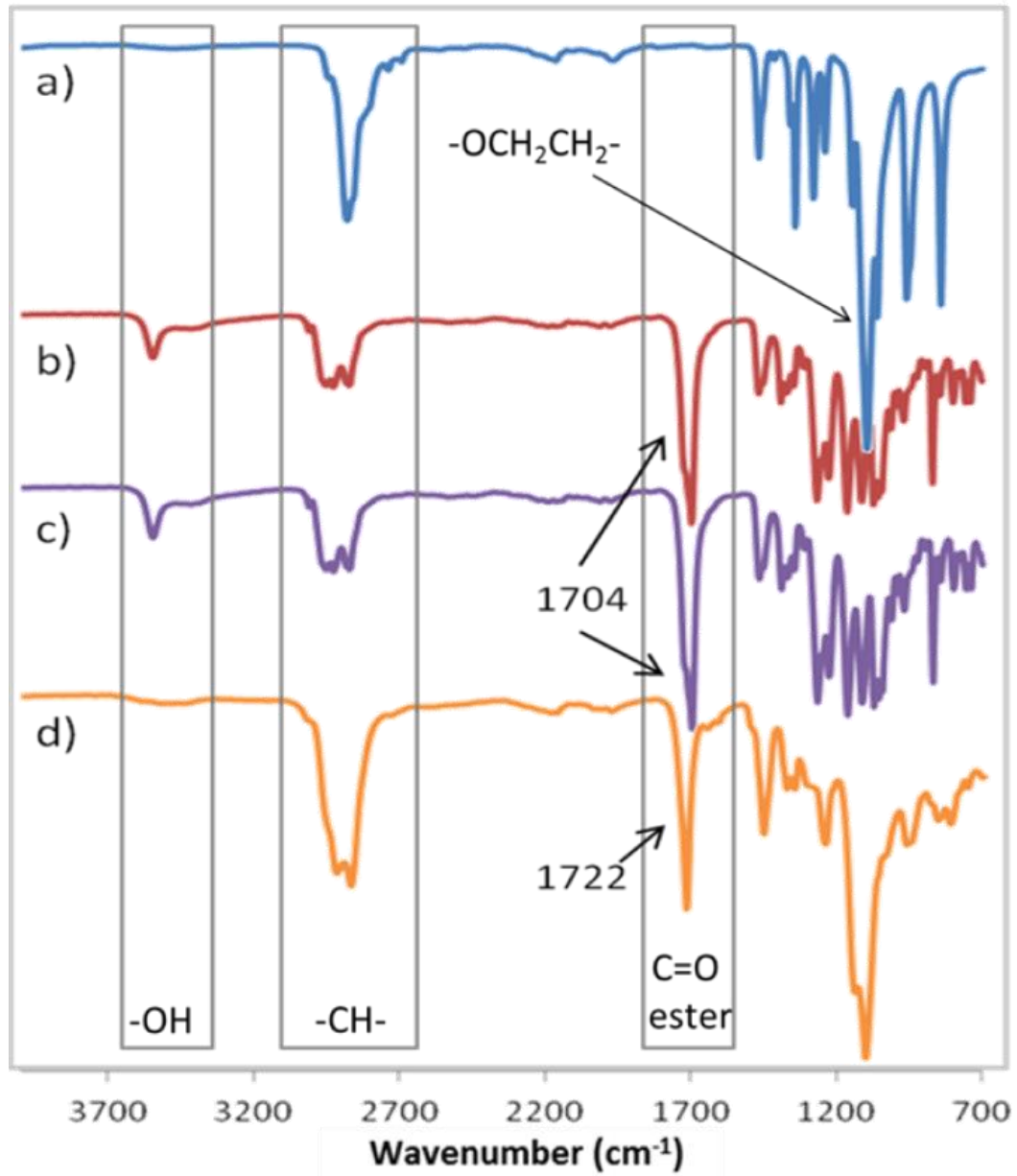


Figure 3.7 FTIR spectra of: a) mPEG, b) simvastatin, c) simvastatin and mPEG blended at the same molar ratio used for the reaction (100:1), and d) poly(ethylene glycol)-*block*-poly(simvastatin).

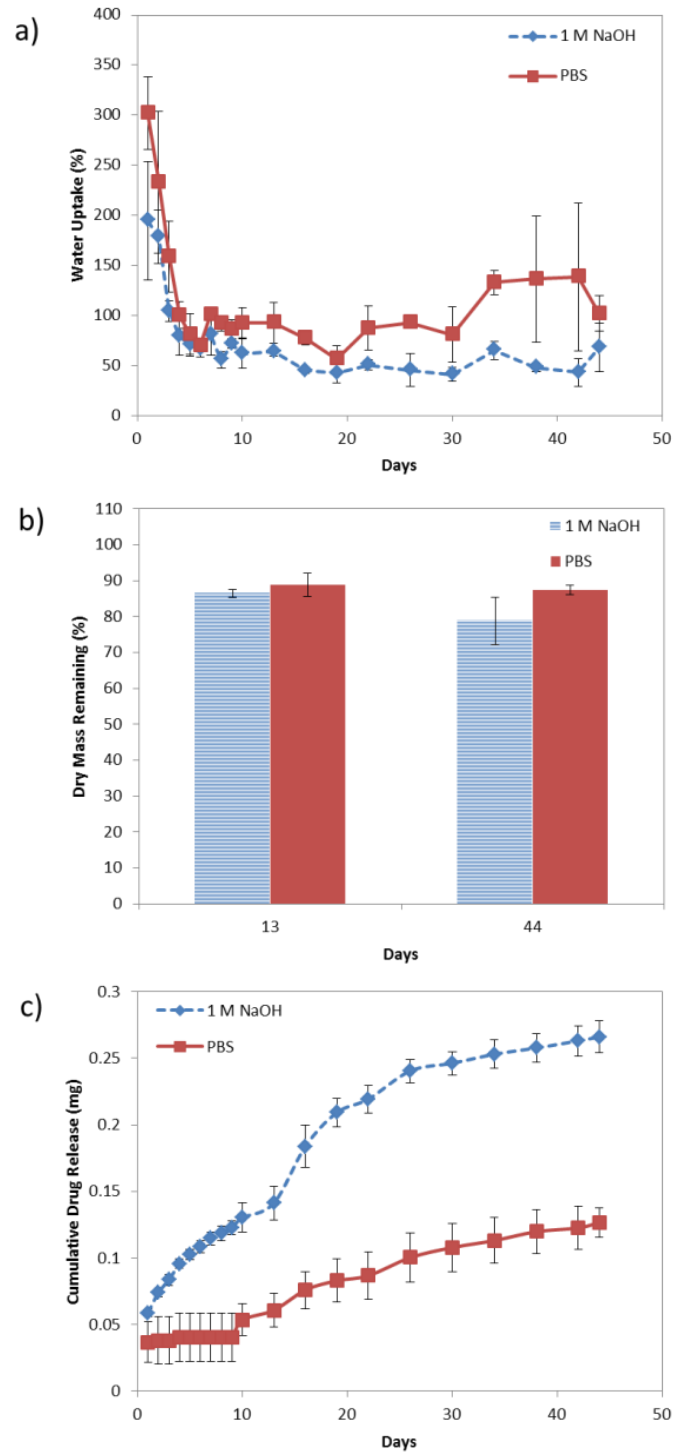
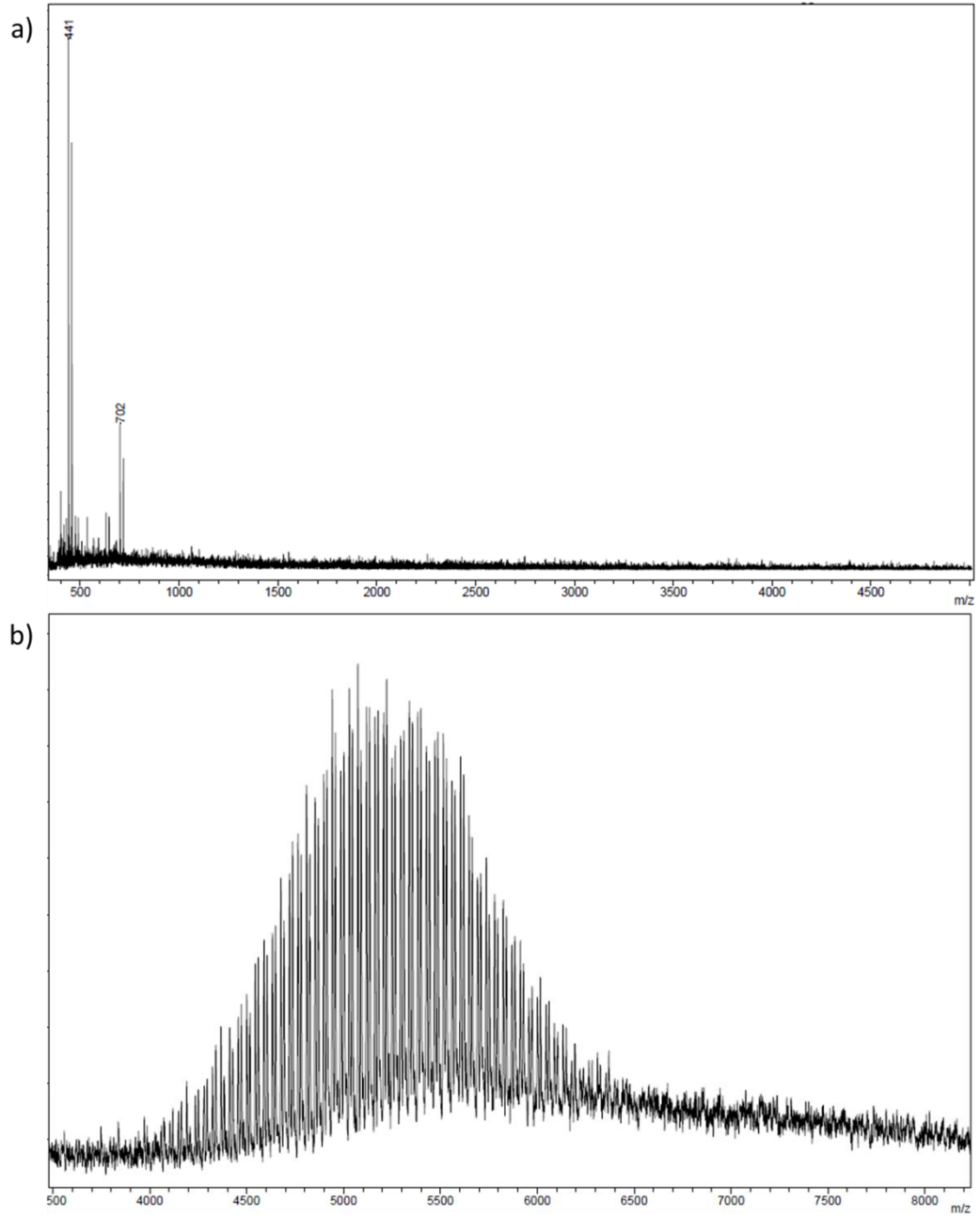


Figure 3.8 Degradation and drug release during incubation of samples in PBS or 1 M NaOH. a) Wet mass loss, b) dry mass loss, and c) drug release. Data are mean \pm standard deviation.



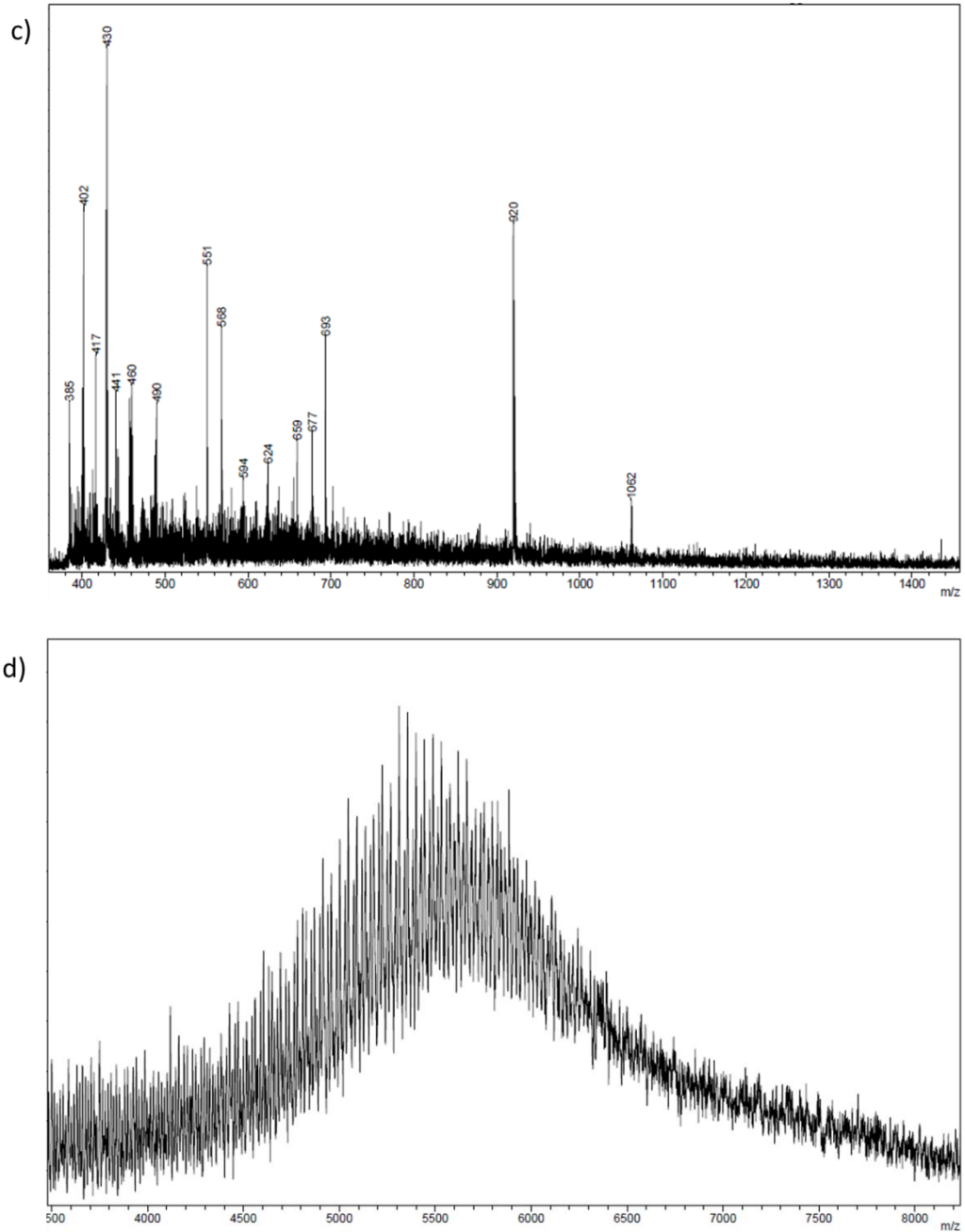


Figure 3.9 Mass spectra of a) simvastatin, b) mPEG (5 kDa), c) low molecular weight degradation products, and d) high molecular weight degradation products.

Mass spectral data identifying different species of degradation products are shown in Figure 3.9. The mass spectrum of simvastatin (Figure 3.9a) shows a peak of the

highest abundance at 441 mass-to-charge ratio (m/z), simvastatin's ion or the parent ion, and another distinct peak at 702 m/z . The mPEG mass spectrum (Figure 3.9b) displayed a pattern of a bell-shaped distribution of peaks with the highest relative abundance at 5207 m/z , which corresponds well with the theoretical molecular weight of the mPEG used for synthesis. Within the low molecular weight spectrum of the degradation products released (Figure 3.9c), the 441 m/z peak is present along with a peak at 460 m/z among a multitude of distinct peaks ranging from 490 to 1062 m/z to the right of the parent ion and 385 to 430 m/z to the left. In the high molecular weight spectrum of degradation products released, the highest relative ion abundance at 5312 m/z (Figure 3.9d) and a similar but rightward shift in the distribution of peaks compared to mPEG. Although present, the abundance of the 441 and 460 m/z peaks were approximately 50, 35, 60, 50, and 35% of the ions represented at a m/z of 402, 430, 551, 920, and 5312, respectively, the peaks of the highest relative abundance representing the degradation products.

3.4 Discussion

3.4.1 Copolymer Characteristics

The molecular and therapeutic properties of simvastatin are desirable for investigating the synthesis of a novel degradable poly(ethylene glycol)-*block*-poly(simvastatin) copolymer for its potential use in drug delivery. Different derivatives of poly(ethylene glycol), which include mPEG, have been used as initiators for the synthesis of block copolymers due to their reactive hydroxyl end groups, biocompatibility, and ability to increase the solubility of hydrophobic counterparts.¹³¹ Reacting simvastatin with mPEG via ROP can lead to a simple one-step synthesis of a

polyprodrug with unique characteristics. The reaction takes advantage of simvastatin being a prodrug, changing its closed-ring form into monomeric units of its active hydroxyacid, the opened-ring form of simvastatin (Figure 3.1a). The ester bond initially in the lactone ring of simvastatin would be embedded in the backbone of its polymer as a result of opening the ring. Thus, polymer degradation and drug release would occur by the hydrolysis of labile ester bonds, allowing the copolymer to degrade into biomolecules of simvastatin hydroxyacid and mPEG (Figure 3.1b). These components are metabolized in the liver and excreted by the kidneys, respectively.¹³²

3.4.2 Polymerization Mechanism

Lactone-based molecules, such as glycolide, lactide, ϵ -caprolactone, and their combinations, have been used as monomers for the synthesis of PLGA, PLA, and other aliphatic polyesters.¹³³⁻¹³⁵ Like these molecules, simvastatin possesses a lactone moiety capable of chemically opening and developing into a polymer block by the ROP mechanism using stannous octoate, a well-known tin metal catalyst. Aluminum and yttrium isopropoxide (metallic), porcine pancreatic and candida antarctica lipases (enzymatic), and various carboxylic acids and amines in the presence of an alcohol (organic) have also been used as catalysts, which in turn dictate the ROP mechanism that occurs.¹³⁶ The mechanism of stannous octoate is pseudo-anionic coordination-insertion ROP.^{136, 137} The metal catalyst first forms a complex with the hydroxyl group of the initiator to form an alkoxide. The more reactive alkoxide begins chain propagation by coordinating with the lactone ring of the monomer, followed by “insertion” of the ring into the alkoxide’s metal-oxygen bond.^{136, 138} Throughout the process, the alkoxide acts as a nucleophile by attacking the carbon of the ring’s carbonyl group, leading to cleavage

of the acyl bond and extended chain formation with its end bonded to the alkoxide, which is otherwise known as a living polymerization.¹³⁸ A 5 kDa mPEG was used in the synthesis of the present polymers so only one reactive hydroxyl group would be available for propagation of the poly(simvastatin) chain, creating a diblock copolymer.

3.4.3 Kinetic Analysis

It was necessary for simvastatin to be in a fluid-like state to ensure homogeneous mixing of all components. This state was possible only above 138 °C, the melting point of simvastatin¹³⁹, hence the high temperature range chosen for conducting melt condensation reactions. However, insignificant growth was seen for the lowest temperature reaction. The same results were also seen for preliminary reactions attempted using tin (II) trifluoromethyl sulfonate, and lanthanum and aluminum isopropoxide at 150 °C and lipase b candida antarctica at 80 °C in toluene (data not shown). Unlike glycolide and lactide, in which the cyclic lactone is their main structure, the lactone ring of simvastatin represents only a portion of the molecule. The other aromatic moieties of simvastatin may interfere with opening the six-membered lactone ring. Lactones of this size also have relatively lower ring strain than do smaller lactones, but their strain is still favorable for polymerization.¹⁴⁰ This characteristic contrasts with the cyclohexane counterpart of the lactone ring of simvastatin that does not polymerize due to the stable chair conformation it assumes without the ester group present.¹⁴¹ Thus, minimal chain growth between 150 and 200 °C may be due to a combination of ring strain and steric hindrance resulting from the bulky side groups attached to the targeted lactone ring of simvastatin, contributing to a lower than necessary reactivity.

Evidently, the simvastatin to mPEG molar ratios present in the 240 and 250 °C reaction products exceeded the initial 1 to 100 molar ratio in the melt. This finding may indicate low mPEG participation in the reaction and increased interactions between neighboring simvastatin molecules due to the higher weight percentage of the molecule within the bulk reaction mixture. In addition to mPEG having a hydroxyl group able to serve as the active group for initiation, simvastatin also possesses a secondary hydroxyl group attached to its lactone ring, which was unprotected during these reactions. Secondary hydroxyl groups are less reactive than their primary counterparts.¹⁴² Regardless, this available hydroxyl may have allowed chain propagation among the monomeric units to create extensively branched chains before interaction with mPEG to create the diblock copolymer. Simvastatin would then be considered a bifunctional latent AB₂ monomer capable of both initiating ROP, via the hydroxyl group on its lactone ring, and chain propagation through the opening of its lactone ring.^{143, 144} Mevalonolactone, a molecule structurally similar to simvastatin, has been used as a monomer for synthesizing branched copolymers.¹⁴⁴ Bifunctionality of the monomer can lead to a dendrimeric architecture of the copolymer, and in this case, it can lead to the synthesis of linear–hyperbranched mPEG–*block*–poly(simvastatin) copolymer chains fully capable of exceeding the initial 1 to 100 mPEG to simvastatin molar ratio, as more simvastatin monomers are added to the branched segments. Also, because simvastatin would be able to compete with mPEG in initiating ROP and is in much greater abundance, more mPEG would likely remain unreacted, which is represented by the low M_n in Table 1. The neighboring monomer interactions and branching may explain why the profiles strayed farther away from achieving a steady state as temperature increased within the given time

period. Regardless, the propagation kinetics of the copolymer reaction exhibited first-order rates, which is generally found to be the rate order of bulk ROP via insertion-coordination initiators.¹⁴⁵ By comparing the temperature-dependent rate constants as a function of temperature via the Arrhenius equation,

$$k = e^{-E_a/RT} \quad (2)$$

where k is the rate constant, R is the universal gas constant, and T is absolute temperature, an activation energy (E_a) of 14.5 kcal mole⁻¹ was obtained. The E_a found of the copolymer reaction is slightly lower but comparable to the activation energy of L-lactide undergoing ROP via insertion-coordination (19.6 kcal mole⁻¹).¹⁴⁶

The limited polymer growth below 200 °C indicates how propagation of the simvastatin chain was a more kinetically-driven reaction. The occurrence of ring opening and subsequent propagation depends on the size of the lactone ring, the bulkiness of side groups attached to the ring, and the inclusion or lack of heteroatoms, all of which affect ring conformation.¹³⁸ High ring strain increases lactone reactivity and largely contributes to the driving force for ROP. Thus, ROP may result from the loss of enthalpy (H) caused by dissipated ring strain. Even with cyclic monomers of low ring strain, heteroatoms present in the ring can increase the degrees of freedom of the resulting polymer, which increases the entropy (S) of the reaction and drives the reaction towards completion.¹¹⁹ Also, depending on the reaction conditions used, such as the solvent and states of the monomer and its polymer (*i.e.*, liquid, gas, or amorphous or crystalline solid), the monomer would be limited to: a) polymerizing above a floor temperature (+ ΔH and ΔS); b) polymerizing below a ceiling temperature (- ΔH and ΔS); c) polymerizing at any

temperature ($-\Delta H$, $+\Delta S$); or d) not polymerizing at all ($+\Delta H$, $-\Delta S$).¹⁴⁷ The M_w growth data show an evident floor temperature with polymerization possible above 150 °C under the given the melt condensation conditions. A more obvious indication of the reaction having a floor temperature relates to the high melting point of simvastatin and physical state necessary for the reaction to proceed. Without solvent present in the reaction vessel, polymerization was limited to temperatures above 138 °C.

3.4.4 Polydispersity

Linear polymers made via ROP of lactone rings with low ring strain often have broader molecular weight distributions than those made from lactone rings with high strain, a major factor necessary for opening the ring and progressing the formation of a polymer chain.¹³⁸ High PDIs may result from reactions such as transesterification, backbiting, or depolymerization. These occurrences can be represented by PDIs up to a value of 2 by the Flory-Shultz distribution function.¹⁴⁷ Even higher PDI values may represent nonlinear forms of polymerization (*i.e.*, branching). In the present studies, reactions above 200 °C produced higher PDIs, possibly from poly(simvastatin) branching considering that there was low mPEG participation in the reaction. An increased occurrence of side reactions likely contributed to a portion of the synthesized crude copolymer due to substantially increased kinetic rates at high temperatures. Although stannous octoate is an efficient catalyst, it is also known to promote transesterification¹⁴⁸, which would only be exacerbated at higher temperatures. Uncontrolled side reactions would in turn contribute to higher PDI values.

The PDIs measured represent solely the copolymer peaks. The baseline did not completely return back to its original intensity after the elution of the copolymer peak,

indicating that there was still a residual amount of intermediates and unreacted simvastatin remaining in the purified product sample. Further removal would require an additional purification step in the procedure.

3.4.5 NMR Analysis

The chemical shifts labeled 'g' and 'h' in the copolymer spectrum represent the mPEG block,¹⁴⁹ while the remaining labeled shifts relate to the poly(simvastatin) block. The broadened peaks that represent simvastatin up-field between 2.91 and 0.067 ppm indicate polymerization that has occurred to form the poly(simvastatin) block. However, the integration ratio of the poly(simvastatin) area upfield (2.91 to .067) to the area downfield (7.22 to 6.71, ratio; 17.0) is far from 1, suggesting some sort of degradation or other form of conjugation that may have occurred due to the high temperature of the reaction. The residual side products as a result may explain the shifts seen beyond 6.71 ppm or it may be an artifact of the environment of copolymer's proposed branched structure.

3.4.6 Functional Groups and Bond Formation

The carbonyl shift shown in the IR spectrum of the copolymer suggested new ester bond formation. The change in height of the -CH-CH- stretch may be a representation of monomer addition (with a -C=O group) to the mPEG block (without a -C=O group). Also, the copolymer spectrum showing peaks characteristic of both components indicated that a chemical bond between the two blocks occurred compared to the mixed control, which showed only peaks characteristic of simvastatin, regardless of the presence of mPEG.

3.4.7 Degradation

The samples in PBS showed an increasing trend in percentage wet mass in the last 3 weeks compared to those in NaOH. An increase in surface area due to disk breakage, despite a minimal loss in dry mass, may have aided in an increased absorbance of medium. The high water absorbance seen in both groups can also be explained by the presence of the hydrophilic mPEG block of the copolymer. The initial burst and subsequent zero-order release observed may indicate small molecules of free simvastatin and oligosimvastatin close to the sample surface being easily dispersed into the medium with the aid of water absorption by mPEG. The first-order rate seen in the NaOH group may be influenced by the existing concentration of simvastatin in medium or by the scission process in which poly(simvastatin) breaks down into simvastatin, which is only then detectable in solution. Even though 108 to 266 μg of simvastatin were released from the samples during a 6 week period, release of other degradation byproducts, some of which do not have maximum absorption at 240 nm, would account for the remaining mass loss measured.

Degradation of the copolymer is expected to occur by the hydrolysis of labile ester bonds in the polymer chains. In alkaline solutions, simvastatin is also known to hydrolyze into its active open-ring form, simvastatin α -hydroxyacid.¹⁵⁰ The simvastatin hydroxyacid may be included in the components resulting from breakdown, along with byproducts that may include oligosimvastatin chains, mPEG, and mPEG with minimal monomers of simvastatin attached. The hypothesized byproducts are based on the presence of ester bonds that would be present between the monomeric units and between the block components. The degradation process and products of other polyesters, such as

PLGA, have been well-documented in identifying soluble oligomers that then degrade into the final products of lactic and glycolic acid in abiotic conditions.¹⁵¹

The mass spectra of the low molecular weight degradation products showed m/z values of 441 and 460, indicating the presence of simvastatin in its closed and open ring forms, respectively. The m/z values for simvastatin and simvastatin hydroxyacid have most likely been influenced by salt adducts in the analytes (i.e. Na^+ , K^+ , and H^+) because the ions are produced by cationization.¹⁵² Salt adducts can be produced from any salts present within the sample, such as the PBS to which degradation products and simvastatin and mPEG controls were exposed before prepping the samples for MS analysis. Despite desalting the final sample solutions, a small amount of the salts remained present for detection but not nearly enough to inhibit the generation of a clear and readable spectrum. However, salt detection can still contribute to decreased ionization efficiency, which possibly influenced the increased baseline noise seen in the low molecular weight region, along with low concentration.

A parent ion value of 441 m/z is likely the result of an attachment of Na^+ (22 m/z) to the parent ion (419 m/z). A simvastatin hydroxyacid ion would gain a molar mass value of 18 due to hydrolysis, leading to an m/z value of 460, seen in the spectrum, if the salt adduct is the same as the one on the parent ion and the H^+ ion also attached. The lower value peaks may represent a combination of fragmented ions of simvastatin,¹⁵³ the CHCA matrix (189 m/z), and salt adducts present in the sample. The same indication holds true for the peaks ranging from 490 to 693 m/z and the peak at 702 m/z in simvastatin's spectrum, along with the incorporation of ion clusters produced from the matrix¹⁵⁴ (i.e., molecule (M): $2\text{M}+\text{Na}^+$ and $2\text{M}+\text{H}^+$; 379 and 401 m/z , respectively) and

the parent ion. The peaks of 920 and 1062 may incorporate dimer ions of simvastatin along with the other combinations previously mentioned.

The pattern of peaks seen in the mPEG mass spectrum represents the repeating –CH₂CH₂O– unit of the polymer. The rightward shift in peak distribution seen in the high molecular weight degradation products indicates simvastatin monomers remaining attached to the mPEG block. Salt adducts and the presence of complex ions can lead to less defined peaks otherwise seen as a rise in the baseline under the peaks of the high molecular weight products. Thus, the mass spectral data suggests that the supernatants collected from the degrading copolymer contained a broad distribution of degradation products, including simvastatin, simvastatin hydroxyacid, dimerized simvastatin, mPEG, and mPEG with simvastatin monomers attached, some of which are possibly branched.

Despite the possibility of a branched architecture being known to accelerate degradation rates because of an increased number of end-groups present per polymer chain⁶³ and the large amount of water uptake of the samples within a 6 week period, limited degradation and slow simvastatin release rates were still seen within neutral and alkaline environments. This effect was attributed to the slow cleavage rate of bonded simvastatin monomers being the limiting factor and/or possible side reactions during polymerization leading to less labile bonds. Thus, investigating methods to improve the synthesis procedure to better control the ROP reaction would be beneficial in minimizing the side reaction byproducts produced in the crude copolymer.

3.5 Conclusions

A degradable poly(ethylene glycol)-*block*-poly(simvastatin) copolymer can be useful as a polymeric drug delivery system. The poly(simvastatin) block formed at and

above 200 °C, showing potential for increasing the weight percentage of the prodrug in the biomaterial. ROP of simvastatin reveals a new approach for polymerizing prodrugs in the statin family and possibly in other classes of lactone-containing prodrugs that may have less steric hindrance. Less bulkiness could provide better chain propagation at more ambient reaction conditions. The minimal synthesis steps of ROP needed to polymerize prodrugs, such as simvastatin, can be desirable in scaled-up production. Although M_w increased with temperature and initial degradation was observed, the rate of bond cleavage between simvastatin monomers and possible byproducts from side reactions hindered mass loss and subsequent drug release. Despite slow degradation, release of open and closed-ring simvastatin as well as simvastatin in poly(oligo)meric forms was demonstrated. By minimizing the side reactions, degradability of the mPEG-poly(simvastatin) diblock copolymer could be improved, potentially providing sufficient concentrations of simvastatin for extended treatment periods.

Ch. 4 Tuning Properties of Poly(ethylene glycol)-*block*-poly(simvastatin) Copolymers Synthesized via Triazabicyclodecene

This chapter was reproduced from a manuscript accepted for publication, “Asafo-Adjei T.A., T.D. Dziubla, D.A. Puleo, Tuning Properties of Poly(ethylene glycol)-*block*-poly(simvastatin) Copolymers Synthesized via Triazabicyclodecene, (2017), Reactive and Functional Polymers.”

4.1 Introduction

A wide range of catalysts with different mechanisms of action have been used to synthesize degradable polyesters for biomedical applications. Common catalysts that mediate ring-opening polymerization (ROP) of lactone-incorporated monomers include tin (II) ethyl-hexanoate (stannous octoate) and other organotin compounds.²⁹ Aluminum-, lanthanum-, and zinc-based alkoxides have also been used in the synthesis of high molecular weight (MW) poly(lactic acid) (PLA), poly(lactic-co-glycolic acid), and poly(ϵ -caprolactone).^{29, 31, 155}

Stannous octoate and other metal and alkaline earth catalysts are known to be efficient¹⁴⁸, while enzymatic, acidic, and organic catalysts have reportedly shown lower reactivity, producing low MW polymers.^{29, 156} Catalyst reactivity, however, can be altered by modifying reaction conditions, the type or size of lactone monomer incorporated into the feed, or functional groups of these catalysts. For example, changing the diamine bridge of aluminum salen complexes from ethylene to dimethylpropylene led to significantly increased polymerization rates of small L-lactide, ϵ -caprolactone, ϵ -decalactone, and β -butyrolactone monomers, while low reactivities with ω -pentadecalactone and other macrolactones were not significantly affected.¹⁵⁷ Also, ROP

reactions with diazabicycloundecene and N-methylated triazabicyclodecene (TBD) organocatalysts generated polylactide MWs of 18 and 21 kDa, respectively, in the presence of pyrenebutanol in chloroform under optimized conditions.⁵⁴ The type of catalyst used under specific reaction conditions can affect the degree of polymerization and the resulting quality of the polymer synthesized.

In our previous studies, stannous octoate-mediated coordination-insertion ROP was used to synthesize a newly developed poly(simvastatin)-poly(ethylene glycol) diblock copolymer with potential anti-inflammatory, angiogenic, and osteogenic properties following degradation. While the catalyst was successful in mediating poly(simvastatin) propagation with a methyl-terminated poly(ethylene glycol) (mPEG) initiator, a narrow and high reaction temperature window served as a limitation that also promoted undesirable transesterification reactions. After preliminary attempts with other metal and organocatalysts, TBD was ultimately selected because of its efficient performance at ambient temperatures,⁵⁴ ability to work without a co-catalyst, metal-free process, and accessibility. TBD was also reported to rapidly catalyze synthesis of 26 kDa PLA, of which the MW could be modified by changing the molar ratio of initiator to monomer in the feed.¹⁵⁸

In the present study, the TBD-mediated poly(simvastatin) reaction was compared with the stannous octoate-mediated reaction under similar conditions. Polymerization via TBD was also evaluated with different MW mPEGs, catalyst percentages, and molar ratios of simvastatin to mPEG. Hydrolytic degradation of the resulting poly(ethylene glycol)-*block*-poly(simvastatin) (PSIM-mPEG) copolymers was also analyzed by measuring mass loss and drug release.

4.2 Experimental

4.2.1 Materials

Simvastatin was purchased from Haorui Pharma-Chem (Edison, NJ). Triazabicyclodecene, monomethyl ether poly(ethylene glycol) (mPEG), anhydrous toluene, anhydrous diethyl ether, dichloromethane (DCM), and deuterated chloroform (CDCl_3) were obtained from Sigma-Aldrich (St. Louis, MO). Tetrahydrofuran (THF) stabilized with 3,5-di-tert-butyl-4-hydroxytoluene (BHT) was procured from Fisher Scientific (Pittsburgh, PA).

4.2.2 Methods

4.2.2.1 Synthesis of poly(ethylene glycol)-block-poly(simvastatin). Microscale reactions of PSIM-mPEG using stannous octoate have been previously described.¹⁵⁹ Macroscale reactions (2 g) were conducted using simvastatin as the monomer and mPEG (550, 2000, or 5000 Da) as the initiator. Molar ratios of 100:2 for simvastatin to mPEG 550, and 100:1 for simvastatin to mPEG 2000 or 5000 Da were used in the feed to synthesize PSIM-mPEG(550), PSIM-mPEG(2k), and PSIM-mPEG(5k), respectively. Simvastatin and mPEG were dried in a round bottom flask embedded in a silica sand bath at 120 °C for 1 hr under a continuous flow of nitrogen gas. The internal bulk temperature was increased to 150 °C for an additional hour before adding 1 wt% of TBD to the homogeneous melt. Each reaction ran for 24 hr.

Microscale reactions (0.4 g) were also conducted for PSIM-mPEG(550) copolymers with a TBD catalyst percentage of 0.1 or 1 wt%, a 100:1, 100:2 or 100:10 simvastatin to mPEG molar ratio, and crude samples taken at 0, 4, 12, 18, or 24 hr reaction times.

Polymer dissolved in DCM was slowly added to cold diethyl ether at a 1:7 v/v ratio of DCM to ether and vacuum filtered to purify the crude PSIM-mPEG(5k) product,. The purification process for PSIM copolymers with lower MW mPEG blocks involved slowly adding cold diethyl ether to the polymer in DCM solution at a 1:20 v/v ratio, followed by centrifugation and decantation of the supernatant.

4.2.2.2 Gel Permeation Chromatography (GPC). A Shimadzu Prominence LC-20 AB HPLC system connected to a Waters 2410 refractive index detector was used to measure the weight-average molecular weights of simvastatin, mPEG (550, 2000, and 5000 Da), and the crude PSIM copolymers. Two Resipore columns in series (300 x 7.5 mm, 3 μ m particle size; Agilent Technologies) were used for separation. Samples were dissolved in THF at 5 to 10 mg/ml. THF was also used as the mobile phase at a 1.0 ml/min flow rate. Polystyrene standards were used to calculate MW ranged from 160 Da to 430 kDa.

4.2.2.3 Nuclear Magnetic Resonance (NMR) Spectroscopy. H-NMR spectra were obtained to characterize the PSIM-mPEG (5k) copolymer and a melted mixture of simvastatin and mPEG at a 100:1 molar ratio using a 400 MHz Varian Gemini NMR instrument connected to a VnmrJ software interface. Samples weighing 5 to 7 mg each were dissolved in 1 ml of CDCl₃, transferred into NMR tubes, and analyzed for additional structural characterization. The number of simvastatin monomers present in the diblock copolymer was calculated by integrating the area under the peaks representing simvastatin relative to those associated with 5 kDa mPEG, of which the number of H atoms in its structure was known. With this ratio, the number of protons in the poly(simvastatin) block of the copolymer was calculated and divided by the known

number of protons in simvastatin to get the number of simvastatin monomers in the diblock copolymer.

4.2.2.4 Matrix-Assisted Laser Desorption/Ionization – Time of Flight Mass Spectrometry (MALDI-TOF MS). Degradation products of PSIM-mPEG(5k) were analyzed using a positive ion mode Bruker Ultraflex extreme MALDI-TOFMS. The procedure used for sample analysis was previously described.¹⁵⁹

4.2.2.5 In Vitro Degradation. Films of each copolymer (10-15 mg) were made by adding a small amount of DCM to polymer to create a viscous solution (700% w/v) that was pipetted onto a Teflon sheet to dry overnight. Each film was gently shaken in 1.5 ml of phosphate-buffered saline (PBS), pH 7.4, at 37 °C. Supernatant was collected and the medium completely replaced every 12 hr the first day, every other day the first week, and at 2 to 5 d for the remainder of the 44 d degradation period. The remaining samples were dried and weighed after 6 weeks to measure total mass loss.

4.2.2.6 High Performance Liquid Chromatography (HPLC). A Shimadzu Prominence LC-20 AB HPLC system was used to analyze supernatants collected from the mass loss study. One Luna C18 column (150 x 4.60 mm, 5 µm particle size) was used with an isocratic mobile phase of acetonitrile and water with 0.1% trifluoroacetic acid (70:30 v/v). Absorbance was measured at 240 nm.

4.2.2.7 Statistical Analysis. Two-way ANOVA with a Bonferroni post-test was performed on the kinetic data to test effects of reaction time, catalyst percentage, and molar ratio on MW, yield, and percent composition of the copolymer. The same analysis was applied to the simvastatin amounts released during copolymer degradation. Values

of $p \leq 0.05$ were deemed statistically significant. Data are plotted as mean and standard deviation.

4.3 Results and Discussion

4.3.1 Polymerization Mechanism

The ROP mechanism governed by TBD is anionic. From the literature, one theorized mechanism suggests that the amidine imine nitrogen of the nucleophilic catalyst attacks the carbonyl group on the lactone ring of simvastatin to form a temporary intermediate as the acyl bond is broken. The secondary amine in the guanidine-based organocatalyst attracts the alcohols within the reaction mixture (i.e., both on mPEG and the propagating poly(simvastatin) block) via hydrogen bonding. This action propagates the PSIM block of the PSIM-mPEG diblock copolymer.¹⁵⁸ However, computational analysis comparing the transitional state energies of proposed TBD-mediated ROP reactions with L-lactide and methanol showed that the intermediate steps carried out via hydrogen bonding had lower energy transitional states compared to nucleophilic attraction throughout the reaction. The lower energy states due to hydrogen bonding indicated a relatively more stable mechanism.¹⁶⁰

In the proposed mechanism shown in Figure 4.1, the amidine imine nitrogen of TBD attracts the hydrogen on the alcohol, in this case mPEG, to activate it. The activated alcohol then attacks the carbon of the carbonyl group of the lactone ring of simvastatin. The catalyst then changes orientation, subsequently hydrogen bonding to the oxygen in the C–O bond in the lactone ring, while the secondary amine remains hydrogen bonded to the oxygen in the carbonyl group. This transitional state initiates opening of the lactone

ring. TBD is reformed after the hydrogen migrates away from the amidine imine to form the hydroxyl end-group of the propagating polymer.¹⁶⁰

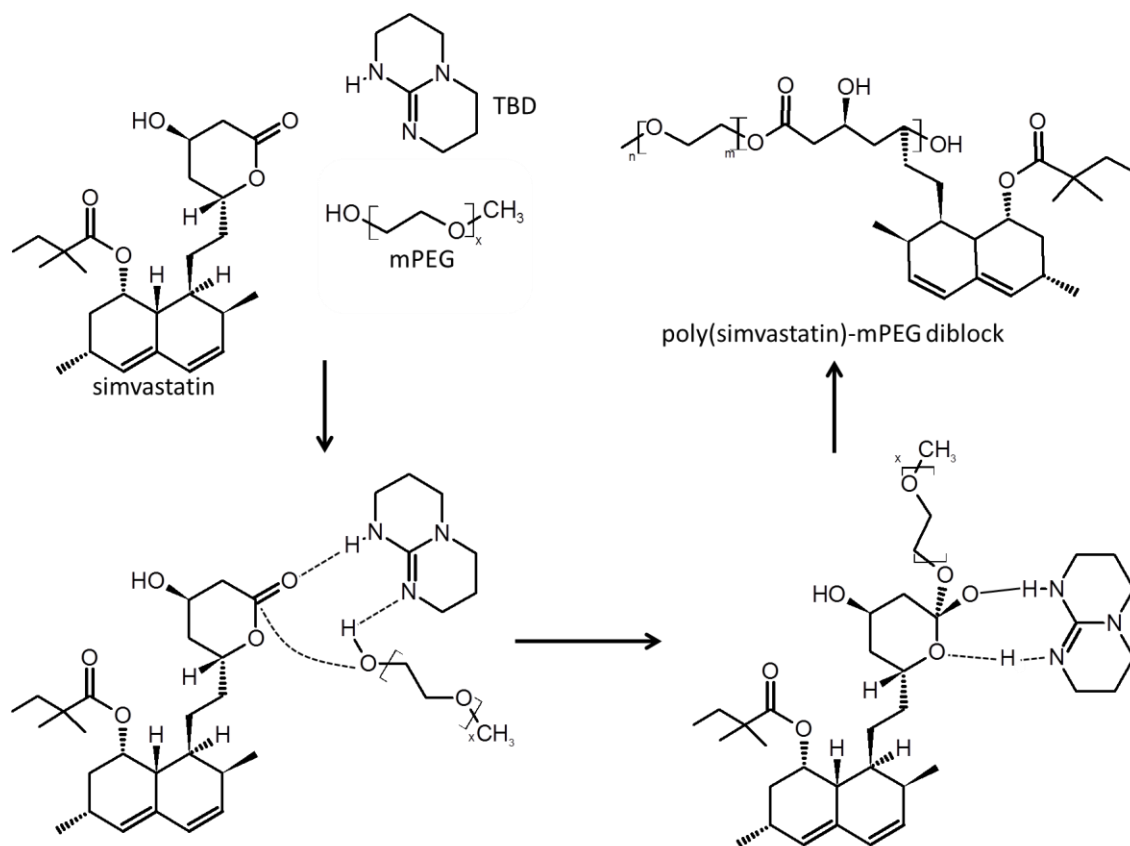


Figure 4.1. ROP mechanism using TBD catalyst via hydrogen bonding.

4.4.2 Stannous Octoate vs. TBD Catalyst Mediated Reactions

The mole percentages of simvastatin, intermediates, and copolymer throughout the reaction using stannous octoate or TBD as a catalyst are displayed in Figure 4.2. Within 24 hr, a decrease in simvastatin monomer was observed at a conversion rate of 0.052 hr^{-1} with 27.2% of simvastatin remaining when using TBD as a catalyst at $150 \text{ }^\circ\text{C}$. In contrast, stannous octoate did not lead to monomer conversion at this temperature. At

200 and 230 °C, however, stannous octoate catalyzed rapid conversion, at 0.179 and 0.351 hr⁻¹, respectively, 3 and 7 times the rate for TBD. Total monomer consumption was reached at 12 and 8 hr for the stannous octoate mediated reactions at 200 and 230 °C, respectively.

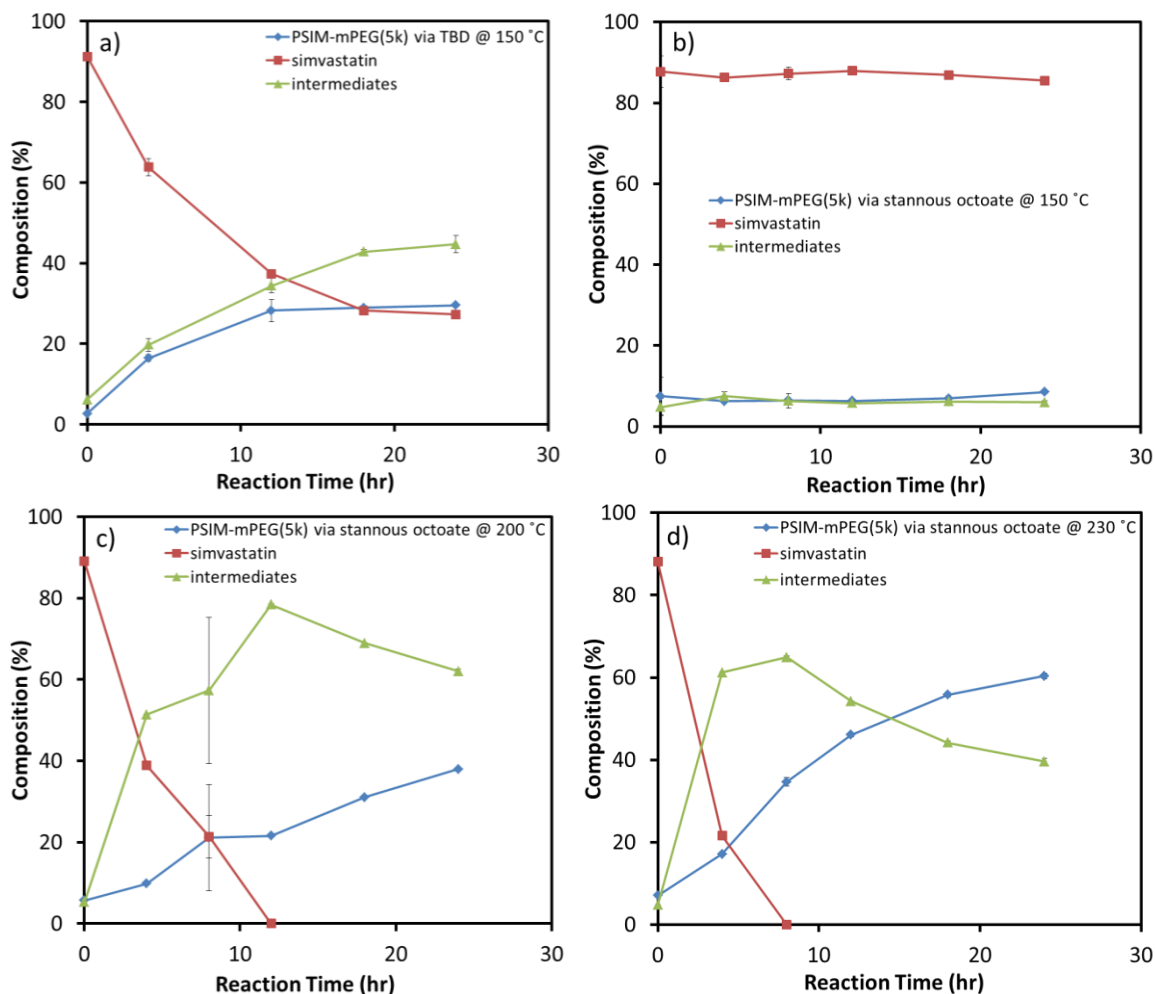


Figure 4.2 GPC measurements of the percentages of copolymer, intermediates, and simvastatin monomer throughout the reactions in the crude products of a) PSIM-mPEG(5k) synthesized via TBD at 150 °C, b) PSIM-mPEG(5k) synthesized via stannous at 150 °C, c) PSIM-mPEG(5k) synthesized via stannous at 200 °C, and d) PSIM-mPEG(5k) synthesized via stannous at 230 °C.

The degree of polymerization achieved by an ROP reaction is greatly influenced by the nature of the catalyst, cyclic monomer, or alcohol incorporated in the feed. Stannous octoate has the necessary electrophilic qualities possessed by its metal cation center, and it gains nucleophilic properties once formed into an alkoxide, becoming a stereoselective catalyst in the mediation of ROP. The newly formed tin alkoxide is subsequently attracted to the carbon of the lactone carbonyl group and cleaves the lactone ring of the monomer at the acyl bond, propagating the polymer chain via a pseudo-anionic coordination-insertion ROP mechanism. However, stannous octoate is a much larger molecule than TBD with a MW of 405 Da, three times that of TBD at 139 Da (Figure 4.3). After forming a complex with the alcohol, or 5 kDa mPEG, the resulting metal alkoxide complex becomes even larger.

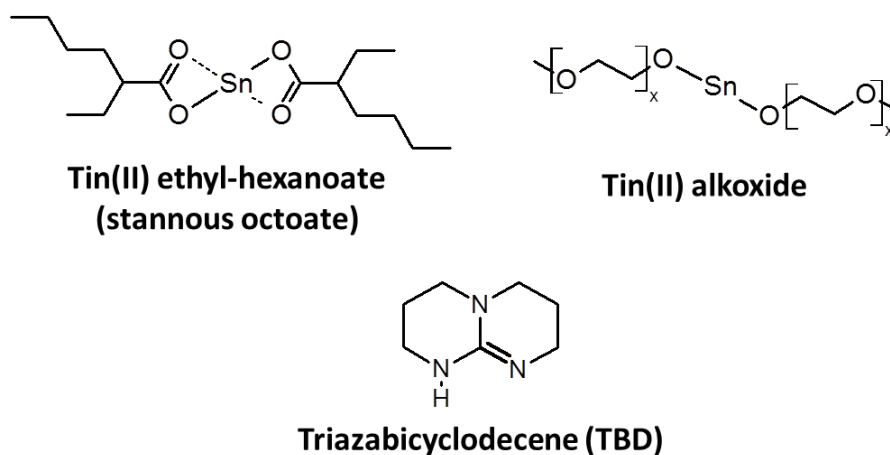


Figure 4.3 Structures of stannous octoate and TBD catalysts used in the ROP of PSIM.

TBD is highly basic (pK_a 26) and requires no cocatalyst, such as thiourea, in the ring-opening of cyclic esters, compared to some of its monocyclic phosphazene, amidine, and guanidine counterparts. The bicyclic structure of TBD also has two active nitrogen centers that allow for electrophilic and nucleophilic bifunctionality, activating simvastatin's lactone ring and the hydroxyl group of the mPEG initiator, respectively, via hydrogen bonding.^{161, 162} This bifunctionality removes a possible limiting step otherwise necessary for stannous octoate to form an alkoxide in order to initiate polymerization. These advantageous characteristics associated with the smaller and less sterically hindered structure may give TBD relatively heightened sensitivity, selectivity, and ease in mediating ROP with mPEG and simvastatin at a lower temperature. These characteristics may also explain why TBD was able to catalyze a ROP reaction of PSIM at 150 °C, where stannous octoate was unsuccessful. TBD-mediated reactions were also carried out at internal temperatures lower than 150 °C (results not shown). Those reactions, however, did not produce significant polymerization, showing that the window for polymerization is still small, but still with a lower temperature threshold than would be necessary for stannous octoate to polymerize simvastatin.

Monomer conversion increased with reaction temperature when catalyzed by stannous octoate. Even after total monomer consumption, however, the polymer composition in the crude product continued to increase as the relative percentage of intermediates declined, suggesting an addition of intermediate products to the copolymer structure after monomer consumption. This may be due to the secondary hydroxyl group on the simvastatin lactone ring acting as another reactive site, potentially forming

intermediates of dimers and small oligomers that are subsequently incorporated into the copolymer.

4.3.3 NMR and mass spectrometry of PSIM-mPEG (5k) via TBD

H-NMR was performed to further support the MW of PSIM-mPEG(5k) measured via GPC. As seen in the control of Figure 4.4a, the chemical shifts represented by r, s, and t (4.21, 3.71, and 3.48 ppm) represent mPEG within the mixture. Simvastatin was identified by the remaining chemical shifts within the spectrum. Seventeen simvastatin monomers were calculated to be incorporated into the PSIM-mPEG(5k) copolymer sample tested, leading to a MW of 12 kDa.

In the NMR control spectrum, the repeating ethylene oxide unit of mPEG is represented by the chemical shift at 3.71 ppm, and the hydroxyl and methyl oxide groups of the polymer block are represented by the 4.21 and 3.48 ppm chemical shifts, respectively. The disappearance of the 4.21 ppm chemical shift in the copolymer spectrum reflects incorporation of the mPEG hydroxyl moiety into the copolymer backbone after initiation. The absence or shift change of e and f, which represent the lactone ring (Figure 4.4a) in the copolymer spectrum reflect a change in the lactone structure or molecular environment as a result of ROP. The broadened peaks in Figure 4.4b indicate synthesis of a polymerized form of simvastatin. Broadening of the base of the peaks was observed between 5.38 to 6.05 ppm, with letters a through d representing more aromatic portions of the simvastatin monomers.

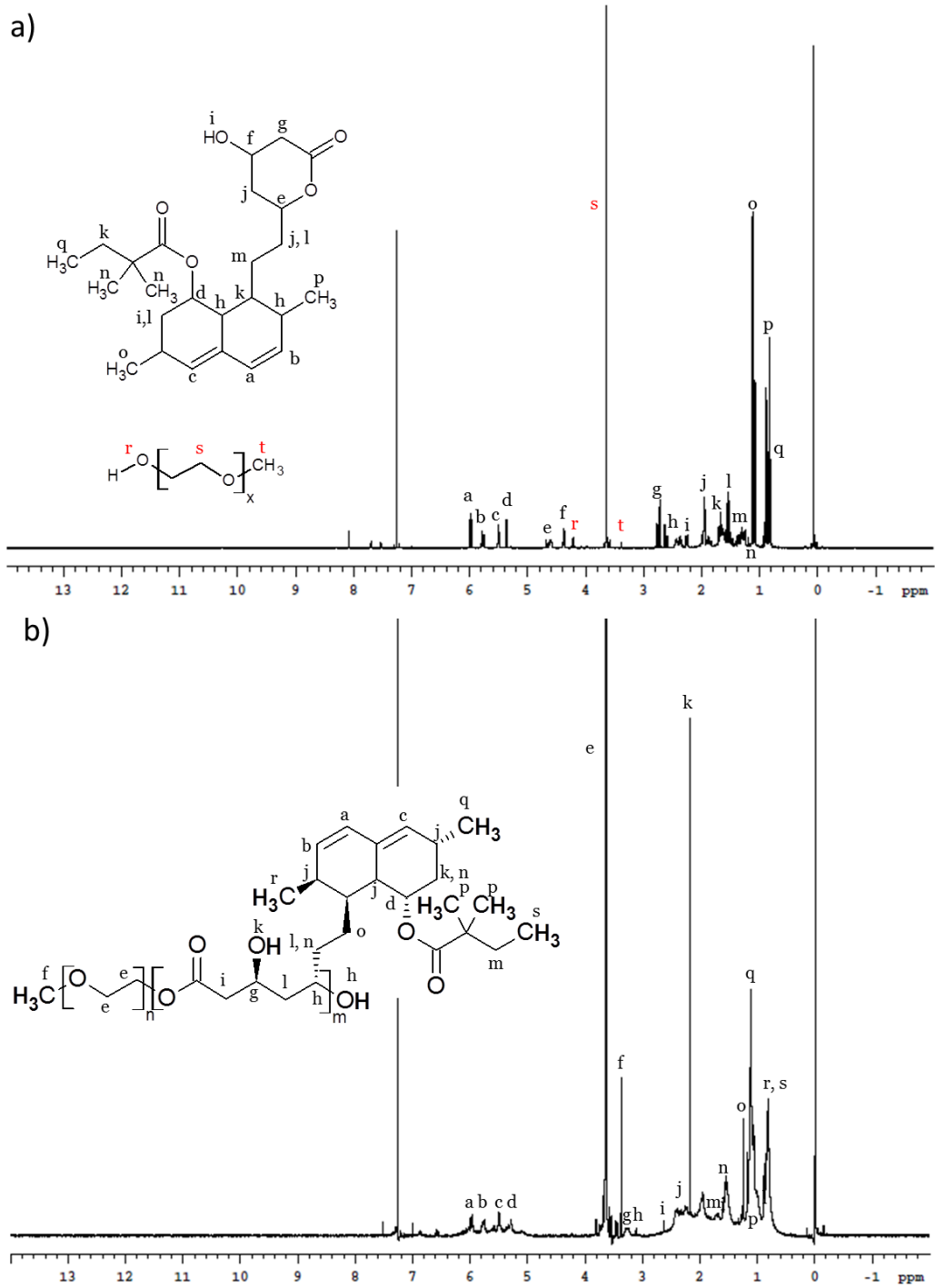


Figure 4.4 $^1\text{H-NMR}$ spectra of a) a 100:1 mixed control of simvastatin and mPEG and b) the PSIM-mPEG(5k) copolymer synthesized via TBD. Figure 3a was reproduced from Ref. 9 with permission from the Royal Society of Chemistry.

Figure 4.5 displays the mass-to-charge ratio (m/z) spectra of PSIM-mPEG(5k) degradation products. The inset in Figure 4.5a shows simvastatin represented by the parent ion of 441 m/z . The low MW degradation product spectrum (Figure 4.5a) contained multiple peaks close to that of simvastatin at 404, 422, 439, 457, and 480 m/z , but the intensities were low relative to the peak of highest abundance at 522 m/z . To the right of the most abundant species, a multitude of smaller peaks was seen, ranging from 540 to 957 m/z .

In the mass spectra of low MW degradation products, the 404 m/z peak represents fragmented simvastatin. The 422 to 480 m/z peaks, alongside the peak of highest relative abundance at 522 m/z , reflect open or closed-ring simvastatin in the presence of a combination of salt adducts remaining from the PBS (i.e., Na^+ , K^+ , and H^+) used to carry out polymer degradation. The alpha-cyano-4-hydroxycinnamic acid (CHCA) matrix (189 m/z) used in the analysis may also contribute to the m/z values. Peaks ranging from 540 to 957 m/z indicate the presence of simvastatin dimers and combined salt adducts or matrix in the degradation products.

In the spectrum of the higher MW degradation products (Figure 4.5b), a wide distribution was observed, with the highest relative abundance at 5561 m/z . The most prevalent peak was slightly higher than the theoretical average MW of the 5 kDa mPEG polymer used as an initiator in the synthesis of the PSIM-mPEG copolymer. The base of peaks representing the higher MW degradation products was broadened compared to the sharp and distinct peaks seen in the mPEG control (Figure 4b inset), indicating the varied distribution of complex ions present in this m/z range, possibly representing mPEG and mPEG with attached simvastatin monomer degradation products.

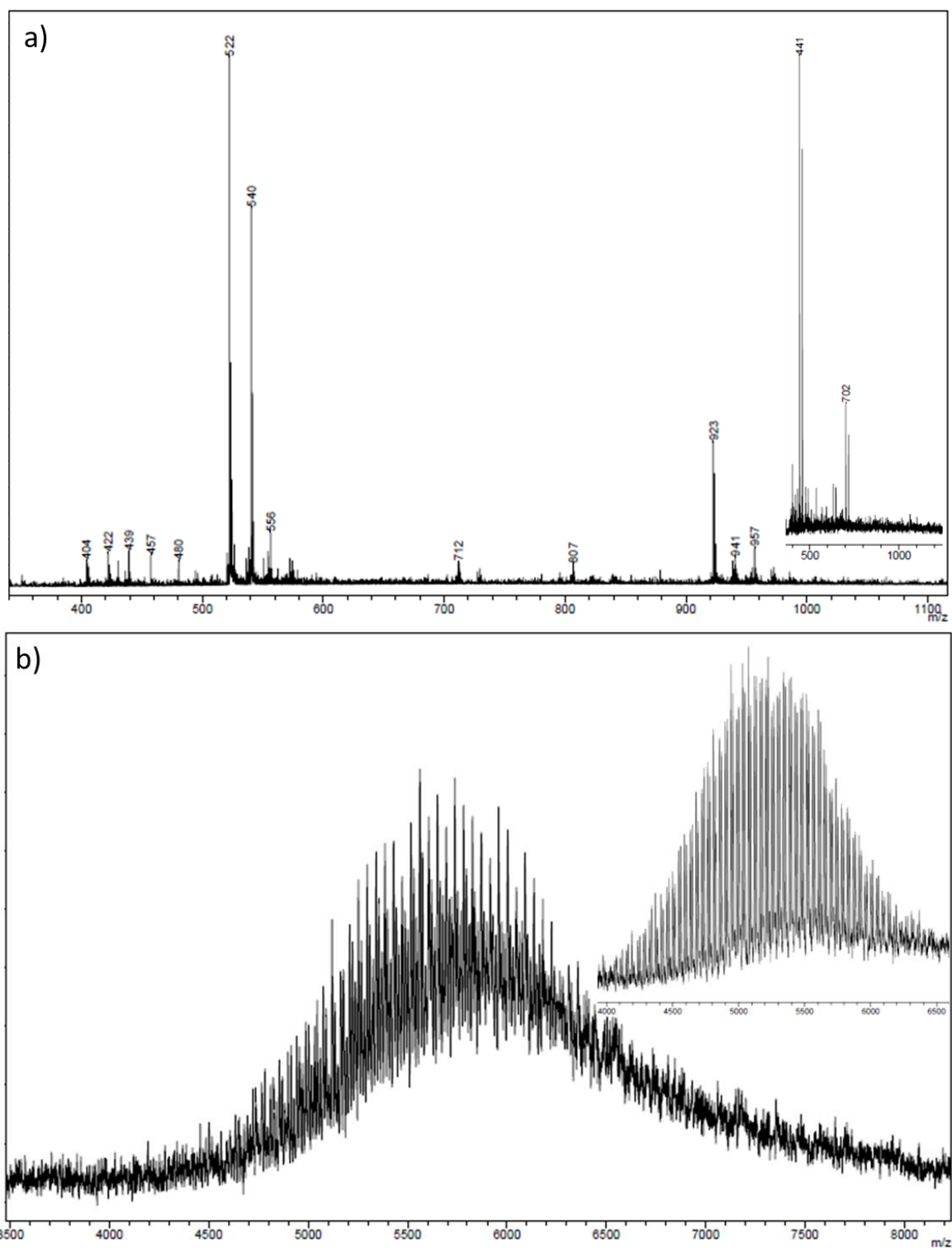


Figure 4.5 Mass spectra of a) low MW PSIM-mPEG(5k) degradation products compared to simvastatin control and b) high MW PSIM-mPEG(5k) degradation products compared to mPEG control. Insets of controls in Figure 2a and 2b were reproduced from Ref. 9 with permission from the Royal Society of Chemistry.

4.3.4 Poly(simvastatin) Copolymer Synthesis using Different mPEGs

Chromatograms of purified PSIM-mPEG copolymers initiated with 5k, 2k, or 550 Da mPEG and catalyzed via TBD are shown along with their respective reactants in Figure 4.6. The resulting weight-average MW of PSIM-mPEG(5k), PSIM-mPEG(2k), and PSIM-mPEG(550) copolymers synthesized were 15, 13, and 20 kDa, respectively, with polydispersity indexes (PDIs) of 2.1, 2.2 and 2.5, respectively. The mPEG initiators with theoretical MWs of 5 and 2 kDa were measured to have slightly higher MW values of 7.4 and 2.5 kDa via GPC, while the 550 Da mPEG and simvastatin registered lower MW values of 0.4 and 0.2 kDa, respectively. ROP reactions with 5k mPEG led to successful simvastatin polymerization when mediated by stannous octoate. With 2k and 550 Da mPEG, however, polymerization reactions were not successful when mediated by stannous octoate or other selected catalysts, such as lanthanum isopropoxide, aluminum isopropoxide, tin triflate, lipase B from *Candida antarctica*, HCl·EtO₂, potassium methoxide (KOMe), 1,3-dimesitylimidazol-2-ylidene (IMes), and diazabicycloundecene (DBU) under varied reaction conditions (results not shown).

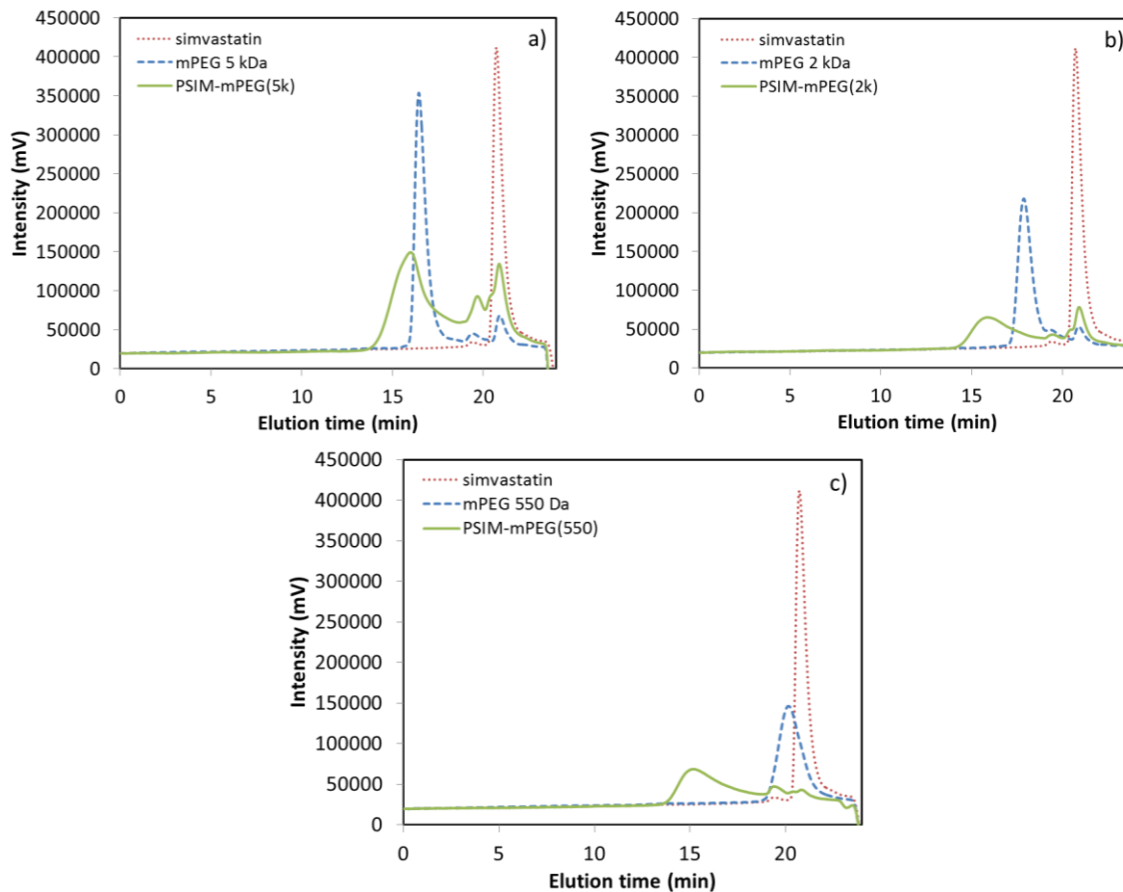


Figure 4.6 GPC chromatograms of poly(simvastatin) synthesized via TBD using a) 5kDa, b) 2kDa, and c) 550 Da mPEG initiators compared with reactants.

TBD successfully catalyzed the synthesis of PSIM-mPEG copolymers using 5k, 2k, and 550 Da mPEG as initiators at 150 °C in melt conditions, possibly as a result of high reactivity combined with less steric hindrance due to its small molecular size. The poor performance of stannous octoate in the same conditions possibly indicated steric hindrance between the catalyst and the simvastatin structure and hindered catalyst stereoselectivity.

4.3.5 Kinetics

Based on the copolymer and mPEG MWs measured via GPC, the PSIM copolymer initiated with the lowest MW mPEG had the highest percentage of simvastatin incorporated in the copolymer at 98%. PSIM-mPEG(2k) and PSIM-mPEG(5k) had 80 and 51% of drug incorporated, respectively. Percent yields of the three copolymers exhibited an opposite trend, however, with the 550 Da mPEG-initiated copolymer having the lowest yield, which increased as the MW of the mPEG block increased (Table 4.1). This trend may be due in part to the decreased solubility of mPEG in ether as its MW increases.

Table 4.1. GPC measurement of simvastatin and mPEG composition in copolymers

Copolymer	Molar ratio	Percent of sim in copolymer	# of sim monomers per mPEG initiator	Percent yield	Percent of mPEG in copolymer
PSIM-mPEG 5k	100:1	51	39	~17 to 30%	49
PSIM-mPEG 2k	100:1	80	52	~13%	20
PSIM-mPEG 550	100:2	98	96	~2%	2

The initial MWs measured for the three PSIM copolymers were significantly different ($p < 0.0001$) due to the MW differences of the mPEG initiators used for each reaction (Figure 4.7a). The MW of the PSIM-mPEG(5k) copolymer remained significantly greater than for the other two copolymers throughout the reaction

($p < 0.0001$). PSIM-mPEG(2k) also had a significantly greater MW than PSIM-mPEG(550) did after 12 and 18 hr ($p < 0.001$) and 24 hr ($p < 0.0001$).

The difference between the initial and highest weight-average MW reached throughout the reaction, which correlates with the number of simvastatin monomers attached, was greatest for the 550 Da mPEG initiator. This difference decreased as MW of the mPEG initiator increased. The trend was further reflected by the rates of polymerization throughout the 24 hr reaction period. Within the first 4 hr, the PSIM-mPEG(550) reaction had the greatest change in MW, increasing by 5 kDa and plateauing at approximately 6.1 kDa for the remainder of the reaction period. PSIM-mPEG(5k) had the smallest change in MW growth in the first 4 hr, and the slowest first-order polymerization rate of 0.021 h^{-1} for 18 hr before undergoing a MW decrease from 13.4 to 12.6 kDa. The PSIM-mPEG(2k) reaction showed a smaller 4 hr MW change and had a lower polymerization rate than PSIM-mPEG(5k) did, but its rate was higher than for the PSIM-mPEG(550) reaction. The total MW increase achieved was 6 kDa at a rate of 0.037 h^{-1} . From initial MWs of 0.67, 3, and 9 kDa, copolymer MWs of 5.8, 9, and 13 kDa were achieved for PSIM-mPEG(550), PSIM-mPEG(2k), and PSIM-mPEG(5k), respectively.

Although the differences in MW growth within the first 4 hr were not significant in Figure 4.7b, there was a noticeably greater change observed for the reaction initiated with a 100:10 ratio of simvastatin to 550 Da mPEG. Unexpectedly, reactions with the smaller amounts of 550 Da mPEG (100:1 and 100:2 molar ratios of simvastatin to mPEG) achieved lower MWs after 4 hr ($p < 0.0001$ and $p < 0.001$, respectively) compared to the feed containing the most mPEG (100:10 sim to mPEG). The MW obtained from

the 100:1 molar ratio feed remained significantly lower than the others after 12 (p<0.001), 18, and 24 hr (p<0.0001). The 100:2 molar ratio feed generated a significantly lower MW than only the 100:10 feed after 4 hr (p<0.001).

The 100:1 and 100:10 sim to 550 Da mPEG molar ratios with the smallest amount of catalyst resulted in the greatest MW growth (Figure 4.7c) when comparing the effects of different molar ratios and weight percentages of TBD. MW growth was statistically insignificant in the 100:10 melt with 0.2 wt% TBD during the first 4 hr. Despite the initial lag, the polymerization rate during the first 12 hr was 0.221 hr⁻¹, leading to an 8.3 kDa crude copolymer. In the last 12 hr, the rate decreased to 0.008 hr⁻¹, resulting in a 9.1 kDa crude copolymer product formed. In the 100:1 melt with 0.2 wt% TBD, a 5.1 kDa MW was formed during the first 4 hr, followed by a 0.026 h⁻¹ rate for the remainder of the reaction to yield a 9.9 kDa polymer. MW differences between the two ratios at 0.2 wt% were insignificant after 4 hr. Reactions with 1 wt% TBD were completed within 4 hr. Upon completion, however, MWs plateaued at lower values than their counterparts did with 0.2 wt% TBD, which were 8.4 and 6.1 kDa for the 100:10 and 100:1 molar ratio feeds, respectively. The final MWs were 8.5 and 5.8 kDa for the 100:10 and 100:1 molar ratio feeds, respectively. The 100:2 melt with 1 wt% TBD reached a MW of 6.9 kDa within the first 4 hr and had a first-order rate of 0.011 h⁻¹ for the rest of the reaction period, resulting in an 8.5 kDa crude product.

Due to the low yield of PSIM-mPEG(550), the amount of catalyst and molar ratios of monomer to initiator were modified to improve yield and the degree of polymerization. The kinetics of the PSIM-mPEG(2k) and PSIM-mPEG(5k) copolymers were also monitored over a 24 hr period. The slower rate of polymerization as the MW

of the mPEG initiator increased suggests that the larger mPEG molecules provided greater steric hindrance. The computational analysis of Chuma *et al.* showed that alcohols with bulky, more sterically hindering side groups increase the potential for destabilizing the transition state needed to initiate and continue polymerization.¹⁶⁰ Although mPEG does not have bulky side groups, this reasoning could apply to the mPEG size and resulting conformations it assumes in the melt.

The majority of MW growth of PSIM-mPEG(550) synthesized with 1 wt% TBD was complete within 4 hr, which plateaued for the remainder of the 24 hr reaction period. This may be explained by the rapidly reactive nature of TBD. At 0.1 mol%, TBD was shown to fully polymerize lactic acid into PLA in 1 min.⁵⁴ Also, a 6 d polymerization reaction with cyclic trimethylene carbonate, carried out by MTBD, a guanidine equivalent of TBD, was shown to be complete in a significantly shorter time of 15 min when mediated by TBD.^{162, 163} TBD is known to be the most basic of its “superbase” counterparts, resulting in polymerization rates that almost equal those catalyzed by N-heterocyclic carbenes, which can take seconds to complete a reaction. Future potential avenues could investigate the kinetics of TBD-mediated PSIM copolymer reactions in a shorter time period for more precise polymerization rates within the 4 hr period.

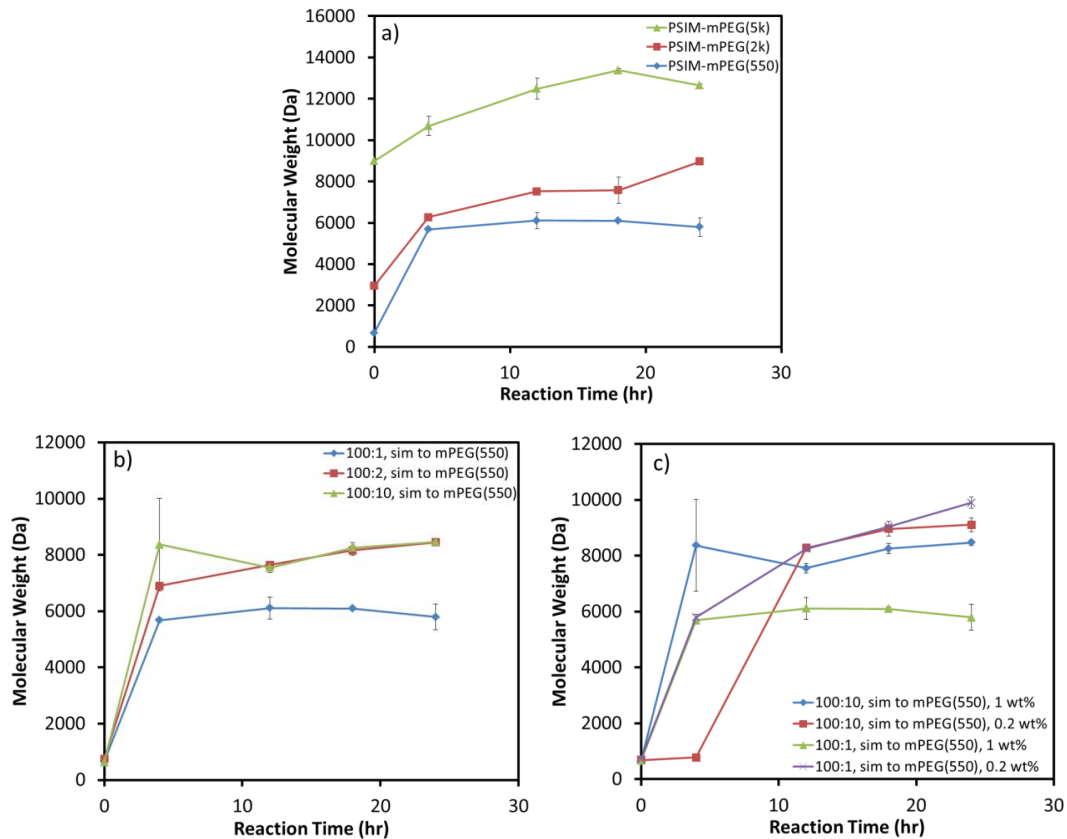


Figure 4.7 MW growth kinetics for PSIM-mPEG copolymers synthesized with: a) different mPEG MWs with 1 wt% TBD, b) different molar ratios of simvastatin to mPEG (550 Da), and c) two different amounts of catalyst at two different molar ratios.

Opposing relationships between catalyst concentration and molecular weight of various polymers have been presented in literature.^{156, 164, 165} One of these investigations includes the analysis of trioxane monomer to p-chlorophenyldiazonium hexafluorophosphate catalyst molar ratios ranging from 5,000 to 20,000. At ratios up to 8,000, the resulting polymer molecular weight was inversely proportional to catalyst concentration, reaching maximum MW values. As the catalyst concentration continued to decrease with monomer to catalyst ratios between 8,000 and 20,000, the relationship to

polymer molecular weight became directly proportional.¹⁶⁴ A range of different initiator concentrations tested with trioxane had no effect on the resulting poly(trioxane) MW in melt conditions, but the same range explored in solution caused a decrease in MW as the initiator concentration increased.¹⁶⁵ The type of catalyst used can also influence the relationship between catalyst concentration and MW. Increasing concentrations of catalysts such as sulfuric acid and titanium (IV) butylate were shown to mediate synthesis of lower molecular weight poly(lactic acid) during polycondensation of L-lactide.¹⁵⁶ A similar inverse relationship was seen in the present studies where polymerization rates and resulting MWs of PSIM-mPEG(550) reactions increased as the TBD catalyst weight percentage decreased. This relationship may result from the chosen catalyst to reactant ratios leading to reactions above or below a specific energy threshold, where the relationship between simvastatin monomer and TBD catalyst is inversely proportional. Mechanistically, increasing the catalyst content between 0.2 and 1 wt% may contribute to an increase of chain transfer reactions mediated by the catalyst, where the hydroxyl terminal end group of a propagating chain, activated by the TBD catalyst, may attack the ester group within the backbone of another neighboring or growing chain.¹⁶⁶ This action can lead to a decrease in MW of the polymer chain and, ultimately, a reduced weight-average MW.

An increased monomer to initiator ratio typically results in greater MW because fewer initiation sites are present, which leads to longer polymer chains at high monomer conversion. An example of this occurrence is seen with the ROP of ϵ -caprolactone using a calcium methoxide catalyst, which increased the resulting poly(ϵ -caprolactone) MW from 5 to 11.4 kDa at 100% conversion as monomer/initiator ratio increased from 20 to

100.¹⁶⁷ While this trend was maintained in PSIM-mPEG(550) crude products with 0.2 wt% TBD, the resulting MW decreased as the initial simvastatin to 550 Da mPEG initiator ratio increased using 1 wt% TBD. This unexpected latter observation may be influenced by low monomer conversion in the crude product for the most hydrophobic copolymer, which partially explains its low yield. Increasing the initiator present in the melt (i.e., lowering the monomer to initiator ratio) provides more initiator sites for potential polymer propagation. Even though this would lead to shorter chains or a lower MW polymer at nearly 100% conversion, the crude products show monomer conversion is still far from complete. At this stage, a larger number of chains present compared to the remaining monomer in the crude may exert a greater influence on the overall average MW increase seen in the crude products as the 550 Da mPEG initiator amount increased in the feed.

Transesterification reactions and depolymerization with extended time may explain the slight decreases in MW nearing the end of reaction for PSIM-mPEG(5k) and PSIM-mPEG(550) with 1wt% TBD. TBD and similar organocatalysts show significantly greater binding affinity to cyclic lactones than acyclic esters, which contributes to transesterification reactions and may contribute to the low PDIs measured in the crude products after 24 hr.¹⁶²

4.3.6 Crude vs Purified Polymers

Figure 4.8 shows chromatograms of the PSIM-mPEG(550) copolymer before and after purification via DCM/cold ether. The crude copolymer in the kinetic reactions reached a maximum of MW of 6-7 kDa in contrast to the purified 19-20 kDa copolymer noted earlier. After precipitation, the purified product showed a peak that noticeably

shifted left to an elution time of 15.1 min compared to the crude peak, which remained at 16.7 min. The measured weight-average MW of the polymer peak in the crude product was 9 kDa, while the purified form was 21 kDa.

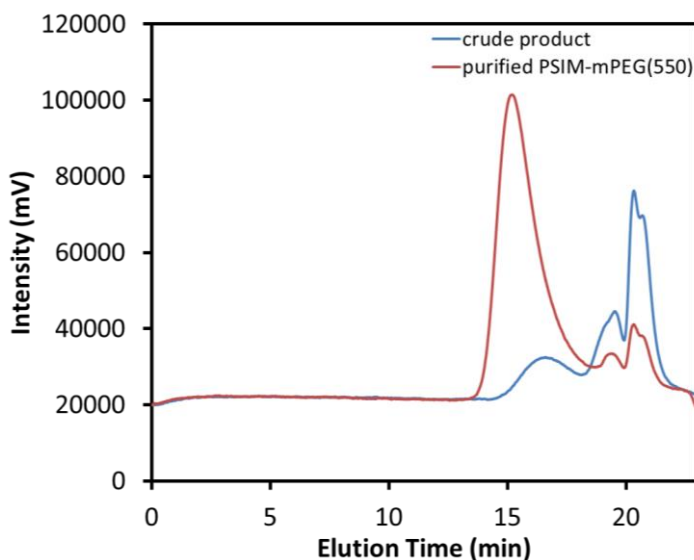


Figure 4.8 Chromatograms of PSIM-mPEG(550) before and after purification.

The significant difference in MW distribution between the crude PSIM-mPEG(550) (approximately 6 kDa) and the purified copolymer (20 kDa) was due to the large amount of low MW products remaining in the crude samples decreasing the weight average MW. Also, the high MW purified product represented only approximately 2% of the crude product. The PSIM copolymer yield increased as the MW of the mPEG incorporated into the feed increased. Analysis of purified samples may have resulted in a different MW trend between the copolymers, but the small amounts of crude product collected from the microscales reactions (5 to 10 mg) made purification impractical.

For macroscale reactions, investigating new solvent/anti-solvent phase precipitation systems may help to improve the yield of the PSIM-mPEG(550) copolymer.

The increased hydrophobicity of the copolymer may be influencing its solubility in the DCM/diethyl ether combination used for purifying PSIM-mPEG(5k) and PSIM-mPEG(2k), thereby affecting its yield.

4.3.7 Degradation

A degradation study was conducted to compare mass loss and cumulative amounts of simvastatin released from the PSIM copolymers (Figure 4.9). After 6 wk, an average total mass loss of 28, 29, and 7% was observed, from which cumulative amounts of 12, 5.2, and 0 μg of simvastatin were released from PSIM-mPEG(5k), PSIM-mPEG(2k), and PSIM-mPEG(550), respectively. While mass loss for the 5 kDa and 2 kDa mPEG-initiated PSIM copolymers was similar, both exhibited significantly greater mass loss compared to PSIM-mPEG(550), the most hydrophobic copolymer ($p < 0.05$). PSIM-mPEG(5k) and PSIM-mPEG(2k) each exhibited differing rates of simvastatin release in later stages of degradation compared to the rates seen initially. From 12 hr up to 10 days, 0.578 and 0.230 $\mu\text{g}/\text{d}$ of simvastatin was released from PSIM-mPEG(5k) and PSIM-mPEG(2k), respectively, which changed to slower rates of 0.124 and 0.052 $\mu\text{g}/\text{d}$, respectively, for the remainder of the 44 d study. In the first 12 hr, a burst release of 1.6 and 1.1 μg was measured from the two copolymers, respectively. PSIM-mPEG(5k) released a significantly greater amount of simvastatin than PSIM-mPEG(550) did during the 44 d period ($p < 0.0001$) and PSIM-mPEG(2k) on day 3 ($p < 0.001$) and the remainder of the study ($p < 0.0001$). Simvastatin release from the PSIM-mPEG(550) copolymer was negligible over the 44 d period. From observation, PSIM-mPEG(5k) experienced the

most erosion, which began the earliest. PSIM-mPEG(550) remained the most intact with breakage observed much later during the degradation period.

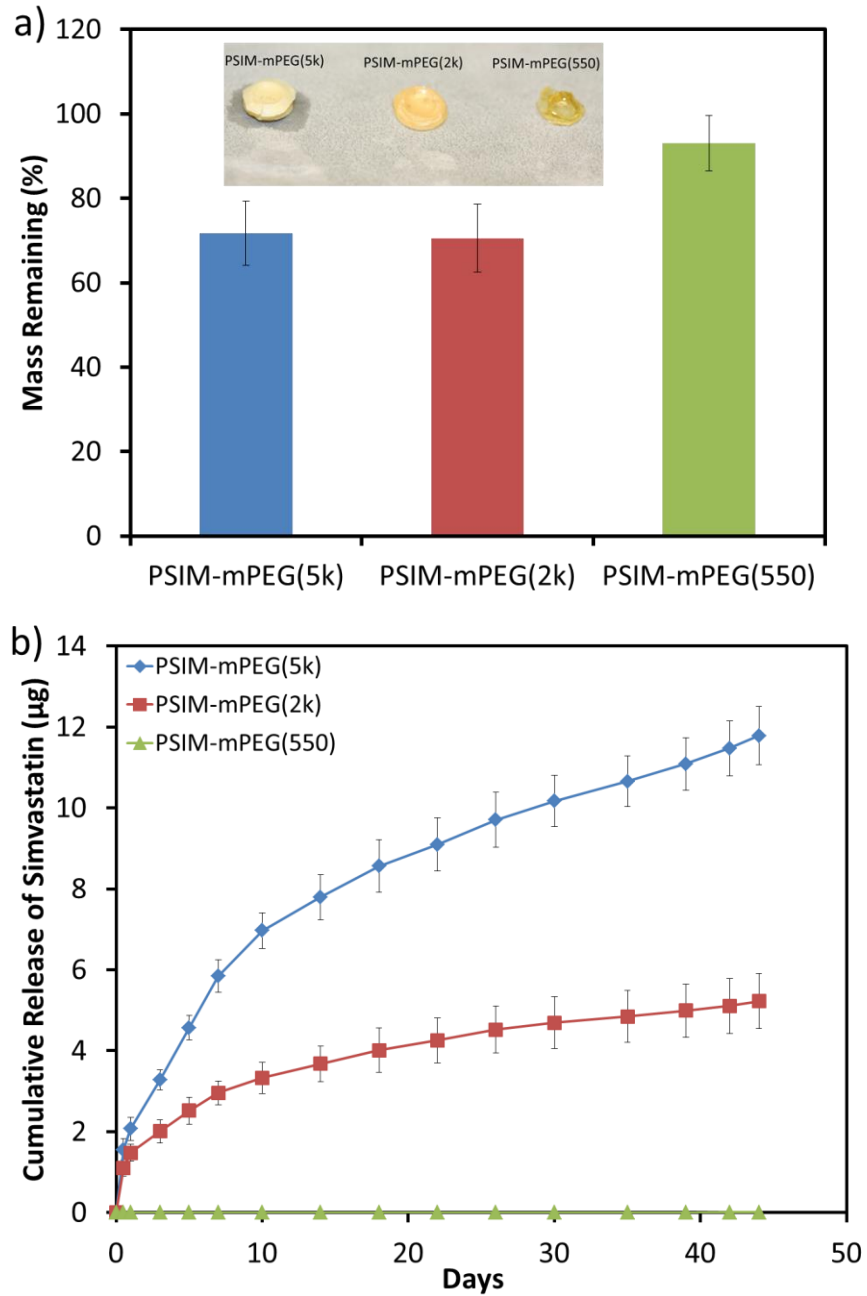


Figure 4.9 Degradation of PSIM-mPEG(5k, 2k, and 550) diblock copolymers showing a) final mass remaining and b) resulting simvastatin release.

Degradation of poly(simvastatin) is caused by cleavage of hydrolytically labile ester bonds throughout the polymer chain, ultimately releasing molecules of simvastatin. The degradation rate of poly(simvastatin) can potentially be tuned by modifying the composition of the diblock copolymer. While simvastatin, and subsequently its respective polymerized form, is hydrophobic, mPEG is hydrophilic, giving the resulting PSIM-mPEG copolymer an amphiphilic nature. The higher the MW of mPEG incorporated into the diblock copolymer, the more hydrophilic the resulting copolymer becomes. Generally, the more hydrophilic the copolymer, the faster it should degrade in a physiological environment. While PSIM-mPEG(2k) had a slightly higher average mass loss than PSIM-mPEG(5k), this difference was insignificant.

The order of increasing mass loss during degradation of the PSIM copolymers correlated with cumulative release of simvastatin. An increasing degradation rate with increasing hydrophilicity was more evident when comparing the amount of simvastatin released. PSIM-mPEG(5k) released 2.3 times more simvastatin than did the less hydrophilic PSIM-mPEG(2k) copolymer, with both releasing significantly more than PSIM-mPEG(550), which experienced insignificant degradation. Concentrations of 0.3-2.4 $\mu\text{g/ml}$, 0.07-0.8 $\mu\text{g/ml}$, and 0-0.01 $\mu\text{g/ml}$ were reached for PSIM-mPEG(5k), PSIM-mPEG(2k), and PSIM-mPEG(550), respectively. Concentrations from PSIM-mPEG(5k) were within and above the range reported for simvastatin to have therapeutic effects *in vitro*, while the range for PSIM-mPEG(2k) was at the bottom and slightly below this window¹⁶⁸. Note, however, the small size (10-15 mg) of the samples; the total amount of simvastatin release can be adjusted via the mass of copolymer used. The negligible amount of simvastatin released from PSIM-mPEG(550), the most hydrophobic of the

PSIM copolymers, during the 8 wk time period may be due to hydrophobic interactions between the PSIM block within the copolymer matrix and potentially free simvastatin trapped within the matrix. Both are extremely hydrophobic, which would lead to a considerably slow rate of simvastatin release from the matrix into the aqueous medium, as seen by similar drugs incorporated in hydrophobic block copolymer delivery systems.¹⁶⁹ A loss of other degradation products, such as mPEG, simvastatin oligomers, or mPEG with limited simvastatin monomers attached, most likely contributed to the significantly greater total mass loss than simvastatin released. Within a 44 d degradation period, the PSIM-mPEG(5k) copolymer synthesized via TBD lost twice as much mass than did the same copolymer synthesized via stannous octoate in a previous study.¹⁵⁹ The comparison may indicate a greater amount of side reactions leading to less degradable byproducts formed in the stannous octoate mediated reaction as a result of being conducted at a higher temperature of 230 °C.

4.4 Conclusions

Triazabicyclodecene, a highly reactive organocatalyst, was able to mediate the ROP of poly(simvastatin) diblock copolymer using different MW mPEGs at a lower reaction temperature than the previously used stannous octoate catalyst. This provides the advantage of modifying hydrophilicity or hydrophobicity of the biomaterial that, in turn, alters degradation rate for therapeutic treatments of different timescales. The potential to polymerize simvastatin at a lower temperature also decreases the incidence of side reactions that generate undesirable byproducts that interfere with degradation of the polymeric biomaterial. Lower reaction or processing temperatures would also be more energy- and cost-efficient at an industrial manufacturing scale. The resulting hydrophilic

copolymer synthesized via TBD was capable of losing significantly more mass within the same time period than the same copolymer synthesized via stannous octoate. Simvastatin release was modified as a result of using different MW mPEG initiators for synthesis. Synthesizing and developing a poly(simvastatin)-mPEG diblock copolymer with tunable degradation properties is desirable for tissue therapeutic applications.

Ch. 5 Tuning Degradation and Mechanical Properties of Poly(ethylene glycol) – Poly(simvastatin)-based Diblock copolymer blends

This chapter was reproduced from a manuscript in preparation, “Asafo-Adjei T.A., T.D. Dziubla, D.A. Puleo, Tuning Degradation and Mechanical Properties of Poly(ethylene glycol) – Poly(simvastatin)-based Diblock copolymer blends, (2017).”

5.1 Introduction

Polymeric biomaterials are frequently used for drug delivery applications due to the ability to tune the time-scale of polymer degradation to that of therapeutic treatment. By changing comonomer or monomer to initiator ratios, blending with other polymers, conjugating hydrophilic or hydrophobic blocks to the polymer, or by modifying the end-group, architecture, or molecular weight, one can substantially alter degradation rate.¹⁷⁰⁻
¹⁷⁴ Poly(lactic-co-glycolic acid) (PLGA), poly(lactic acid) (PLA), and poly(ϵ -caprolactone) (PCL) are biocompatible polyesters widely used as drug delivery vehicles that benefit from their tunable characteristics.^{25, 175, 176} Examples of FDA-approved products include Arestin[®], Respiredal[®], Consta[™], Trelstar[®] Depot, and Sandostatin LAR[®] Depot, which release minocycline, resperidone, triptorelin, pamoate, and octreotide acetate for periodontal disease, psychosis, prostate cancer, and acromegaly, respectively.¹⁷⁷ These diverse PLGA microparticle system therapeutics aim to circumvent the disadvantages of their oral administration, which include frequent dosage due to insufficient bioavailability, burst drug release, and toxic effects.¹⁷⁸ In addition, aliphatic polyester carriers in drug delivery serve to protect drugs against premature degradation, extending their half-life in the body to increase bioavailability of these drugs

as opposed to forms of oral administration. In addition, specific polyesters, such as PCL, degrade extremely slow, providing low dose, yet sustained, drug release.

While polymers that degrade in weeks to months are desirable for bone healing applications, the period of polymer degradation exhibited by polymers such as PCL may extend beyond the necessary period of treatment, impeding rather than aiding the healing process.¹⁷⁹ Furthermore, the associated slow rate of drug release may be therapeutically ineffective. As a result, copolymerization with poly(ethylene glycol) (PEG), a hydrophilic macromolecule, has been investigated to accelerate the degradation rate of hydrophobic and crystalline polyesters, such as PCL.¹⁸⁰ PEG-PCL block copolymers have been used as *in situ* gels, porous scaffolds, and in collagen/hydroxyapatite/hydrogel composites for bone tissue regeneration.^{179, 181, 182} Past investigations have also controlled degradation of relatively less hydrophobic and more amorphous PLA and PLGA polymers by copolymerizing with PEG to use as composite scaffolds, micro- and nanoparticle systems for tissue healing, anti-cancer and gene therapy, and other targeted drug delivery applications.^{65, 183, 184} Blending polyesters into different polymers potentially combines the desirable physical properties of the individual polymers. For example, Tsuji *et al.* reported that blending a minimal amount of PCL with poly(D,L-lactic acid) (PDLLA) significantly enhanced elongation before failure, as well as the Young's modulus of the blend, with the opposite effect seen when the same amount of PDLLA was added to PCL.¹⁸⁵

To further combat the disadvantages of high burst release and insufficient drug release, advanced drug delivery systems include polymer chains consisting of repeating monomeric units of the drug, such as aspirin, poly(morphine), poly(trolox ester), and

curcumin polymers, providing sustained and pseudo-zero order release for select systems.^{42, 186-188} These polydrugs include the previously reported synthesis of polymerized simvastatin.¹⁵⁹ Most well-known for regulating cholesterol, simvastatin also has osteogenic, angiogenic and anti-inflammatory properties desirable for tissue regeneration.^{120-122, 127}

While the weight percentage of simvastatin in poly(ethylene glycol)-*block*-poly(simvastatin) (PSIM) can be controlled by the drug to initiator ratio, the hydrophobic nature of the poly(simvastatin) block results in slow polymer degradation even following copolymerization with mPEG. Tailorable properties of the block would be more advantageous for regenerative drug delivery applications. Thus, the objective of the present studies was to investigate the effects of blending poly(ethylene glycol)-*block*-poly(lactic acid) (PLA) copolymers on the degradation and structural properties of PSIM.

5.2 Experimental

5.2.1 Materials

Simvastatin and D,L-lactide were purchased from Haorui Pharma-Chem (Edison, NJ) and Alfa Aesar, respectively. Monomethyl ether poly(ethylene glycol) (mPEG), triazabicyclodecene (TBD), tin (II) ethyl-hexanoate (stannous octoate), carboxyl esterase from porcine liver, anhydrous toluene, anhydrous diethyl ether, dichloromethane (DCM), ethanol (EtOH) and an HMG-CoA Reductase kit were purchased from Sigma-Aldrich (product CS1090; St. Louis, MO). Tetrahydrofuran (THF) stabilized with 3,5-di-tert-butyl-4-hydroxytoluene (BHT) and acetonitrile (ACN) were purchased from Pharmco-Aaper (Shelbyville, KY).

5.2.2 Methods

5.2.2.1 Poly(ethylene glycol)-*block*-poly(simvastatin) synthesis via TBD. Macroscale reactions (3 g) were conducted to synthesize copolymers using simvastatin as the monomer and mPEG (550, 2000, or 5000 Da) as initiator at a molar ratio of 100 to 1. Within a round bottom flask immersed in a silicone oil bath, simvastatin and mPEG were dried at 130 °C for 1 hr under a continuous flow of nitrogen gas. The temperature was increased to 150 °C for an additional hour before adding 1 wt% of TBD to the homogeneous melt. Each reaction ran for 24 hr. The reaction procedure and mechanism of copolymer polymerization via a metal catalyst, stannous octoate, has been previously studied.¹⁵⁹

5.2.2.2 Poly(ethylene glycol)-*block*-poly(lactic acid) Synthesis via Stannous Octoate. Macroscale reactions were conducted (5g) using D,L-lactide and mPEG (550, 2000, or 5000 Da) at a molar ratio of 100:1 monomer to initiator. Components were mixed and dried at 140 °C for 1 hr under a continuous nitrogen gas purge. The temperature was decreased to 120 °C for an additional hour before 1 wt% of stannous octoate dissolved in toluene was added to the melt. Each reaction ran for 6 h.¹⁸⁹

5.2.2.3 Purification. Crude PSIM copolymers using 5000, 2000, or 550 Da mPEG (PSIM-mPEG(5k), (2k), or (550)) and the PLA copolymers were purified by dissolving the crude products in DCM and pipetting the polymer solution into excess cold diethyl ether as the anti-solvent. The purified products were isolated via vacuum filtration.

5.2.2.4 Gel Permeation Chromatography (GPC). A Shimadzu Prominence LC-20 AB HPLC system with a waters 2410 refractive index detector was used to measure the MW of the copolymers synthesized. Two 300 x 7.5 mm, 3 μ m particle size ResiPore columns (Agilent Technologies) in series were used for sample separation. Samples were injected using THF as the eluent at a 1.0 ml/min flow rate. Standard curves were prepared using polystyrene standards ranging from 162 Da to 483 kDa.

5.2.2.5 Film Formulation. Purified PLA-mPEG with block components of 5000, 2000, or 550 Da mPEG (PLA-mPEG(5k), (2k) or (550)) and PSIM-mPEG(5k) were dissolved in DCM at 700 μ g/ml for a viscous solution. Each PLA-mPEG copolymer was blended with PSIM-mPEG(5k) at 20 wt%, and labelled 80:20 PSIM(5k):PLA(5k), 80:20 PSIM(5k):PLA(2k), and 80:20 PSIM(5k):PLA(2k), respectively. The PSIM-mPEG(5k) and PLA-mPEG(5k) block copolymers were also blended at a 60:40 weight ratio (60:40 PSIM(5k):PLA(5k)), respectively. The mixture was also dissolved in DCM at 70 wt% and vortexed into a homogeneous mixture before droplets were pipetted onto a Teflon sheet. Discs were dried overnight.

5.2.2.6 *In vitro* Degradation. A destructive mass loss study was conducted with each of the purified copolymers and blended copolymers. After recording initial mass, each copolymer disk was gently shaken at 37 °C in 1.5 ml of phosphate-buffered saline (PBS), pH 7.4, for 60 d. Additionally, disks of the same polymer blends were shaken in 1.5 ml of 0.1% porcine liver carboxyesterase^{190, 191} in PBS at 37 °C for 60 d. At 0.5, 1, 3, 7, 14, 42, and 60 d, three film samples from each copolymer group were withdrawn and dried overnight to determine mass loss. After the first day, where supernatant was collected

every 12 hr, PBS was replaced every 2-3 days the first week, followed by every 3-5 days for the remainder of the 60 d period.

5.2.2.7 High Performance Liquid Chromatography (HPLC). Simvastatin concentrations in release supernatants were measured using a Hitachi Primaide system equipped with a Kinetix Luna C18 column (150 x 4.60 mm, 5 μ m particle size; Phenomenex). Acetonitrile and water with 0.1 wt% trifluoroacetic acid (70:30 v/v) was used as the mobile phase, and UV absorbance was measured at 240 nm.

5.2.2.8 Mechanical Testing. A Teflon mold was used to form cylindrical samples with a 2:1 height to diameter ratio (5 by 2.5 mm). Samples were made from PSIM-mPEG(5k), the PLA-mPEG copolymers, and the copolymer blends. Using a Bose Electroforce 3300 mechanical testing instrument, uniaxial compression tests were run at 0.05 mm/s until a displacement of 2.5 mm was reached.¹⁹² Compressive strength and modulus were calculated from the load-displacement data and physical dimensions of the samples. When measuring compressive strength, more crystalline polymers were measured at yield, which was also peak strength. For the semi-crystalline polymers, strength was measured just above yield and before the plastic region of the load vs. deformation curve. The modulus was determined from the slope of the initial linear elastic region of each curve.

5.2.2.9 X-Ray Diffraction (XRD). Powder and film samples, 10 to 20 mg each, were analyzed using a Siemens D500 Diffractometer to determine the relative of crystallinity of the PSIM and PLA copolymers and their blends. A 2θ angle range of 10 to 50 $^{\circ}$ was used for measurement at a rate of 1 $^{\circ}$ /min. Diffraction was performed at 30 mA and 40 kV. A VisxDACO software interface was used to obtain and analyze data. Relative

percentage crystallinity was calculated by measuring the total area of crystalline peaks to the total area of both crystalline and amorphous peaks in the diffractogram.

5.2.2.10 Biochemical Activity of Degradation Products. The activity of PSIM and PLA degradation products in supernatants was tested by evaluating inhibitory activity on 3-hydroxy-3-methylglutaryl coenzyme A (HMG CoA) reductase. A commercially available assay kit was used to monitor oxidation of NADPH, which is dependent on the conversion of HMG CoA to mevalonate.¹⁹³⁻¹⁹⁵ The optical density of each reaction sample was immediately read at 340 nm using a PowerWave HT microplate spectrophotometer with a Gen5 analysis software interface.

5.2.2.11 Statistical Analysis. Two-way analysis of variance with a Tukey-Kramer post-test was performed to test the effects of the blending ratio on the degradation rate and release of simvastatin from PSIM(5k). One-way analysis of variance was used to compare means of the mechanical properties and HMG CoA reductase activity. A value of $p \leq 0.05$ was deemed statistically significant. Data are presented as mean and standard deviation.

5.3 Results

The starting MW of the PSIM-mPEG(5k), PLA-mPEG(5k), PLA-mPEG(2k), and PLA-mPEG(550) copolymers and blends degraded in the mass loss study was 13, 20, 16, and 19 kDa, respectively. Figure 5.1 displays the mass loss and subsequent release of simvastatin from the copolymer and blended films. Within the first 24 hr, significant mass loss was observed, with 25, 37, 21, 21, and 20% initial loss from PSIM-mPEG(5k), 60:40 PSIM(5k):PLA(5k), 80:20 PSIM(5k):PLA(5k), 80:20 PSIM(5k):PLA(2k), and

80:20 PSIM(5k):PLA(2k), respectively. The PLA copolymers lost up to 22% within the first 24 hr.

At 60 d, the PLA copolymer with the smallest mPEG size experienced the least mass loss at 26%. The amount of mass lost increased with increasing MW of the mPEG block incorporated into the PLA copolymer, with up to 94% lost from the PLA-mPEG(5k) copolymer films. PSIM-mPEG(5k) and its blended films underwent mass loss within this range. After the initial loss, the rate of mass loss for PSIM and its blends was similar, with rates of 0.44, 0.54, 0.6, 0.73, and 0.46 $\mu\text{g}/\text{d}$ from the first 24 hr to end of the 60 d for PSIM-mPEG(5k), 60:40 PSIM(5k):PLA(5k), 80:20 PSIM(5k):PLA(5k), 80:20 PSIM(5k):PLA(2k), and 80:20 PSIM(5k):PLA(550), respectively. The blend with the highest amount of PLA copolymer (60:40) and highest MW mPEG showed the greatest mass loss of 75%. Blends with a smaller PLA copolymer content (80:20) retained more mass than did the 60:40 blend and continued a trend of decreasing mass loss as the mPEG MW in the PLA copolymer decreased, from 63 to 45%. A total mass loss of 50% from the PSIM copolymer was comparable to that of its blend with the PLA copolymer having the lowest MW mPEG.

The largest amount of simvastatin, 15 μg after 60 d, was released from the 80:20 blend with the highest MW mPEG block (5kDa) incorporated into both of the individual copolymers. The two remaining 80:20 blends and PSIM-mPEG(5k) exhibited similar release profiles with an insignificant difference in total simvastatin released, ranging from 7.8 to 8.3 μg . The 60:40 blend released 6.2 μg , the smallest total amount of simvastatin. Increasing zero-order release rates of 0.24, 0.28, 0.3, 0.33, and 0.72 $\mu\text{g}/\text{d}$ were observed during the first 10 d followed by lower zero-order rates of 0.078, 0.11, 0.093, 0.094, and

0.168 a $\mu\text{g/d}$ for 60:40 PSIM(5k):PLA(5k), PSIM-mPEG(5k), 80:20 PSIM(5k):PLA(550), 80:20 PSIM(5k):PLA(2k), and 80:20 PSIM(5k):PLA(5k), respectively. The 80:20 PSIM(5k):PLA(5k) blend released a greater amount of simvastatin than PSIM-mPEG(5k) and 60:40 PSIM(5k):PLA(5k) did from 3 d ($p<0.01$) to 5 d ($p<0.0001$) and the remaining 60 d period ($p<0.0001$), along with 80:20 PSIM(5k):PLA(2k) ($p<0.001$) and 80:20 PSIM(5k):PLA(550) ($p<0.01$) from 7 to 60 d ($p<0.0001$). Simvastatin released from PSIM-mPEG(5k) and 80:20 PSIM(5k):PLA(550) was greater than the amount released from 60:40 PSIM(5k):PLA(5k) from 49 to 60 d ($p<0.05$).

Overall, approximately 62 wt% of simvastatin was polymerized into the diblock copolymer. An 8 to 15 μg amount of the drug (0.06 to 0.2 % of the monomer) was released during the 8 week period. Throughout degradation of PSIM-mPEG(5k) and the 60:40 blend, concentrations of 0.08 to 0.5 $\mu\text{g/ml}$ were reached, while the 80:20 blend releasing the largest drug amounts reached concentrations between 0.2 and 1.2 $\mu\text{g/ml}$.

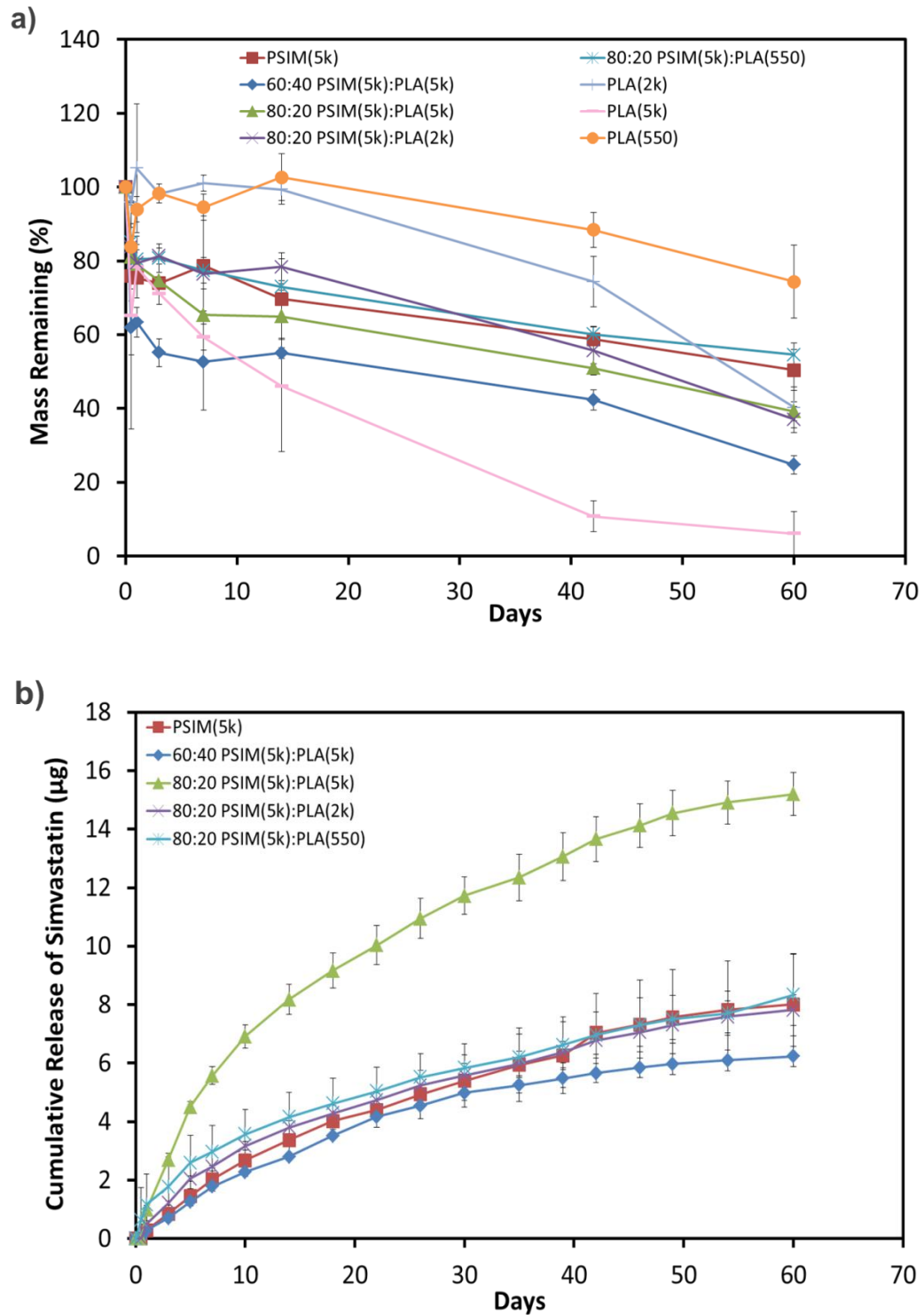


Figure 5.1 Degradation of PSIM and PLA copolymers and their blends in PBS, pH 7.4, showing a) mass loss and b) drug release profiles.

To evaluate the sensitivity of the synthesized polymers to enzymatic degradation, another mass loss study was conducted using PBS supplemented with 0.1 mg/ml carboxylesterase. Table 5.1 compares cumulative release of simvastatin with and without enzyme after 2 months of degradation. While the average simvastatin amount released was lower in esterase solution for 80:20 PSIM(5k):PLA(5k) and 80:20 PSIM(5k):PLA(550), no significant difference in release was seen comparing PBS and esterase solution conditions with each copolymer or copolymer blend.

Table 5.1: Comparison of simvastatin released from PSIM and blends in PBS and PBS containing 0.1 wt% esterase.

Cumulative Sim Released (μg)	PSIM(5k)	60:40 PSIM(5k): PLA(5k)	80:20 PSIM(5k): PLA(5k)	80:20 PSIM(5k): PLA(2k)	80:20 PSIM(5k): PLA(550)
PBS	8.01 ± 1.71	6.24 ± 0.344	15.2 ± 0.733	7.82 ± 0.523	8.33 ± 1.40
PBS with 0.1 wt% esterase	13.3 ± 1.28	8.14 ± 2.93	8.50 ± 3.49	8.98 ± 5.27	2.83 ± 0.933

Figure 5.2 shows images of samples used for mechanical testing. Although characteristically orange in color, the PSIM copolymer samples appear somewhat transparent along with their PLA copolymer counterparts, as opposed to the blends of PSIM with each of the PLA copolymers, which appear opaque. The PLA-mPEG(5k) copolymer was the least translucent of the three PLA copolymers, followed by PLA-

mPEG(550), and lastly PLA-mPEG(2k). The mPEG block polymers tested also had a characteristic opaqueness, white in color at room temperature.



Figure 5.2. Cylindrical mechanical testing samples of PSIM copolymers and blends. From *left to right*: mPEG (5kDa), mPEG (2kDa), PLA(5k), PLA(2k), PLA(550), PSIM(5k), 80:20 PSIM(5k):PLA(5k), and 60:40 PSIM:PLA.

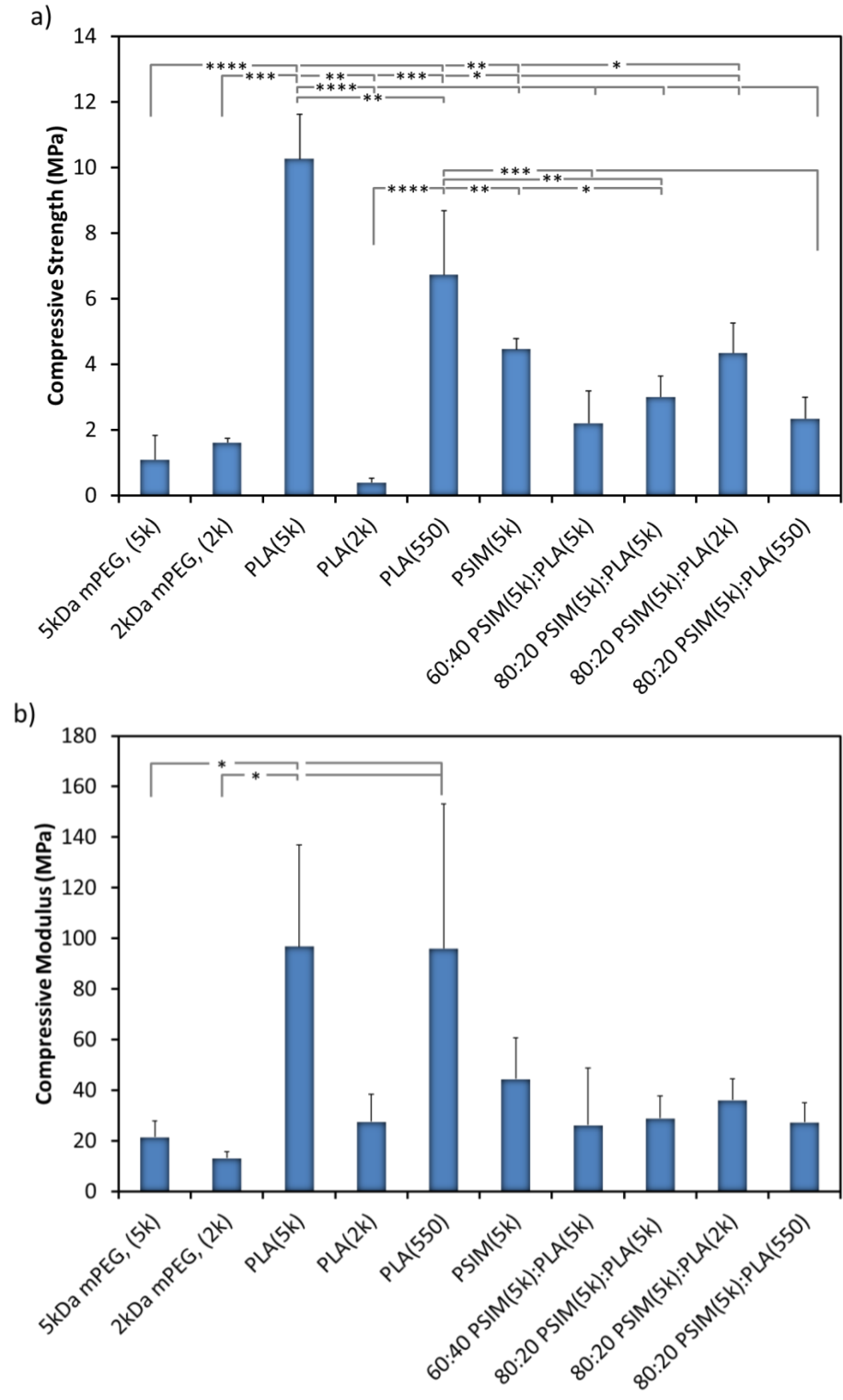


Figure 5.3 Mechanical properties of PSIM and PLA copolymers and blended samples: a) compressive strength and b) modulus. * $p < 0.05$, ** $p < 0.01$, *** $p < 0.001$, **** $p < 0.0001$

The average compressive modulus and strength of PSIM-mPEG(5k) were 44 and 4.5 MPa, respectively (Figure 5.3). Blending PSIM with PLA copolymers noticeably decreased the resulting compressive modulus and strength to ranges of 26-36 MPa and 2.4-5.4 MPa, respectively. In contrast, no significant difference in modulus and strength was seen between PSIM-mPEG(5k) and its blends. Also, there was no significant difference in modulus between the blends and the respective PLA copolymers used for each type, with the exception of 60:40 PSIM(5K):PLA(5K), which exhibited a significantly lower modulus than did PLA-mPEG(5k).

Significant differences in compressive strength were seen between the blends and the respective PLA copolymers incorporated in each blend type. The compressive strength of 2 kDa and 5 kDa mPEG was significantly lower than that of PSIM-mPEG(5K). There was a noticeable decrease in compressive modulus and large decrease in strength ($p < 0.0001$) as the mPEG block length in the PLA copolymer shortened from 5 to 2 kDa. However, the PLA copolymer with the shortest mPEG length (550 Da) exhibited a higher modulus (although with high variability) and strength ($p < 0.0001$) than did PLA-mPEG(2k), which had a similar modulus but significantly lower strength ($p < 0.01$) compared to PLA(5k).

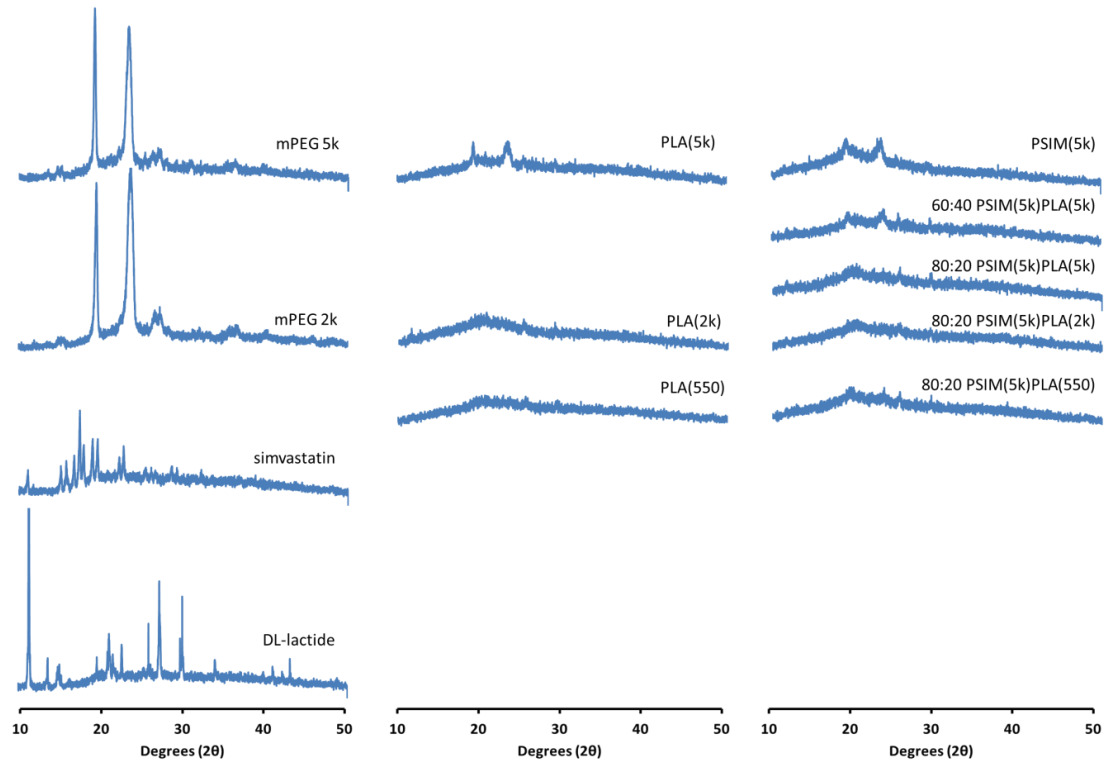


Figure 5.4 X-ray diffractograms of mPEG block components, simvastatin and D,L-lactide monomer components, PLA-mPEG copolymers, the PSIM-mPEG(5k) copolymer, and PSIM:PLA blends.

Figure 5.4 displays the comparative crystalline and amorphous peaks between the mPEG, PLA and PSIM polymers and blends, and their respective monomers obtained via X-ray diffraction. The 5 kDa mPEG was normalized at 100% as the most crystalline in the group when determining the relative crystalline index (CrI) between mPEG block components and copolymers. The 2 kDa mPEG followed with 90%, and then PSIM-mPEG(5k), PLA-mPEG(5k), 60:40 PSIM(5k):PLA(5k), and 80:20 PSIM(5k):PLA(5k) with 16, 14, 12, and 7.8% relative crystallinity, respectively. Similar amorphous properties to the 5 kDa mPEG-containing blends were exhibited by 80:20 PSIM(5k):PLA(2k), 80:20 PSIM(5k):PLA(550), PLA(2k) and PLA(550) with 9, 11, 11,

and 8.5% relative crystallinity, respectively. Distinctive peaks were observed at 20 and 24° (2θ) in the more crystalline polymers and blends.

The diffraction patterns of simvastatin and D,L-lactide also showed a semi-crystalline nature of the monomers used in copolymerization, at 47.5 and 62.5% crystallinity, respectively. Distinctive peaks of crystallinity characteristic to simvastatin were seen at 11.1° and from 15 to 27° (2θ). The diffraction pattern characteristic to D,L-lactide exhibited multiple crystalline peaks throughout the 2θ angle range of 11 to 43°.

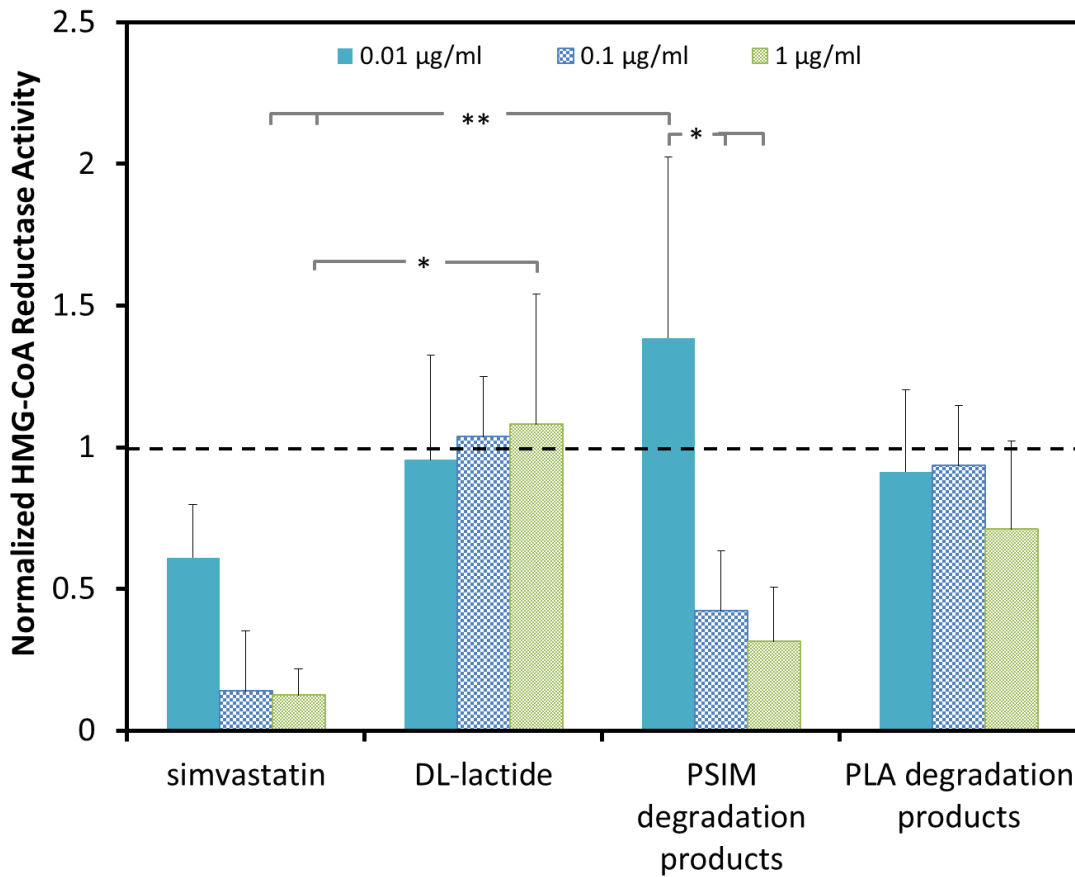


Figure 5.5. Inhibition of HMG-CoA reductase activity in the presence of simvastatin, lactide, and PSIM and PLA degradation products at different concentrations. (n = 3)

*p<0.05, **p<0.01

HMG CoA reductase activity was analyzed in the presence of PLA-mPEG(5k) and PSIM-mPEG(5k) degradation products (Figure 5.5). Inhibition of enzyme activity was seen with simvastatin at 0.01, 0.1, and 1 $\mu\text{g/ml}$ concentrations and with PSIM degradation products at the higher concentrations of 0.1 and 1 $\mu\text{g/ml}$. Compared to fresh enzyme activity, the levels of enzyme inhibition were 39, 86, and 88% for simvastatin at 0.01, 0.1, and 1 $\mu\text{g/ml}$, respectively, and 58 and 68% for PSIM degradation products at 0.1 and 1 $\mu\text{g/ml}$, respectively,. The presence of lactide and PLA degradation products exhibited minimal to no effect of enzyme inhibition at the concentrations analyzed. While multiple noticeable differences in inhibition were observed, statistical significance was seen for the PSIM degradation products at 0.1 and 1 $\mu\text{g/ml}$ ($p < 0.05$) compared to the same products at 0.01 $\mu\text{g/ml}$, for which there was no noticeable enzyme inhibition. No significant difference in inhibition was seen between the different simvastatin concentrations, but the products of PSIM at 0.01 $\mu\text{g/ml}$ exhibited significantly different activity from simvastatin at 0.1 and 1 $\mu\text{g/ml}$ ($p < 0.01$). Simvastatin at 1 $\mu\text{g/ml}$ also significantly reduced reductase activity compared to D,L-lactide at 1 $\mu\text{g/ml}$ ($p < 0.05$). D,L-lactide and PLA degradation products did not show significant activity at any of the concentrations tested.

5.4 Discussion

5.4.1 Degradation

The most influential factor affecting mass loss from the PSIM:PLA blends was relative hydrophobicity between PSIM and PLA copolymers within the blends. This factor, in turn, determined the rate of ester bond hydrolysis within the polymer backbone

and degree of erosion that occurred. Simvastatin is hydrophobic due to the aromatic rings found within its structure, a characteristic that increases in degree as simvastatin is polymerized into its respective polymeric block. Lactide, a lactone molecule that lacks aromatic moieties in its structure, is comparatively less hydrophobic, resulting in the synthesis of a less hydrophobic polymer. Differences in mass loss between the blends can be explained by relative hydrophobicity when evaluating the differences between the PLA-mPEG diblock copolymers incorporated in the blends. Increasing the mPEG block MW from 550 to 5000 Da created copolymers that decreased in hydrophobicity. This trend led to an increased degradation rate as the association of water with oxygen-rich mPEG, and subsequent access of water into the polymer matrix, increased with block length.

The degree of compatibility between the PSIM-mPEG(5k) and PLA copolymers in the blends and loss of residual mPEG and simvastatin reactants were possible contributing factors to the significant initial erosion of the blends observed during the first 24 hr. The initial mass loss from blends that had 20 and 40% of PLA-mPEG(5k) may indicate phase separation between the two copolymers that was only exacerbated upon increasing the weight percentage of PLA and/or leaching of PLA oligomers from the bulk samples. The amount of PLA lost would not account for the total loss during this period, however, as a detectable amount of simvastatin and intermediate PSIM-mPEG(5k) degradation products were also present in the release supernatant. The slightly larger mass loss from PSIM-mPEG(5k) compared 80:20 blends may result from leaching of free mPEG and monomer from the polymer matrix.

The PLA degradation products, residual mPEG and simvastatin reactants, and PSIM-mPEG(5k) intermediary degradation products, such as simvastatin oligomers, would account for the three orders of magnitude difference in mass lost and simvastatin monomer released from the blends, because only simvastatin monomer is accounted for in the release profiles. The 80:20 blend most likely released the largest amount of simvastatin due to a potentially lower internal pH environment in the bulk relative to the other blends and PSIM-mPEG(5k) as a result of the higher degradation rate of PLA-mPEG(5k) within the blended matrix. This comparatively accelerated process would, in turn, enhance degradation of PSIM-mPEG(5k), leading to greater cumulative release of simvastatin. In contrast, the 60:40 blend releasing the lowest amount of drug was possibly linked with the blend prematurely breaking up resulting in the early loss of PLA-mPEG(5k) from the blended matrix. Without the faster degrading polymer, pH of the internal environment within the remaining PSIM-mPEG(5k) matrix may not have been low enough to accelerate cleavage of labile ester bonds to ultimately free larger amounts of simvastatin. Blended polyester systems have shown an increase in polymer degradation in the presence a secondary acid producing biodegradable polymer (such as PLA) within the matrix.¹⁹⁶ In contrast, effects of neutralization to reduce degradation rate have also been seen following incorporation of basic products in the blends.¹⁶⁸ Relatively better integrity observed in the remaining blends correlated with higher amounts of simvastatin released.

The simvastatin concentration range generated from the least hydrophobic 80:20 blend was within the concentration range of 0.5 to 1.5 μM (i.e., 0.21 to 0.42 $\mu\text{g/ml}$) deemed to have a therapeutic effect *in vitro*. Similar simvastatin concentrations were

reported by Song et al. to induce significant alkaline phosphatase activity in bone marrow stromal cells.¹⁹⁷ Concentrations from PSIM-mPEG(5k) were also within this range. Another study found that a slightly higher concentration range of 1 to 10 μM of simvastatin also induced VEGF mRNA expression in osteoblastic cells, showing similar therapeutic concentration windows for different effects promoted by simvastatin.¹⁹⁸

During degradation of the PSIM copolymer and its blends, open and/or closed-ring simvastatin and mPEG and other intermediate products may be produced as a result of the breakdown of hydrolytically unstable ester bonds. Potential degradation products include mPEG with a few monomers of simvastatin attached and oligomers of simvastatin in the absence of mPEG, leading to increasingly hydrophobic macromolecules as the number of simvastatin monomers on the oligomeric chain increases. Some arguments have been made that *in vitro* degradation studies of polymer drug delivery systems do not accurately represent performance in the physiological environment due to the lack of enzymatic components and other biological factors that may accelerate degradation of biodegradable polymeric systems. Tracy *et al.* showed that PLGA microspheres injected into Sprague-Dawley rats exhibited degradation rate constants 1.7 to 2.6 times faster than their degradation *in vitro* in a HEPES and KCl buffer. As a result, the microspheres lasted a shorter time *in vivo*, from 14 to 60 d compared to ~35 to over 60 d *in vitro*.¹⁹⁹ In the present studies, there were no significant differences seen between the PSIM:PLA blends degraded in PBS with or without carboxylesterase. Porcine liver carboxylesterase was chosen because hepatic carboxylesterases are known to contribute to metabolizing simvastatin.²⁰⁰ Decreased affinity of porcine liver carboxylesterase for PSIM macromolecules, despite its ability to

metabolize simvastatin, could possibly explain the insignificant differences between groups. Different types of liver carboxyl esterases exist show similar activity, but they differ in conformation,²⁰¹ which may have better affinity for PSIM. Further analysis of PSIM degradation with different liver carboxyl esterases would better determine if their structures would in turn influence affinity for PSIM. The aromatic side groups of simvastatin, more prominent in its polymerized form, may further inhibit access of the enzyme to ester bonds compared to PLA and PLGA polyesters, which lack large side groups. This potential concern of interfering side groups may be further exacerbated by the random entanglement of polymer chains.

5.4.2 Mechanical and crystalline properties

While internal defects and voids within the samples played a part in their relative opaqueness, inherent differences in their appearance may be due to possible differences of indices between the two copolymers blended together. Refractive differences increase light scattering between phases.²⁰² For copolymers with similar, if not the same, refractive index, light would transmit more easily creating the transparent appearance seen in the PLA and PSIM copolymer samples. The opaqueness of the mPEG polymers was due to their highly crystalline nature, much like the appearance of PCL, which is also mostly crystalline at room temperature. Thus, PLA copolymers with the highest MW mPEG appeared the least translucent of the three.

Mechanical properties of biodegradable copolymers play an influential role in the balance of bone resorption and growth as the surrounding tissue heals. The average compressive modulus and strength of trabecular bone in elderly adult human mandibles are 56 ± 29.6 and 4 ± 2.7 MPa, respectively. For the cortical bone of elderly adult human

mandibles, the compressive modulus was found to be higher at 96.2 ± 40.6 MPa.²⁰³ The mechanical properties of developed polymeric biomaterials for tissue regenerative therapies are intended to mimic the properties of the surrounding bone to minimize under- or over-compensation of loading put on bone, as described by Wolff's law, which would otherwise lead to decreased or increased bone turnover, respectively.²⁰⁴ However, for the device to combat fatigue from damage and repeated loading, the argument of developing implants with mechanical properties stronger than their surroundings has been made because of their typically smaller cross-sectional areas than bone and lack of reconstructive capability.²⁰⁵ In either case, being able to easily modify the mechanical properties of biodegradable polymers via blending is advantageous.

The modulus and strength of PSIM-mPEG(5k) remaining within the same order of magnitude of those for mandibular trabecular bone.²⁰³ Incorporating the same percentages of each PLA copolymer in the blends (80:20) and also blending two different amounts of PLA-mPEG(5k) (80:20 and 60:40) further decreased the modulus and strength of the resulting blends (excluding the strength of 80:20 blend with PLA-mPEG(2k)) compared to PSIM-mPEG(5k). The relative crystallinity of PSIM compared to its respective blends correlated with the modulus comparisons between PSIM-mPEG(5k) and the respective blends. This result may indicate a plasticizing effect of the PLA copolymers incorporated,²⁰⁶ however the presence of small voids within the blended sample matrix cannot be discounted as a contributor to the decreased properties. Miscibility of the two polymers can also influence properties. While PEG is known to be miscible with PLA, often referred to as a "compatibilizer" component of block copolymers in polymeric blends, hydrophobic PCL has been shown to be immiscible

with PLA.²⁰⁶ Low miscibility between hydrophobic PSIM and PLA block segments of the copolymers could lead to boundaries between poorly or non-mixed regions within the matrix, which could act as regions of stress concentration, thereby leading to lower modulus and strength as the amount of PLA-mPEG(5k) increased. This effect could explain the lower average strength of the 60:40 blend compared to its 80:20 counterpart. The PLA copolymer samples had a modulus ranging from 26 to 97 MPa, resulting in the PLA-mPEG(5k) and PLA-mPEG(550) samples measuring 1.7 times higher than the values measured for trabecular bone.

The lower modulus and strength of the individual mPEG polymers compared to the copolymers of PLA-mPEG(5k), PLA-mPEG(550), PSIM-mPEG(5k), and the blends is due to the lower molecular weights of the mPEGs, despite their higher crystallinity compared to the copolymers and blends. The properties of 550 Da mPEG were not measured due to the liquid state of the polymer at ambient temperature.

The trends seen between the PLA copolymers may be due to competing effects of plasticization and crystallization as a result of the length of incorporated mPEG blocks and their influence on PLA block segments, relative PEG content of the copolymers, and overall orientation of these block segments within various domains of the polymer matrix. The weight percentage of PEG in PLA-mPEG(550), PLA-mPEG(2k), and PLA-mPEG(5k) was 3, 13, and 25%, respectively. Kulinski *et al.* reported a plasticizing effect of 600 Da PEG within the PLA domains as the PEG content increased from 5% to 12%, resulting in decreased yield stress from 30 to 5 MPa.²⁰⁷ Plasticization may also explain the decrease in modulus and strength of PLA-mPEG(2k) compared to PLA-mPEG(550). The increased plasticization effect predominated the more crystalline nature of 2 kDa

mPEG in PLA-mPEG(2k), compared to 550 Da mPEG in PLA(550), which would otherwise potentially increase modulus and strength. Wu *et al.* showed that attachment of a 5 kDa mPEG block impeded spherulite growth and thus chain folding ability of PLA in the copolymer compared to PLLA homopolymers.²⁰⁸ Among the three PLA copolymers synthesized, PLA-mPEG(5k) had the highest compressive modulus and strength, which can be attributed to the higher crystallinity of the conjugated 5 kDa mPEG block, compared to 2 kDa and 550 Da mPEG, combined with its high percentage in the PLA(5k) copolymer. This effect may indicate that a critical ratio exists where crystallinity of the high MW PEG begins to dominate over an otherwise plasticizing effect. While PEG hindered PLA chain folding, Wu *et al.* still calculated large 5 kDa mPEG crystals even at low PEG ratios because of the ability of mPEG to crystallize.²⁰⁸

While PSIM-mPEG(5k) and PLA-mPEG(5k) exhibited similar crystallinity, the higher modulus of PLA-mPEG(5k) may be the result of the higher MW compared to PSIM-mPEG(5k). Stress concentrators from small defects within the samples may have also played a role in the resulting compressive strength. Compared to the multiple distinct peaks representative of the crystal lattice structure unique to simvastatin and the ordered arrangement of mPEG crystallites in the 5 kDa mPEG polymer, the PSIM-mPEG(5k) diffractogram has peaks similar to mPEG but a much lower relative intensity, in addition to a noticeable halo underneath the two peaks. The observed diffraction maxima observed for PSIM-mPEG(5k) support the conjugation between the mPEG and PSIM blocks and between the simvastatin monomers. The lower peak intensities may be attributed to the PSIM-mPEG(5k) copolymer chains containing a lower mPEG

percentage compared to solely mPEG. The peaks and halo are representative of the crystalline and amorphous regions of the PSIM(5k) copolymer, respectively.²⁰⁹

5.4.3 Bioactivity

Simvastatin is a well-known inhibitor of HMG-CoA reductase, a rate-limiting enzyme in the cholesterol biosynthesis pathway. By inhibiting the enzyme, late-stage prenylation of GTPase proteins (Rho, Ras, etc.) is affected, leading to the expression of multiple properties. Apart from its role in lowering lipids, simvastatin has osteogenic, anti-inflammatory, and angiogenic properties.¹²⁰⁻¹²³

A noticeable concentration-dependent inhibition of enzyme activity was observed with both simvastatin and degradation products from the PSIM copolymer, reflecting the known ability of simvastatin to act as a competitive substrate for HMG-CoA reductase. In contrast, D,L-lactide and PLA degradation products did not show inhibitory activity. As such, the D,L-lactide monomer and degradation products of PLA may serve as controls in other future bioactivity studies. Lower activity of the PSIM degradation products compared to simvastatin at the same concentrations was most likely due to the components incorporated that do not have an effect on reductase activity, such as mPEG or oligosimvastatin macromolecules that have not fully degraded into individual molecules of simvastatin, which contributed to the total concentrations of the PSIM degradation products.

5.5 Conclusions

Blending poly(simvastatin) with PLA provided an easier alternative to copolymerization for enhancing and tuning degradation. Different mPEG sizes

conjugated to PLA and weight ratios chosen to blend PLA with PSIM copolymers led to varied hydrophobicity, which consequently altered degradation and physical properties of the blends. Incorporating PLA copolymers at different ratios plasticized poly(simvastatin), reducing the compressive modulus, within a range comparable to that of trabecular bone. The PSIM degradation products were also active in reductase inhibition, a key factor for simvastatin exhibiting biological effects. PSIM and its tailorable properties may be useful in tissue regenerative applications.

Ch. 6 *In vitro* and *In vivo* bioactivity of poly(simvastatin) – poly(ethylene glycol) diblock copolymer for bone therapeutic applications

This chapter was reproduced from a manuscript in preparation, “Asafo-Adjei T.A., T.D. Dziubla, D.A. Puleo, *In vitro* and *In vivo* bioactivity of poly(simvastatin) – poly(ethylene glycol) diblock copolymer for bone therapeutic applications, (2017).”

6.1 Introduction

Statins such as lovastatin (Mevacor) and simvastatin (Zocor) were approved by the FDA in 1987 and 1988, respectively, as potent cholesterol-lowering agents.^{210, 211} However, these statins were later found to possess multiple properties making them desirable for a range of therapeutic applications. Specific statins are preferred over others for treatment depending on their relative potency at a given dose, relative lipophilicity, bioavailability, and mechanism of metabolism, which may influence interactions with other drugs and potential side effects experienced by patients.^{96, 210} However, simvastatin was the most prescribed statin in 2010, the third most prescribed drug in the U.S., and it continues to be the most investigated statin in the literature.^{210, 212, 213} Its popularity in research is most likely due to the medium-potency and overall cost-effectiveness of the prodrug compared to other statins.²¹⁴ Structurally, simvastatin is the only statin aside from lovastatin that resides in an inactive lactone form before it is introduced into a physiological environment where it becomes active.²¹⁰

When simvastatin is active in its open ring, hydroxyacid form, the molecule competes with 3-hydroxy-3-methyl-glutaryl (HMG) as a substrate for HMG-CoA reductase, inhibiting the rate-limiting and early step of the mevalonate pathway. Isoprenoid precursors, such as geranyl-geranyl and farnesyl pyrophosphates (GGPP and

FPP, respectively), which are indirectly inhibited further down the biosynthesis pathway, inhibit the prenylation of Ras (via GGPP) and Rho (via FPP) proteins.^{215, 216} Rho inhibition results in a significant increase in endothelial cell nitric oxide synthase (eNOS) and subsequent nitric oxide (NO) production.²¹⁶ NO and eNOS promote anti-oxidant and anti-inflammatory activity through limiting platelet adhesion and promote cell survival and blood vessel development through the PI3 kinase/Akt pathway and regulation of vascular endothelial growth factors (VEGF).^{216, 217} Prenylation of T-cells is also inhibited, leading to reduced macrophage activation and inflammation.²¹⁸ Thus, the early inhibition of cholesterol biosynthesis by statins affects other signaling pathways leading to anti-atherosclerotic, angiogenic, anti-inflammatory, and anti-oxidant properties necessary for tissue health and regeneration.¹²⁰⁻¹²³

The discovery by Mundy et al. in 1991 of the osteogenic nature of lovastatin and simvastatin prompted a whole new avenue for using statins in biomedical applications.⁹⁷ Simvastatin was observed to upregulate expression of BMP-2, which consequently induced significant bone formation on the calvaria of ovariectomized mice. Upregulation of BMP-2 by simvastatin has since been shown to be caused by the Ras/Smad/Erk/BMP-2 signaling pathway.²¹⁹ Reduction of mevalonate while BMP-2 is upregulated may also be mediated by factors outside inhibition of the cholesterol biosynthesis pathway, however.²²⁰ Mevalonate reduction has been shown to correlate with increased alkaline phosphatase activity, an indicator of early osteoblast differentiation.^{221, 222} Additionally, Rho inhibition suppresses osteoclast activity, allowing simvastatin to exhibit anti-resorptive effects as well,²²³ although the anti-resorptive effects of statins are not nearly as significant as osteogenic effects.⁹⁷ While simvastatin, as with all treatments, proves to

be ineffective below a therapeutic window unique to the drug, simvastatin at high doses has promoted inflammation, myositis, rhabdomyolysis, and hepatotoxicity.⁹⁹ To better control statin loading and rate of release, a polymerized form of simvastatin was previously synthesized via ring opening polymerization.¹⁵⁹

The objective of the present studies was to compare *in vitro* bioactivity of PSIM and PLA copolymer degradation products with, simvastatin, D,L-lactide, and BMP-2 control groups. A pilot study to evaluate polymer degradation and osteogenic activity *in vivo* was also started.

6.2 Experimental

6.2.1 Materials

Simvastatin and D,L-lactide were purchased from Haorui Pharma-Chem (Edison, NJ) and Alfa Aesar, respectively. Monomethyl ether poly(ethylene glycol) (mPEG), and triazabicyclodecene (TBD), β -glycerophosphate, ascorbic acid, thiazolyl blue tetrazolium bromide, magnesium chloride, 2-amino-2-methyl-1 propanol, sodium dodecyl sulfate, dimethylformamide, and ethylenediaminetetraacetic acid (EDTA) were purchased from Sigma Aldrich. BMP-2 was purchased from (Genscript), Dulbecco's Modified Eagle's Medium was obtained from Corning, Fetal bovine serum (FBS) was obtained from Atlanta Biologicals, and p-nitrophenyl phosphate was purchased from ---.

6.2.2 Methods

6.2.2.1 Copolymer synthesis. A macroscale reaction of PSIM-mPEG(5k) via TBD or stannous octoate (3 g) was conducted using the synthesis procedures previously described.¹⁵⁹ Simvastatin was used as the monomer and mPEG with a weight-average M_w of 5000 Da at a 100 to 1 monomer to initiator molar ratio. A macroscale reaction of

PLA(5k) using a procedure previously described in Section 5.2.2.2 was conducted (5g) using D,L-lactide as the monomer and mPEG with a M_w of 5000 Da at a 100 to 1 monomer to initiator molar ratio. The crude copolymers were purified by dissolving the crude products in DCM and pipetting the polymer solution into excess cold diethyl ether, as the anti-solvent. The purified products were isolated via vacuum filtration.

6.2.2.2 Degradation Products. PSIM(5k) and PLA(5k) were each degraded in 5 mL of 0.1 M NaOH (aq) for 30 d. Afterwards, supernatant with the degraded products from each copolymer was collected and neutralized to pH 7.4 using 1 M HCl. Various concentrations were made from the neutralized PSIM(5k) and PLA(5k) supernatants for cell studies.

6.2.2.3 Cell culture. Murine myoblast C2C12 cells were obtained from American Type Culture Collection (CRL-1772; ATCC, Manassas, VA). Cells were cultured in DMEM with 10% fetal bovine serum (FBS), and incubated at 37 °C in a 5% CO₂ environment. Culture medium was replaced every 3 days.

6.2.2.4 Cytotoxicity. Cytotoxicity upon exposure to its degradation products was assessed using a 3-(4,5-dimethylthiazol-2-yl)-2,5-diphenyltetrazolium bromide (MTT) assay.²²⁴ MTT is reduced into formazan by dehydrogenase enzymes present in viable cells. C2C12 cells were seeded at 20,000 cells/well in a 96-well plate and incubated overnight. Afterwards, 0.001, 0.01, 0.1, 1, and 10 µg/ml of PSIM-mPEG(5k) degradation products, PLA-mPEG(5k) degradation products, simvastatin, D,L-lactide, and BMP-2 were added to the cells. PSIM-mPEG(5k) and PLA-mPEG(5k) were also tested at at 100 µg/ml. After 24 hr, medium was replaced and 5 mg/ml of MTT in PBS

was added to each well before incubating at 37 °C for 2 h. Lysing buffer containing 20% w/v sodium dodecyl sulfate in 50% dimethylformamide, pH 4.7, was added to each well to solubilize the formazan produced by viable cells. The optical density of formazan was read at a maximum absorbance wavelength of 570 nm using a PowerWave HT microplate spectrophotometer with Gen5 analysis software.

6.2.2.5 Alkaline Phosphatase (AP) Activity. C2C12 cells were seeded at 20,000 cells/well in 48-well plates for 24 hr, after which the culture medium was replaced with α MEM containing 10% FBS, 5 mM β -glycerophosphate, and 50 μ g/ml of ascorbic acid. Cells were cultured for 4 days to reach confluence before treating with simvastatin, D,L-lactide, PSIM-mPEG(5k) degradation products, PLA-mPEG(5k) degradation products, simvastatin, BMP-2, or PBS. The same treatments with the addition of 20 μ g/ml of phenamil, active in BMP-2 upregulation, were run in parallel to assess the effects of the compound. Medium with treatments were replaced every 3 days. After 3, 5, and 7 d, buffer containing 50 mM sodium phosphate, 2 M sodium chloride and 2 mM EDTA was added and followed by sonication to ensure cell lysis. Aliquots of lysate were mixed with substrate solution containing 10 mM of p-nitrophenyl phosphate and 4 mM of $MgCl_2$ in 0.6 M of 2-amino-2-methyl-1 propanol buffer, and the absorbance was measured at 400 nm as a function of time.

6.2.2.6 Myotube Staining. C2C12 cells with the same treatment groups were stained with 0.01% of crystal violet for 30 min after fixation with methanol for 5 min. After staining, the dye was aspirated and excess amounts were removed with 4 to 5 washes of DI water. Cells were captured (10x) using an Olympus IX51 inverted microscope.

6.2.2.7 Copolymer Disk Formulation. Poly(simvastatin-*block*-mPEG) disks were formulated by compressing the copolymer, in powder form, into a cylindrical dye with a stainless steel rod under 8000 pounds of pressure for 5 min using a carver press. After removing the samples from the dye, samples were annealed at 30 °C for 24 hr and subsequently at 60 °C for 24 hr to form 4 x 6 mm disks (100 mg).

6.2.2.8 Pilot Animal Study. While *in vivo* analysis is ongoing and will not be completed until late 2017 (Table 1), a trial study using a male Sprague-Dawley rat model was conducted at the University of Kentucky in accordance with the Institutional Animal Care and Use Committee protocol generated for biodegradable poly(simvastatin). A transverse incision was made between the ears and the periosteum was elevated before placing a poly(simvastatin-*block*-mPEG) disk (4 x 6 mm, 100 mg) on the calvarium of each animal. Poly(simvastatin-*block*-mPEG) disks were implanted to observe initial disk behavior and the resulting tissue response up to 4 wk post-implantation. The calvarium with samples still intact were fixated in phosphate buffered formalin for microCT (Scanco Medical) to observe bone morphology at and surrounding the implantation site.

Table 6.1 *In vivo* experimental design

<i>Treatments</i> <i>(50 mg disks)</i>	<i>Weeks after implantation</i>					
	1 wk	2 wks	3 wks	4 wks	6 wks	8 wks
<i>Poly(simvastatin-co-glycolide)</i>	6	6	6	6	6	6
<i>Poly(simvastatin-block-mPEG)</i>	6	6	6	6	6	6
<i>PLGA</i>	6	6	6	6	6	6
<i>PLGA with encapsulated simvastatin</i>	6	6	6	6	6	6

6.2.2.9 Statistical Analysis. One-way ANOVA with a Tukey post-test was used to analyze differences in cytotoxicity, and Two-way ANOVA with a Bonferroni post-test was used for AP expression between treatments. Mean and standard deviation are plotted. A value of $p \leq 0.05$ was deemed statistically significant.

6.3 Results

An MTT assay was conducted to determine the cytotoxicity for each treatment group before selecting the concentrations to be used for AP expression in C2C12 cells. In Figure 6.1, concentrations up to 100 $\mu\text{g/ml}$ of PSIM and PLA degradation products, and up to 10 $\mu\text{g/ml}$ of simvastatin, D,L-lactide, and BMP-2 were cytocompatible with

C2C12 cells after 24 hrs. The positive control of ethanol was the only group showing significant cell cytotoxicity ($p < 0.001$).

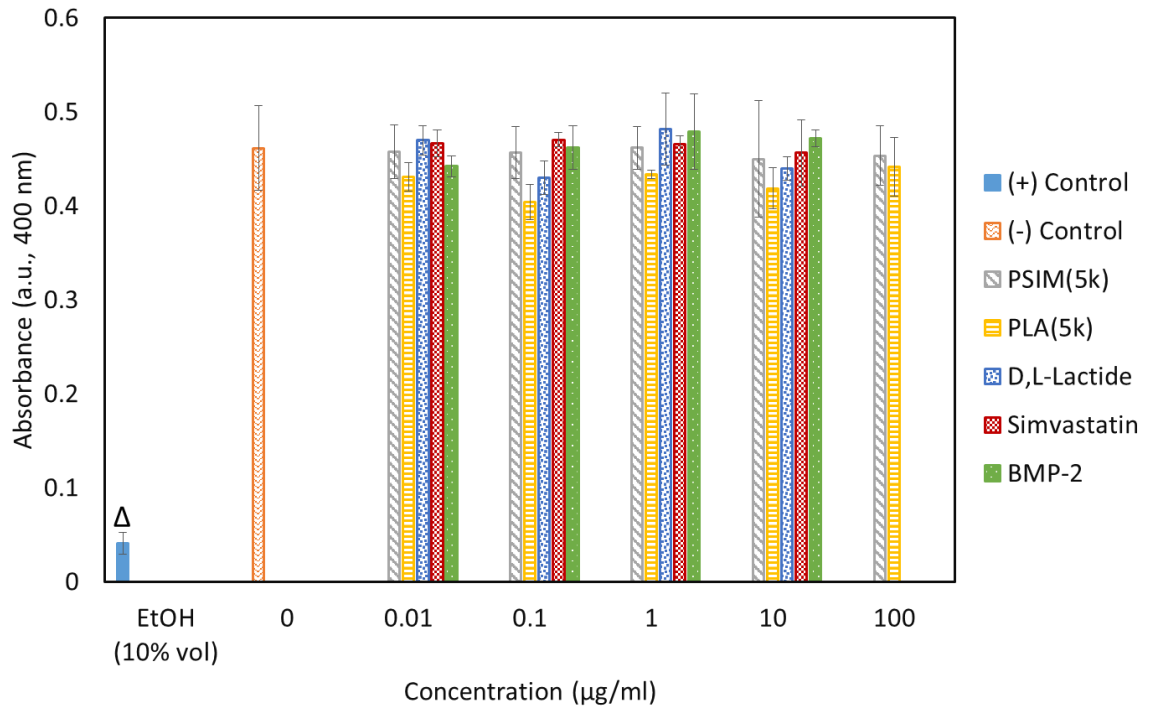


Figure 6.1 Cytocompatibility of simvastatin and lactide monomers and poly(simvastatin) and poly(lactide) degradation products at different concentrations in C2C12 myoblast cell cultures. $\Delta p < 0.001$

Based on effective concentrations for the controls described in the literature and cytocompatibility results, C2C12 cells were treated with 1 µg/ml of simvastatin, D,L-lactide, or BMP-2 and 10 or 50 µg/ml of PSIM or PLA degradation products to measure AP expression after 7d of confluency.

A 24 hr kinetic run of AP activity showed that activity began to plateau for one or more groups after 2 hrs, so the 2 hr timepoint was used to compare groups with and

without phenamil (Figure 6.2) at 3, 5, and 7 days post- confluency. In the absence of phenamil, only simvastatin led to a difference in AP expression at 3d ($p<0.01$), followed by both simvastatin and BMP-2 at 5 ($p<0.01$ and $p<0.001$, respectively) and 7d ($p<0.001$ and $p<0.001$, respectively). While there was a slight increase in AP activity with 50 $\mu\text{g/ml}$ of PSIM(5k) degradation products, and 1.5 times higher than the PBS control, the difference was not significant. BMP-2 promoted AP activity 1.5, 4, and 13 times higher than the PBS control at 3, 5, and 7 d, respectively. Simvastatin promoted 2.5, 3, and 2.4 times more AP activity than PBS at 3, 5, and 7 d, respectively.

Simvastatin promoted greater AP expression with phenamil than without at 3 d ($p<0.001$), followed by diminished expression at days 5 and 7 ($p<0.05$). BMP-2 was the only treatment that resulted in increased AP activity at days 5 ($p<0.001$) and 7 d ($p<0.001$), promoting higher AP expression compared to treatment without phenamil. BMP-2 treatments with phenamil increased activity 1.6, 2.2, and 1.2 times more than BMP-2 did in the absence of phenamil at 3, 5, and 7 d, respectively. Simvastatin with phenamil increased AP activity 1.5 and 1.1 times more at 3 and 5 d, respectively, followed by 0.16 times less activity at 7 d. PSIM(5k) degradation products at 50 $\mu\text{g/ml}$ led to only 1.1 times more AP activity at 5 d.

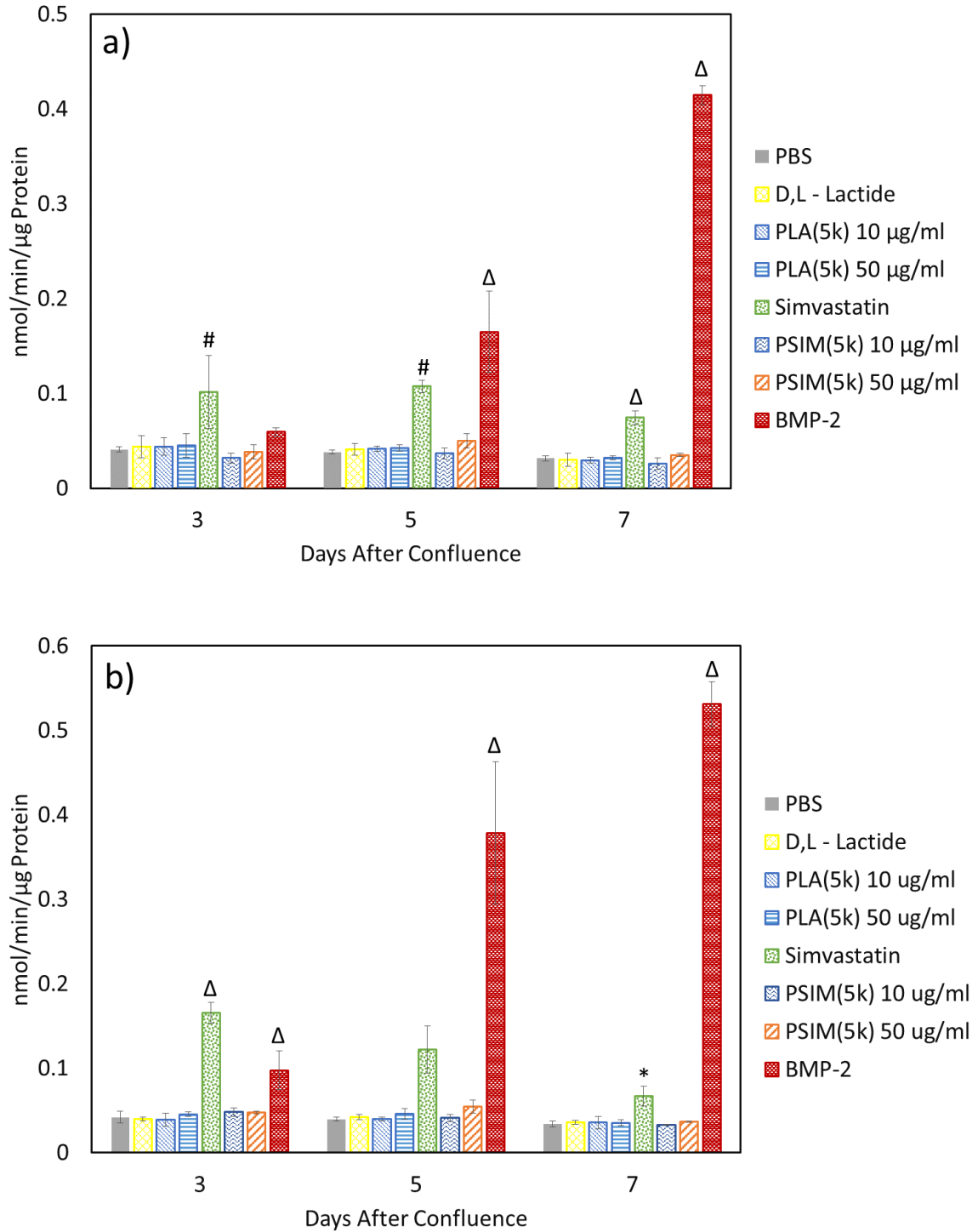
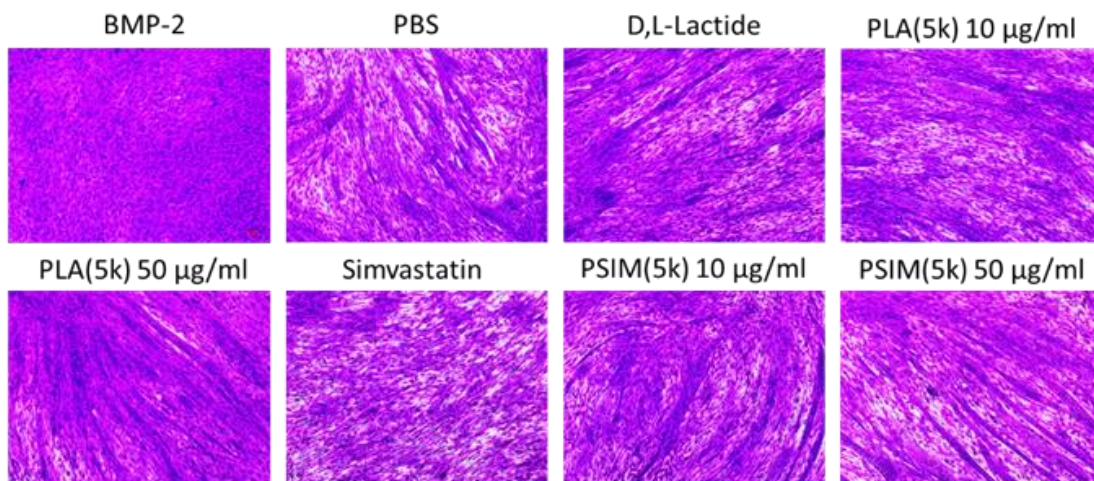


Figure 6.2 Alkaline phosphatase expression by C2C12 myoblast cells in the presence of poly(simvastatin) and poly(lactide) degradation products, simvastatin, D,L-lactide, BMP-2, and untreated controls a) without and b) with phenamil. * $p < 0.05$, # $p < 0.01$, $\Delta p < 0.001$

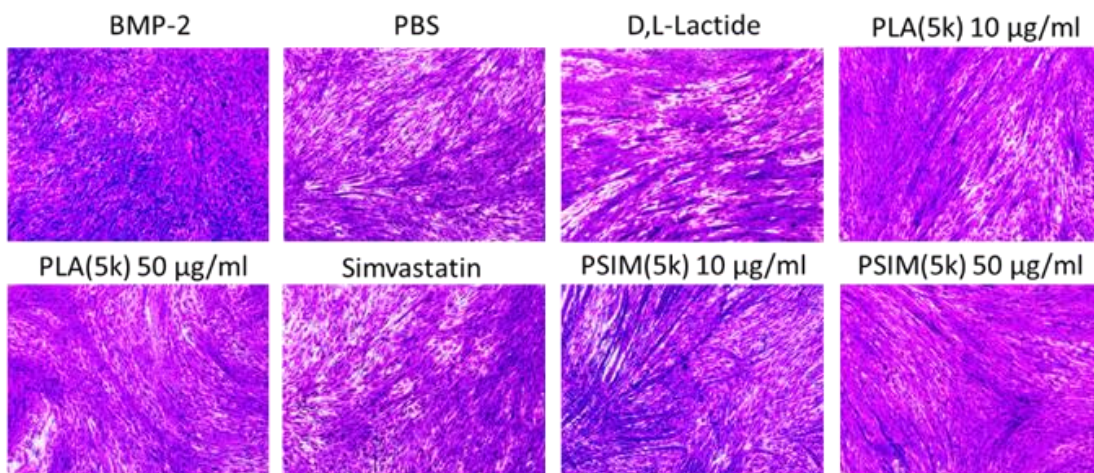
Relative myotube thickness between the groups after 7 d is shown in Figure 6.3. Cells treated with BMP-2 were excluded from the plot because the protein prevents myotube formation, which is seen in Figure 6.3b. In the absence of phenamil, only C2C12 myoblasts treated with simvastatin had significantly smaller myotube diameters compared to the PBS control and remaining treatments ($p < 0.001$), including D,L-lactide ($p < 0.01$). Between the remaining groups, D,L-lactide treatment led to significantly smaller myotubes formed than PLA(5k) did at 10 $\mu\text{g/ml}$ ($p < 0.001$), but it was not different from the PBS control. A difference in myotube diameter was also seen between PLA(5k) at 10 $\mu\text{g/ml}$ having the thickest diameters and PSIM(5k) at 50 $\mu\text{g/ml}$ and D,L-lactide ($p < 0.01$), but it was not significantly different from the PBS control.

When phenamil was present, the PBS control showed a difference in myotube thickness compared to the other treatments ($p < 0.001$). Simvastatin with phenamil resulted in even smaller myotube thickness compared to the remaining treatments ($p < 0.001$), including PLA(5k) at 50 $\mu\text{g/ml}$ ($p < 0.01$). Smaller myotube thickness from PLA(5k) at 10 $\mu\text{g/ml}$ compared to 50 $\mu\text{g/ml}$ was seen as well ($p < 0.05$).

a) (-) phenamil



(+) phenamil



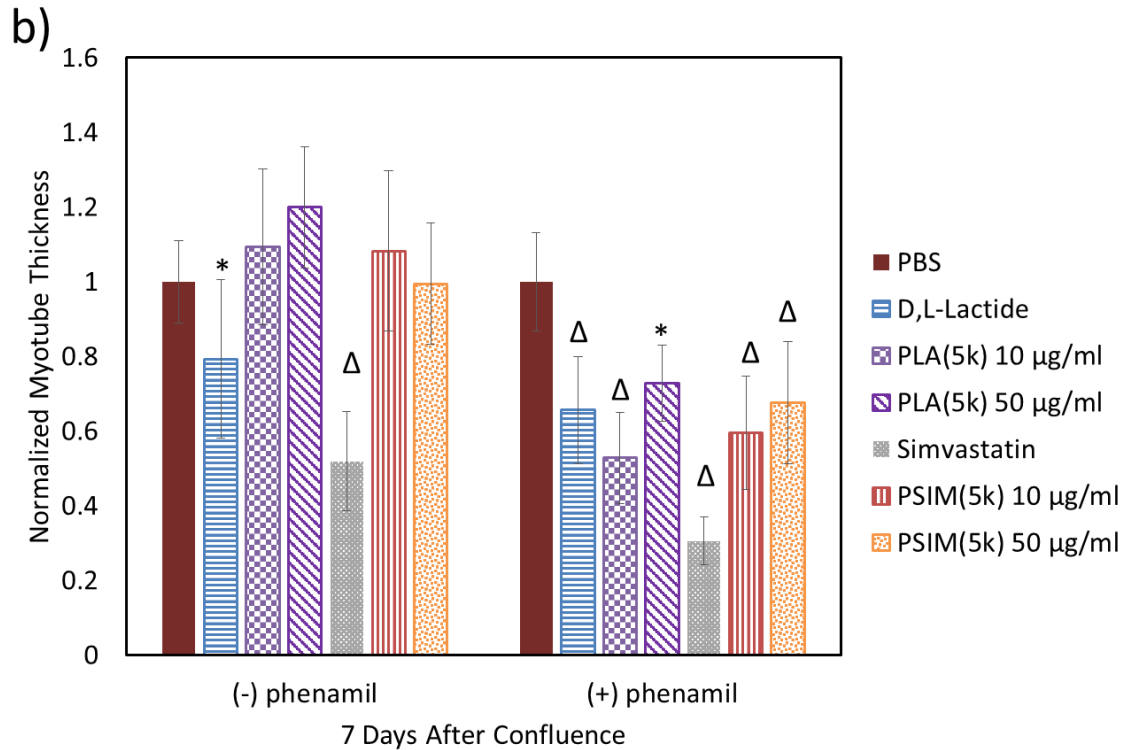


Figure 6.3 a) Relative myotube thickness normalized to PBS control at 7 d and b) cell images comparing myotube formation between groups. BMP-2 was excluded from the plot since myotubes did not form with treatment. $n=10$, $*p<0.05$, $\Delta p<0.001$.

Observations from up to 4 week trial runs of 4 x 6 mm poly(simvastatin) disks implanted on the calvarium, beneath the periosteum, of Sprague-Dawley rats revealed slightly varied findings in the physical and degradation behavior of the disks *in vivo* (Figure 6.4). Within one week, observations ranged from an extensively fragmented disk, to a relatively intact disk encased in a fibrous capsule at the implantation site, to remnants of the disk remaining at the site. At the third week, similar disk conditions of fragmented or intact disks were seen. The intact disks looked to have retained most if not

all of their initial size up to wk 4, despite the disk conditions and the outlier of only particles remaining in one of the animals at wk 1.

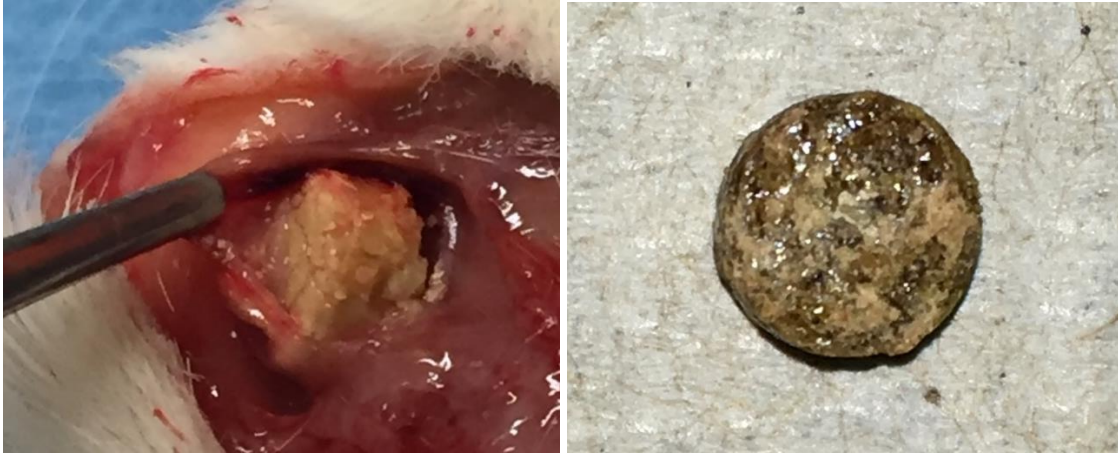


Figure 6.4 Images of fragmented and intact poly(simvastatin) disk samples at wk 1.

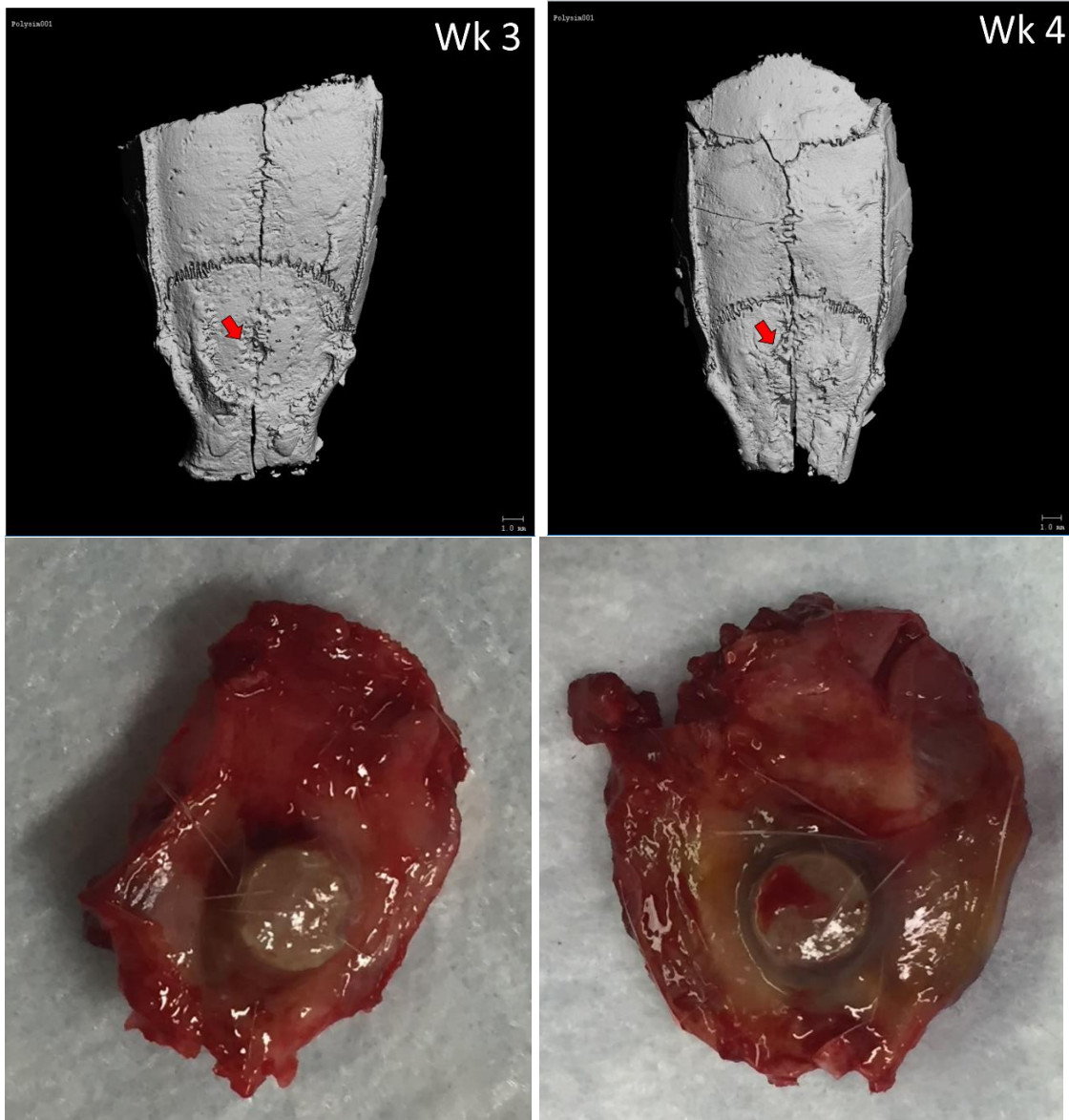


Figure 6.5 a) Photographs of harvested calvaria with disks intact at 3 and 4 wks. b) MicroCT images of calvaria of the same specimens.

The calvarium was harvested with the disk still encased in the fibrous capsule, shown in Figure 6.5. MicroCT shows slight indentation where the implant was or an otherwise different surface morphology compared to bone surrounding the implant,

which will be investigated later, histologically. The observations seen in the pilot aided in adjusting the disk dimensions for continuing with the main *in vivo* study giving insight as to what to expect.

6.4 Discussion

Simvastatin has been shown to inhibit myoblast formation at 1 μM , and BMP-2 at significantly lower concentrations,²²⁵ so the concentration chosen ensured a range where AP activity and myoblast inhibition had been previously seen. C2C12 myoblasts are normally known to differentiate into myotubes, which express characteristic biomarkers indicative of muscle. With BMP-2 treatment, however, differentiation can shift to an osteoblastic pathway in which cells express alkaline phosphatase, osteocalcin, and other known biomarkers of osteoblastic phenotype. This pathway shift diminishes, if not completely inhibits, formation of myotubes within the monolayer.²²⁶ While treating C2C12 cells is not as relevant towards bone promoting applications as MC3T3-E1 pre-osteoblasts, the cell line was used instead to present a clearer distinction between the positive control (BMP-2) and negative control (PBS) regarding AP expression. Osteogenic biomarkers such as AP will not be expressed in C2C12 cells as they mature, unless the treatment given promotes it, unlike MC3T3-E1 subclone 4 cells where AP expression and osteoblast differentiation are inevitable and different forms of treatment dictate the rate of that process.

BMP-2 is a potent stimulator of osteoblastic differentiation which is mediated by a collective family of Smad proteins after BMP-2 binds to the type II receptor that directly activates the type I receptor. Cyclin-dependent kinase 6 (cdk6) is subsequently repressed via the Rho/Smad pathway, a protein that would otherwise play a key role in

inhibiting osteoblastic differentiation.²²⁷ When added to C2C12 cells, the effects of phenamil promoting the expression of osteogenic biomarkers are seen within a day,²²⁸ and are more immediate compared to statins such as simvastatin that must first upregulate BMP-2 in order to have the same effect. While myotube inhibition caused by BMP-2 has been linked to the same Rho mechanism, simvastatin has been found to mediate myotube inhibition via Rac by HMG-CoA reductase inhibition, different from the suppression of Rho leading to BMP-2 upregulation which promotes AP expression in C2C12 cells.²²⁵ Regardless, the signaling pathways previously described explain how BMP-2 and simvastatin are able to promote significant AP expression in both non-osteoblastic and osteoblastic cell lines, which is why they worked well as positive controls.

Phenamil was chosen to supplement treatments due to its ability to augment the osteogenic effects of BMP-2. Its upregulation of BMP-2 is done by stimulating tribbles homolog 3 (Trb3), which enhances the BMP-Smad pathway.²²⁹ A concentration of 20 μM was used since one study found it as the highest to promote a dose-dependent.²³⁰ The synergistic effect phenamil had with the active treatments of BMP-2 at 3, 5, and 7 d, and simvastatin at 3 and 5 d can be attributed to the mediation of the BMP-Smad pathway. The expression level is not cumulative as what would be seen with mineralization of an osteogenic cell line, so the trend with decreasing AP activity up to 7 d post-confluency seen with simvastatin is not unusual. The expression levels of AP and other biomarkers can change dependent on the differentiation stage of the cell line. The small effect of the PSIM(5k) degradation products without phenamil may be an indication of the amount of simvastatin present compared to the other possible degradation products, i.e., mPEG(5k), dimerized or trimer simvastatin forms, and simvastatin attached to mPEG.

Simvastatin is a very small percent of the products, with simvastatin release profiles from the PSIM copolymer referenced in Chapter 4 showing amounts of simvastatin released being 2 to 3 orders of magnitude lower than the total mass lost. The simvastatin oligomers may not be active and the rate of degradation into monomers if taken up by the cells, remains to be determined. MPEG could also potentially hinder cellular uptake if simvastatin is still attached contributing to minimized activity because of the size, hydrophilicity, and uncharged nature of mPEG, rendering it difficult to being taken up by cells.

Fragmentation of some disks when implanted over the calvarium may be due to a mechanical stresses imposed on the sample. Possible reasons include initial disk movement before formation of the fibrous capsule over the disk, the high activity and grooming of the animals at or near the implantation site, and the slightly more brittle nature of the disk. The disk fragments may have also induced a large amount of inflammation at the site, further exacerbating the condition of the disk. The outlier of a majority of the disk being resorbed may be due to the residuals being found in the tissue more above the intended site. The indentation seen in microCT may indicate possible wearing of existing lamellar bone under the disk from minor but repeated disk movement within the implantation site. The morphology may otherwise indicate possible formation of new woven bone surrounding the disk as opposed to underneath, accentuating the indentation observed. This observation was seen and quantified in an *in vivo* study conducted by Jeon et al., where the thickness of bone underneath the intermittent and sustained simvastatin releasing devices was significantly lower than the woven bone

thickness surrounding it.²³¹ The observation will be further investigated in the main study with H&E staining.

6.5 Conclusions

Poly(simvastatin) degradation products were cytocompatible with myoblast cells at concentration levels at and above therapeutic levels of simvastatin. However, they promoted low to minimal osteogenic activity, which may be attributed to a significant percentage of the degradation products still in a conjugated and inactive state. Poly(simvastatin) disks *in vivo* were shown to affect the surface morphology of bone under and at the periphery of the disks. Whether these changes are an indication of new bone growth remains to be determined, but alongside its cytocompatibility, this copolymer shows potential for use as a regenerative biomaterial with further development.

Ch. 7 Summary and Conclusions

Polymerizing a commercialized cholesterol-regulating prodrug known as simvastatin via ROP was explored as a proof of concept. Degradation, simvastatin release, physical properties, and bioactivity of the resulting polymer were evaluated for potential use in bone regenerative applications.

By modifying reaction parameters, variation in reaction temperature was ultimately found to have the most effect on increasing the degree of simvastatin polymerization via stannous octoate. Further investigation of different catalysts led to desirably lower reaction temperature conditions, via TBD. Chromatography and spectroscopy techniques used to corroborate simvastatin conjugation supported the feasibility of utilizing the lactone ring of simvastatin to synthesize a diblock copolymer backbone comprised of simvastatin monomers in the secondary block. This observation opens a window to the ROP of many other lactone-incorporated drug precursors implemented in a variety of therapeutic drug delivery treatments that would benefit from an increased drug wt% while providing controlled release.

Using the TBD catalyst also allowed for the synthesis of PSIM copolymers initiated by mPEGs of decreasing sizes, releasing more simvastatin with decreased hydrophobicity. Blending different hydrophobic PLA-mPEG copolymers with poly(simvastatin) also resulted in modified rates of mass loss, simvastatin release and modified mechanical properties. These examples of copolymerization and blending demonstrate methods to easily tune poly(simvastatin) degradation and mechanical

properties, to better match different time periods of treatments. Lactide, glycolide, ϵ -caprolactone, or ricinoleic acid lactones, their respective polymers, or different PEG structures could be randomly or block copolymerized with simvastatin to further alter degradation or mechanical properties of the resulting copolymers more suitable to different delivery applications. Likewise, poly(simvastatin)-incorporated blends with these alternative polyesters or composites utilizing hydroxyapatite or calcium-based components could be considered to investigate the osteogenic nature of the resulting biomaterial alongside its structural properties and conformity to abnormal shapes of wound-sites in load-bearing bone.

Degradation products of PSIM inhibited HMG-CoA reductase potential enhancement of osteogenic expression and biocompatibility *in vitro* and *in vivo*. These observations demonstrate the potential to promote bone growth. Because HMG-CoA inhibition is linked to the expression of simvastatin's osteogenic properties, in addition to angiogenic and anti-atherosclerotic properties, future investigations of degradable poly(simvastatin) can potentially be broadened to include localized applications for maintaining vascular health. The tailorable qualities provided by copolymerizing pleiotropic simvastatin and co-blending its polymerized form can result in biomaterials suitable for a broad range of therapeutic drug delivery applications from vascular to bone regeneration.

Copyright © Theodora Atta Asafo-Adjei 2017

REFERENCES

1. Stebbins ND, Faig JJ, Yu W, Guliyev R and Uhrich KE. Polyactives: controlled and sustained bioactive release via hydrolytic degradation. *Biomaterials science*. 2015; 3: 1171-87.
2. Global strategies to reduce the health care burden of craniofacial anomalies: report of WHO meetings on international collaborative research on craniofacial anomalies. *The Cleft palate-craniofacial journal : official publication of the American Cleft Palate-Craniofacial Association*. 2004; 41: 238-43.
3. Dimitriou R, Jones E, McGonagle D and Giannoudis PV. Bone regeneration: current concepts and future directions. *Bmc Med*. 2011; 9.
4. Scheller EL and Krebsbach PH. Gene Therapy: Design and Prospects for Craniofacial Regeneration. *J Dent Res*. 2009; 88: 585-96.
5. Bostrom MPG and Seigerman DA. The Clinical Use of Allografts, Demineralized Bone Matrices, Synthetic Bone Graft Substitutes and Osteoinductive Growth Factors: A Survey Study. *HSS Journal*. 2005; 1: 9-18.
6. Giannoudis PV, Dinopoulos H and Tsiridis E. Bone substitutes: An update. *Injury*. 2005; 36: 20-7.
7. Porter JR, Ruckh TT and Popat KC. Bone Tissue Engineering: A Review in Bone Biomimetics and Drug Delivery Strategies. *Biotechnol Progr*. 2009; 25: 1539-60.
8. Bostrom MP and Seigerman DA. The clinical use of allografts, demineralized bone matrices, synthetic bone graft substitutes and osteoinductive growth factors: a survey study. *Hss Journal*. 2005; 1: 9-18.
9. Giannoudis PV, Dinopoulos H and Tsiridis E. Bone substitutes: an update. *Injury*. 2005; 36 Suppl 3: S20-7.
10. Mourino V and Boccaccini AR. Bone tissue engineering therapeutics: controlled drug delivery in three-dimensional scaffolds. *J R Soc Interface*. 2010; 7: 209-27.
11. Suchanek W and Yoshimura M. Processing and properties of hydroxyapatite-based biomaterials for use as hard tissue replacement implants. *J Mater Res*. 1998; 13: 94-117.
12. Rezwani K, Chen QZ, Blaker JJ and Boccaccini AR. Biodegradable and bioactive porous polymer/inorganic composite scaffolds for bone tissue engineering. *Biomaterials*. 2006; 27: 3413-31.
13. Low KL, Tan SH, Zein SHS, Roether JA, Mourino V and Boccaccini AR. Calcium phosphate-based composites as injectable bone substitute materials. *J Biomed Mater Res B*. 2010; 94B: 273-86.
14. Shindo ML, Costantino PD, Friedman CD and Chow LC. Facial Skeletal Augmentation Using Hydroxyapatite Cement. *Arch Otolaryngol*. 1993; 119: 185-90.
15. Garlotta D. A literature review of poly(lactic acid). *J Polym Environ*. 2001; 9: 63-84.
16. Dhandayuthapani B, Yoshida Y, Maekawa T and Kumar DS. Polymeric Scaffolds in Tissue Engineering Application: A Review. *Int J Polym Sci*. 2011.
17. Ajioka M, Enomoto K, Suzuki K and Yamaguchi A. The Basic Properties of Poly(Lactic Acid) Produced by the Direct Condensation Polymerization of Lactic-Acid. *J Environ Polym Degr*. 1995; 3: 225-34.
18. Maurus PB and Kaeding CC. Bioabsorbable implant material review. *Operative Techniques in Sports Medicine*. 2004; 12: 158-60.
19. Kaito T, Myoui A, Takaoka K, et al. Potentiation of the activity of bone morphogenetic protein-2 in bone regeneration by a PLA-PEG/hydroxyapatite composite. *Biomaterials*. 2005; 26: 73-9.
20. Kim HW, Lee HH and Knowles JC. Electrospinning biomedical nanocomposite fibers of hydroxyapatite/poly(lactic acid) for bone regeneration. *Journal of biomedical materials research Part A*. 2006; 79: 643-9.

21. Jain RA. The manufacturing techniques of various drug loaded biodegradable poly(lactide-co-glycolide) (PLGA) devices. *Biomaterials*. 2000; 21: 2475-90.
22. Advanced healthcare materials. Weinheim: Wiley-VCH,, 2012.
23. Middleton JC and Tipton AJ. Synthetic biodegradable polymers as orthopedic devices. *Biomaterials*. 2000; 21: 2335-46.
24. Bala I, Hariharan S and Kumar MN. PLGA nanoparticles in drug delivery: the state of the art. *Crit Rev Ther Drug Carrier Syst*. 2004; 21: 387-422.
25. Wu XS and Wang N. Synthesis, characterization, biodegradation, and drug delivery application of biodegradable lactic/glycolic acid polymers. Part II: biodegradation. *Journal of biomaterials science Polymer edition*. 2001; 12: 21-34.
26. Clark A. Treating Proximal Tibial Growth Plate Injuries Using Poly (Lactic-co-Glycolic Acid) Scaffolds.
27. Song CX, Labhasetwar V, Cui XM, Underwood T and Levy RJ. Arterial uptake of biodegradable nanoparticles for intravascular local drug delivery: Results with an acute dog model. *J Control Release*. 1998; 54: 201-11.
28. Hakkarainen M. Aliphatic polyesters: Abiotic and biotic degradation and degradation products. *Adv Polym Sci*. 2002; 157: 113-38.
29. Labet M and Thielemans W. Synthesis of polycaprolactone: a review. *Chem Soc Rev*. 2009; 38: 3484-504.
30. Lowry KJ, Hamson KR, Bear L, et al. Polycaprolactone/glass bioabsorbable implant in a rabbit humerus fracture model. *J Biomed Mater Res*. 1997; 36: 536-41.
31. Ikada Y and Tsuji H. Biodegradable polyesters for medical and ecological applications. *Macromol Rapid Comm*. 2000; 21: 117-32.
32. Storey RF and Sherman JW. Kinetics and mechanism of the stannous octoate-catalyzed bulk polymerization of epsilon-caprolactone. *Macromolecules*. 2002; 35: 1504-12.
33. Chuenjittkuntaworn B, Inrung W, Damrongsri D, Mekaapiruk K, Supaphol P and Pavasant P. Polycaprolactone/hydroxyapatite composite scaffolds: preparation, characterization, and in vitro and in vivo biological responses of human primary bone cells. *Journal of biomedical materials research Part A*. 2010; 94: 241-51.
34. Williams JM, Adewunmi A, Schek RM, et al. Bone tissue engineering using polycaprolactone scaffolds fabricated via selective laser sintering. *Biomaterials*. 2005; 26: 4817-27.
35. Hill JW. Studies on polymerization and ring formation XVII Friedel-Crafts syntheses with the polyanhydrides of the dibasic acids. *J Am Chem Soc*. 1932; 54: 4105-6.
36. Rosen HB, Chang J, Wnek GE, Linhardt RJ and Langer R. Bioerodible Polyanhydrides for Controlled Drug Delivery. *Biomaterials*. 1983; 4: 131-3.
37. Kumar N, Langer RS and Domb AJ. Polyanhydrides: an overview. *Adv Drug Deliver Rev*. 2002; 54: 889-910.
38. Jain JP, Modi S, Domb AJ and Kumar N. Role of polyanhydrides as localized drug carriers. *J Control Release*. 2005; 103: 541-63.
39. Jampel HD, Leong KW, Dunkelburger GR and Quigley HA. Glaucoma Filtration Surgery in Monkeys Using 5-Fluorouridine in Polyanhydride Disks. *Arch Ophthalmol-Chic*. 1990; 108: 430-5.
40. Kimura H, Ogura Y, Moritera T, et al. Injectable Microspheres with Controlled Drug Release for Glaucoma Filtering Surgery. *Invest Ophth Vis Sci*. 1992; 33: 3436-41.
41. Masters DB, Berde CB, Dutta S, Turek T and Langer R. Sustained Local-Anesthetic Release from Bioerodible Polymer Matrices - a Potential Method for Prolonged Regional Anesthesia. *Pharmaceut Res*. 1993; 10: 1527-32.
42. Schmeltzer RC, Anastasiou TJ and Uhrich KE. Optimized synthesis of salicylate-based poly(anhydride-esters). *Polym Bull*. 2003; 49: 441-8.

43. Odian GG. *Principles of polymerization*. New York,: McGraw-Hill, 1970, p.xviii, 652 p.
44. Hoffman AS. Hydrogels for biomedical applications. *Ann N Y Acad Sci*. 2001; 944: 62-73.
45. Maffezzoli A, Della Pietra A, Rengo S, Nicolais L and Valletta G. Photopolymerization of dental composite matrices. *Biomaterials*. 1994; 15: 1221-8.
46. Xing JF, Zheng ML and Duan XM. Two-photon polymerization microfabrication of hydrogels: an advanced 3D printing technology for tissue engineering and drug delivery. *Chem Soc Rev*. 2015; 44: 5031-9.
47. Sawhney AS, Pathak CP and Hubbell JA. Bioerodible Hydrogels Based on Photopolymerized Poly(Ethylene Glycol)-Co-Poly(Alpha-Hydroxy Acid) Diacrylate Macromers. *Macromolecules*. 1993; 26: 581-7.
48. Domb AJ, Ron E and Langer R. Poly(Anhydrides) .2. One-Step Polymerization Using Phosgene or Diphosgene as Coupling Agents. *Macromolecules*. 1988; 21: 1925-9.
49. Hyon SH, Jamshidi K and Ikada Y. Synthesis of polylactides with different molecular weights. *Biomaterials*. 1997; 18: 1503-8.
50. Odian G. Step polymerization. *Principles of Polymerization*. Fourth Edition ed. 2004, p. 39-198.
51. Carbone AL, Song M and Urrich KE. Iodinated salicylate-based poly(anhydride-esters) as radiopaque Biomaterials. *Biomacromolecules*. 2008; 9: 1604-12.
52. Kim Y and Verkade JG. Living polymerization of lactide using titanium alkoxide catalysts. *In Macromolecular Symposia*. 2005; 224: 105-18.
53. Kurcok P, Penczek J, Franek J and Jedlinski Z. Anionic-Polymerization of Lactones .14. Anionic Block Copolymerization of Delta-Valerolactone and L-Lactide Initiated with Potassium Methoxide. *Macromolecules*. 1992; 25: 2285-9.
54. Lohmeijer BGG, Pratt RC, Leibfarth F, et al. Guanidine and amidine organocatalysts for ring-opening polymerization of cyclic esters. *Macromolecules*. 2006; 39: 8574-83.
55. Jensen TR, Breyfogle LE, Hillmyer MA and Tolman WB. Stereoelective polymerization of D,L-lactide using N-heterocyclic carbene based compounds. *Chemical communications*. 2004: 2504-5.
56. Shibasaki Y, Sanada H, Yokoi M, Sanda F and Endo T. Activated monomer cationic polymerization of lactones and the application to well-defined block copolymer synthesis with seven-membered cyclic carbonate. *Macromolecules*. 2000; 33: 4316-20.
57. Gopferich A. Mechanisms of polymer degradation and erosion. *Biomaterials*. 1996; 17: 103-14.
58. Mata-Perez F and Perez-Benito JF. The kinetic rate law for autocatalytic reactions. *Journal of Chemical Education*. 1987; 64: 925-7.
59. Urrich KE, Cannizzaro SM, Langer RS and Shakesheff KM. Polymeric systems for controlled drug release. *Chem Rev*. 1999; 99: 3181-98.
60. Breitenbach A, Li YX and Kissel T. Branched biodegradable polyesters for parenteral drug delivery systems. *J Control Release*. 2000; 64: 167-78.
61. Wang M, Gan D and Wooley KL. Linear and hyperbranched poly (silyl ester)s: Synthesis via cross-dehydrocoupling-based polymerization, hydrolytic degradation properties, and morphological analysis by atomic force microscopy. *Macromolecules*. 2001; 34: 3215-23.
62. Qiu LY and Bae YH. Polymer architecture and drug delivery. *Pharmaceut Res*. 2006; 23: 1-30.
63. McKee MG, Unal S, Wilkes GL and Long TE. Branched polyesters: recent advances in synthesis and performance. *Prog Polym Sci*. 2005; 30: 507-39.
64. Zhang J, Zhao YJ, Su ZG and Ma GH. Synthesis of monomethoxy poly(ethylene glycol) without diol poly(ethylene glycol). *J Appl Polym Sci*. 2007; 105: 3782-6.

65. Avgoustakis K, Beletsi A, Panagi Z, et al. Effect of copolymer composition on the physicochemical characteristics, in vitro stability, and biodistribution of PLGA-mPEG nanoparticles. *Int J Pharmaceut.* 2003; 259: 115-27.
66. Banerjee SS, Aher N, Patil R and Khandare J. Poly(ethylene glycol)-Prodrug Conjugates: Concept, Design, and Applications. *Journal of drug delivery.* 2012; 2012: 103973.
67. Knop K, Hoogenboom R, Fischer D and Schubert US. Poly(ethylene glycol) in Drug Delivery: Pros and Cons as Well as Potential Alternatives. *Angew Chem Int Edit.* 2010; 49: 6288-308.
68. Olivier JC. Drug transport to brain with targeted nanoparticles. *NeuroRx : the journal of the American Society for Experimental NeuroTherapeutics.* 2005; 2: 108-19.
69. Tormala P. Determination of Glass-Transition Temperature of Poly(Ethylene Glycol) by Spin Probe Technique. *Eur Polym J.* 1974; 10: 519-21.
70. Li FJ, Zhang SD, Liang JZ and Wang JZ. Effect of polyethylene glycol on the crystallization and impact properties of polylactide-based blends. *Polym Advan Technol.* 2015; 26: 465-75.
71. Sungsanit K, Kao N and Bhattacharya SN. Properties of linear poly(lactic acid)/polyethylene glycol blends. *Polym Eng Sci.* 2012; 52: 108-16.
72. Wischke C and Schwendeman SP. Principles of encapsulating hydrophobic drugs in PLA/PLGA microparticles. *Int J Pharm.* 2008; 364: 298-327.
73. Butler SM, Tracy MA and Tilton RD. Adsorption of serum albumin to thin films of poly(lactide-co-glycolide). *J Control Release.* 1999; 58: 335-47.
74. Cleek RL, Ting KC, Eskin SG and Mikos AG. Microparticles of poly (DL-lactic-co-glycolic acid)/poly (ethylene glycol) blends for controlled drug delivery. *J Control Release.* 1997; 48: 259-68.
75. Ringsdorf H. Structure and Properties of Pharmacologically Active Polymers. *J Polym Sci Pol Sym.* 1975: 135-53.
76. Joshi HN. Recent Advances in Drug Delivery Systems: Polymeric Prodrugs. *Pharmaceutical Technology.* 1988: 118.
77. Gupta P, Authimoolam SP, Hilt JZ and Dziubla TD. Quercetin conjugated poly(beta-amino esters) nanogels for the treatment of cellular oxidative stress. *Acta Biomater.* 2015; 27: 194-204.
78. Patil VS, Dziubla TD and Kalika DS. Static and dynamic properties of biodegradable poly (antioxidant β -amino ester) networks based on incorporation of curcumin multiacrylate. *Polym Bull.* 2015; 75: 88-96.
79. Jeon JH, Thomas MV and Puleo DA. Bioerodible devices for intermittent release of simvastatin acid. *Int J Pharm.* 2007; 340: 6-12.
80. Jeon JH and Puleo DA. Alternating release of different bioactive molecules from a complexation polymer system. *Biomaterials.* 2008; 29: 3591-8.
81. Sundararaj SC, Thomas MV, Peyyala R, Dziubla TD and Puleo DA. Design of a multiple drug delivery system directed at periodontitis. *Biomaterials.* 2013; 34: 8835-42.
82. Fisher PD, Palomino P, Milbrandt TA, Hilt JZ and Puleo DA. Improved small molecule drug release from in situ forming poly(lactic-co-glycolic acid) scaffolds incorporating poly(beta-amino ester) and hydroxyapatite microparticles. *Journal of biomaterials science Polymer edition.* 2014; 25: 1174-93.
83. Brown ME, Zou Y, Peyyala R, Dziubla TD and Puleo DA. Temporal separation in the release of bioactive molecules from a moldable calcium sulfate bone graft substitute. *Curr Drug Deliv.* 2014; 11: 605-12.
84. Orellana BR, Hilt JZ and Puleo DA. Drug release from calcium sulfate-based composites. *J Biomed Mater Res B Appl Biomater.* 2015; 103: 135-42.
85. Wozney JM. Overview of bone morphogenetic proteins. *Spine.* 2002; 27: S2-S8.

86. Ebara S and Nakayama K. Mechanism for the action of bone morphogenetic proteins and regulation of their activity. *Spine (Phila Pa 1976)*. 2002; 27: S10-5.
87. Rao SM, Ugale GM and Warad SB. Bone morphogenetic proteins: periodontal regeneration. *North American journal of medical sciences*. 2013; 5: 161-8.
88. Rai B, Teoh SH, Hutmacher DW, Cao T and Ho KH. Novel PCL-based honeycomb scaffolds as drug delivery systems for rhBMP-2. *Biomaterials*. 2005; 26: 3739-48.
89. Kempen DH, Lu L, Hefferan TE, et al. Retention of in vitro and in vivo BMP-2 bioactivities in sustained delivery vehicles for bone tissue engineering. *Biomaterials*. 2008; 29: 3245-52.
90. Laurencin CT, Attawia MA, Lu LQ, et al. Poly(lactide-co-glycolide)/hydroxyapatite delivery of BMP-2-producing cells: a regional gene therapy approach to bone regeneration. *Biomaterials*. 2001; 22: 1271-7.
91. Zhou AJ, Clokie CM and Peel SA. A novel peptide to enhance recombinant BMP-2 production in mammalian cell cultures. *BMC Proc*. 2011; 5 Suppl 8: P96.
92. Wozney JM, Rosen V, Celeste AJ, et al. Novel regulators of bone formation: molecular clones and activities. *Science*. 1988; 242: 1528-34.
93. Chen NF, Smith ZA, Stiner E, Armin S, Sheikh H and Khoo LT. Symptomatic ectopic bone formation after off-label use of recombinant human bone morphogenetic protein-2 in transforaminal lumbar interbody fusion: Report of 4 cases. *Journal of Neurosurgery: Spine*. 2010; 12: 40-6.
94. Davignon J and Mabile L. Mechanisms of action of statins and their pleiotropic effects. *Ann Endocrinol-Paris*. 2001; 62: 101-12.
95. Elavarasu S, Suthanthiran TK and Naveen D. Statins: A new era in local drug delivery. *Journal of pharmacy & bioallied sciences*. 2012; 4: S248-51.
96. Schachter M. Chemical, pharmacokinetic and pharmacodynamic properties of statins: an update. *Fund Clin Pharmacol*. 2005; 19: 117-25.
97. Mundy G, Garrett R, Harris S, et al. Stimulation of bone formation in vitro and in rodents by statins. *Science*. 1999; 286: 1946-9.
98. Yazawa H, Zimmermann B, Asami Y and Bernimoulin JP. Simvastatin promotes cell metabolism, proliferation, and osteoblastic differentiation in human periodontal ligament cells. *J Periodontol*. 2005; 76: 295-302.
99. Keogh A, Macdonald P, Kaan A, Aboyoum C, Spratt P and Mundy J. Efficacy and safety of pravastatin vs simvastatin after cardiac transplantation. *J Heart Lung Transpl*. 2000; 19: 529-37.
100. Issues in Aesthetic, Craniofacial, Maxillofacial, Oral, and Plastic Surgery. In: Acton QA, (ed.). Atlanta, Georgia: ScholarlyEditions, 2013.
101. Tonetti MS, D'Aiuto F, Nibali L, et al. Treatment of periodontitis and endothelial function. *N Engl J Med*. 2007; 356: 911-20.
102. Yoshito I and Tsujih H. Biodegradable polyesters for medical and ecological applications. *Macromol Rapid Commun*. 2000; 21: 117-32.
103. Gunaitllake PA and Adhikari R. Biodegradable Synthetic Polymers for Tissue Engineering. *Eur Cell Mater*. 2003; 5: 1-16.
104. Dhandayuthapani B, Yoshida Y, Maekawa T and Kumar DS. Polymeric Scaffolds in Tissue Engineering Application: A Review. *Int J Polym Sci*. 2011; 2011.
105. Langer R. New Methods of Drug Delivery. *Science*. 1990; 249: 1527-33.
106. Rohini NA, Agrawal N, Joseph A and Mukerji A. Polymeric Prodrugs: Recent Achievements and General Strategies. *J Antivir Antiretrovir S*. 2013; 2.
107. Duncan R. Polymer conjugates as anticancer nanomedicines. *Nature* 2006; 6: 688-701.
108. Banerjee SS, Aher N, Patil R and Khandare J. Poly(ethylene glycol)-Prodrug Conjugates: Concept, Design, and Applications. *J Drug Delivery*. 2012; 2012.

109. Joshi HN. Recent Advances in Drug Delivery Systems, Polymeric Prodrugs. *Pharm Technol.* 1988; 12: 120-30.
110. Cleek RL, Ting KC, Eskin SG and Mikos AG. Microparticles of poly(dl-lactic-co-glycolic acid)/poly(ethylene glycol) blends for controlled drug delivery. *J Controlled Release.* 1997; 48: 259-68.
111. Yeo Y and Park K. Control of Encapsulation Efficiency and Initial Burst in Polymeric Microparticle Systems. *Arch Pharm Res.* 2004; 27: 1-12.
112. Saltzman WM and Fung LK. Polymeric implants for cancer chemotherapy. *Adv Drug Delivery Rev.* 1997; 26: 209-30.
113. Alexis F, Venkatraman SS, Rath SK and Boey F. In vitro study of release mechanisms of paclitaxel and rapamycin from drug-incorporated biodegradable stent matrices. *J Controlled Release.* 2004; 98: 67-74.
114. Huang X and Brazel CS. On the importance and mechanisms of burst release in matrix-controlled drug delivery systems. *J Controlled Release.* 2001; 73: 121-36.
115. Carbone AL and Uhrich KE. Design and Synthesis of Fast-Degrading Poly(anhydride-esters). *Macromol Rapid Commun.* 2009; 30: 1021-6.
116. Wattamwar PP, Mo Y, Wan R, Palli R, Zhang Q and Dziubla TD. Antioxidant Activity of Degradable Polymer Poly(trolox-ester) to Suppress Oxidative Stress Injury in the Cells. *Adv Funct Mater.* 2010; 20: 147-54.
117. Slivniak R and Domb AJ. Macrolactones and polyesters from ricinoleic acid. *Biomacromolecules.* 2005; 6: 1679-88.
118. Kricheldorf HR, Kreiser-Saunders J and Boettcher C. Polylactones:31. Sn(II)octoate-initiated polymerization of L-lactide: a mechanistic study. *Polym.* 1995; 36: 1253-9.
119. Nuyken O and Pask SD. Ring-Opening Polymerization—An Introductory Review. *Polym.* 2013; 5: 361-403.
120. Sparrow CP, Burton CA, Hernandez M, et al. Simvastatin Has Anti-Inflammatory and Anti-atherosclerotic Activity Independent of Plasma Cholesterol Lowering. *Arterioscler Thromb Vasc Biol.* 2001; 21: 115-21.
121. Kureishi Y, Luo Z, Shiojima I, et al. The HMG-CoA reductase inhibitor simvastatin activates the protein kinase Akt and promotes angiogenesis in normocholesterolemic animals. *Nature medicine.* 2000; 6: 1004-10.
122. Chen PY, Sun JS, Tsuang YH, Chen MH, Weng PW and Lin FH. Simvastatin promotes osteoblast viability and differentiation via Ras/Smad/Erk/BMP-2 signaling pathway. *Nutrition research.* 2010; 30: 191-9.
123. Istvan ES and Deisenhofer J. Structural mechanism for statin inhibition of HMG-CoA reductase. *Science.* 2001; 292: 1160-4.
124. Porter JR, Ruckh TT and Popat KC. Bone tissue engineering: a review in bone biomimetics and drug delivery strategies. *Biotechnol Prog.* 2009; 25: 1539-60.
125. Wong RW and Rabie AB. Statin-induced osteogenesis uses in orthodontics: a scientific review. *World journal of orthodontics.* 2006; 7: 35-40.
126. Prueksaritanont T, Gorham LM, Ma B, et al. In vitro metabolism of simvastatin in humans [SBT]identification of metabolizing enzymes and effect of the drug on hepatic P450s. *Drug metabolism and disposition: the biological fate of chemicals.* 1997; 25: 1191-9.
127. Armitage J, Bowman L, Collins R, Parish S, Tobert J and Group MBHPSC. Effects of simvastatin 40 mg daily on muscle and liver adverse effects in a 5-year randomized placebo-controlled trial in 20,536 high-risk people. *BMC Clin Pharmacol.* 2009; 9.
128. Dziubla TD, Karim A and Muzykantov VR. Polymer nanocarriers protecting active enzyme cargo against proteolysis. *J Controlled Release.* 2005; 102: 427-39.
129. Jing Zhang J, Zhao Y, Su Z and Ma G. Synthesis of Monomethoxy Poly(ethylene glycol) without Diol Poly(ethylene glycol). *J Appl Polym Sci.* 2007; 105: 3780-6.

130. Ambike AA, Mahadik KR and Paradkar A. Physico-chemical characterization and stability study of glassy simvastatin. *Drug development and industrial pharmacy*. 2005; 31: 895-9.
131. Tessmar JK and Gopferich AM. Customized PEG-derived copolymers for tissue-engineering applications. *Macromolecular bioscience*. 2007; 7: 23-39.
132. Knop K, Hoogenboom R, Fischer D and Schubert US. Poly(ethylene glycol) in drug delivery: pros and cons as well as potential alternatives. *Angewandte Chemie*. 2010; 49: 6288-308.
133. Save M, Schappacher M and Soum A. Controlled Ring-Opening Polymerization of Lactones and Lactides Initiated by Lanthanum Isopropoxide. *Macromol Chem Phys*. 2002; 203: 889-99.
134. Puaux J, Banu I, Nagy I and Bozga G. A Study of L-Lactide Ring-Opening Polymerization Kinetics. *Macromol Symp*. 259: 318-26.
135. Kaihara S, Matsumura S, Mikos AG and Fisher JP. Synthesis of poly(L-lactide) and polyglycolide by ring-opening polymerization. *Nature protocols*. 2007; 2: 2767-71.
136. Labet M and Thielemans W. Synthesis of polycaprolactone: a review. *Chem Soc Rev*. 2009; 38: 3484-504.
137. Storey RF. Kinetics and Mechanism of the Stannous Octoate-Catalyzed Bulk Polymerization of ϵ -Caprolactone. *Macromolecules*. 2002; 35: 1504-12.
138. Odian G. *Principles of Polymerization*. 4th ed. Hoboken, NJ: John Wiley & Sons, Inc., 2004.
139. Górnjak A, Karolewicz B, Żurawska-Plaksej E and Pluta J. Thermal, spectroscopic, and dissolution studies of the simvastatin-acetylsalicylic acid mixtures. *J Therm Anal Calorim*. 2013; 111: 2125-32.
140. Aleman C, Betran O, Casanovas J, Houk KN and Hall HKJ. Thermodynamic control of the polymerizability of five-, six-, and seven-membered lactones. *The Journal of organic chemistry*. 2009; 74: 6237-44.
141. Ahuja R, Kundu S, Goldman AS, Brookhart M, Vicente BC and Scott SL. Catalytic ring expansion, contraction, and metathesis-polymerization of cycloalkanes. *Chem Commun (Camb)*. 2008: 253-5.
142. Otera J. Transesterification. *Chem Rev*. 1993; 93: 1449-70.
143. Sunder A, Hanselmann R, Frey H and Mu R. Controlled Synthesis of Hyperbranched Polyglycerols by Ring-Opening Multibranching Polymerization. *Macromolecules*. 1999; 32: 4240-6.
144. Tasaka F, Ohya Y and Ouchi T. One-Pot Synthesis of Novel Branched Polylactide Through the Copolymerization of Lactide with Mevalonolactone. *Macromol Rapid Commun*. 2001; 22: 820-4.
145. Disjstra PJ, Du H and Feijen J. Single site catalysts for stereoselective ring-opening polymerization of lactides. *Polym Chem*. 2011; 2: 520-7.
146. Katiyar V and Nanavati H. Ring-opening polymerization of L-lactide using N-heterocyclic molecules: mechanistic, kinetics and DFT studies. *Polym Chem*. 2010; 1: 1491-500.
147. Duda A and Kowalski A. *Handbook of Ring-Opening Polymerization*. KGaA, Weinheim: Wiley-VCH Verlag GmbH & Co., 2009.
148. Veld PJA, Velner EM, Witte PVD, Hamhuis J, Dijkstra PJ and Feijen J. Melt Block Copolymerization of ϵ -Caprolactone and L-Lactide. *J Polym Sci A Polym Chem*. 1997; 35: 219-25.
149. Xie WH, Zhu WP and Shen ZQ. Synthesis, isothermal crystallization and micellization of mPEG-PCL diblock copolymers catalyzed by yttrium complex. *Polymer*. 2007; 48: 6791-8.

150. Kaesemeyer WH, Caldwell RB, Huang J and Caldwell RW. Pravastatin sodium activates endothelial nitric oxide synthase independent of its cholesterol-lowering actions. *Journal of the American College of Cardiology*. 1999; 33: 234-41.
151. Hakkarainen M and Albertsson A-C. Degradation Products of Aliphatic and Aromatic Polyesters. In: Hakkarainen M, Burman L, Albertsson A-C, Gröning M and Strandberg C, (eds.). *Chromatography for Sustainable Polymeric Materials*. Verlag Berlin Heidelberg: Springer, 2008, p. 85-116.
152. Lewis JK, Wei J and Siuzdak G. Matrix-assisted Laser Desorption/Ionization Mass Spectrometry in Peptide and Protein Analysis. In: Meyers RA, (ed.). *Encyclopedia of Analytical Chemistry*. Chichester: John Wiley & Sons Ltd, 2000, p. 5880-94.
153. Wang H, Wu Y and Zhao Z. Fragmentation study of simvastatin and lovastatin using electrospray ionization tandem mass spectrometry. *Journal of mass spectrometry : JMS*. 2001; 36: 58-70.
154. Keller BO and Li L. Discerning matrix-cluster peaks in matrix-assisted laser desorption/ionization time-of-flight mass spectra of dilute peptide mixtures. *Journal of the American Society for Mass Spectrometry*. 2000; 11: 88-93.
155. Save M, Schappacher M and Soum A. Controlled Ring-Opening Polymerization of Lactones and Lactides Initiated by Lanthanum Isopropoxide, 1. General Aspects and Kinetics. *Macromolecular chemistry and physics*. 2002; 203: 889-99.
156. Hiltunen K, Seppälä JV and Härkönen M. Effect of catalyst and polymerization conditions on the preparation of low molecular weight lactic acid polymers. *Macromolecules*. 1997; 30: 373-9.
157. Pepels MPF, Bouyahyi M, Heise A and Duchateau R. Kinetic investigation on the catalytic ring-opening (co) polymerization of (macro) lactones using aluminum salen catalysts. *Macromolecules*. 2013; 46: 4324-34.
158. Pratt RC, Lohmeijer BG, Long DA, Waymouth RM and Hedrick JL. Triazabicyclodecene: a simple bifunctional organocatalyst for acyl transfer and ring-opening polymerization of cyclic esters. *J Am Chem Soc*. 2006; 128: 4556-7.
159. Asafo-Adjei TA, Dziubla TD and Puleo DA. Synthesis and characterization of a poly(ethylene glycol)-poly(simvastatin) diblock copolymer. *Rsc Adv*. 2014; 4: 58287-98.
160. Chuma A, Horn HW, Swope WC, et al. The reaction mechanism for the organocatalytic ring-opening polymerization of L-lactide using a guanidine-based catalyst: hydrogen-bonded or covalently bound? *J Am Chem Soc*. 2008; 130: 6749-54.
161. Kamber NE, Jeong W, Waymouth RM, Pratt RC, Lohmeijer BG and Hedrick JL. Organocatalytic ring-opening polymerization. *Chem Rev*. 2007; 107: 5813-40.
162. Kiesewetter MK, Shin EJ, Hedrick JL and Waymouth RM. Organocatalysis: opportunities and challenges for polymer synthesis. *Macromolecules*. 2010; 43: 2093-107.
163. Nederberg F, Lohmeijer BG, Leibfarth F, et al. Organocatalytic ring opening polymerization of trimethylene carbonate. *Biomacromolecules*. 2007; 8: 153-60.
164. Chen CSH. Polymerization and copolymerization of trioxane: Factors influencing molecular weight and end groups. *Journal of Polymer Science: Polymer Chemistry Edition*. 1975; 13: 1183-208.
165. Rakova GV, Shaginyan AA and Yenikolopyan NS. Effect of temperature and catalyst concentration on molecular weight during polymerization of trioxane in solution. *Polymer Science USSR*. 1967; 9: 2916-24.
166. Simon L and Goodman JM. The mechanism of TBD-catalyzed ring-opening polymerization of cyclic esters. *J Org Chem*. 2007; 72: 9656-62.
167. Zhong Z, Ankoné MJ, Dijkstra PJ, Birg C, Westerhausen M and Feijen J. Calcium methoxide initiated ring-opening polymerization of ϵ -caprolactone and L-lactide. *Polym Bull*. 2001; 46: 51-7.

168. Ambrosio AM, Allcock HR, Katti DS and Laurencin CT. Degradable polyphosphazene/poly(alpha-hydroxyester) blends: degradation studies. *Biomaterials*. 2002; 23: 1667-72.
169. Allen C, Han J, Yu Y, Maysinger D and Eisenberg A. Polycaprolactone–b-poly (ethylene oxide) copolymer micelles as a delivery vehicle for dihydrotestosterone. *J Control Release*. 2000; 63: 275-86.
170. Park TG. Degradation of Poly(Lactic-Co-Glycolic Acid) Microspheres - Effect of Copolymer Composition. *Biomaterials*. 1995; 16: 1123-30.
171. Park TG. Degradation of Poly(D,L-Lactic Acid) Microspheres - Effect of Molecular-Weight. *J Control Release*. 1994; 30: 161-73.
172. Celikkaya E, Denkbaz EB and Piskin E. Poly (DL- lactide)/poly (ethylene glycol) copolymer particles. I. Preparation and characterization. *J Appl Polym Sci*. 1996; 61: 1439-46.
173. Lee SH, Kim SH, Han YK and Kim YH. Synthesis and degradation of end-group-functionalized polylactide. *J Polym Sci Pol Chem*. 2001; 39: 973-85.
174. Cha Y and Pitt CG. The Biodegradability of Polyester Blends. *Biomaterials*. 1990; 11: 108-12.
175. Oh JK. Polylactide (PLA)-based amphiphilic block copolymers: synthesis, self-assembly, and biomedical applications. *Soft Matter*. 2011; 7: 5096-108.
176. Bae YH, Huh KM, Kim Y and Park K. Biodegradable amphiphilic multiblock copolymers and their implications for biomedical applications. *J Control Release*. 2000; 64: 3-13.
177. Mundargi RC, Babu VR, Rangaswamy V, Patel P and Aminabhavi TM. Nano/micro technologies for delivering macromolecular therapeutics using poly(D,L-lactide-co-glycolide) and its derivatives. *J Control Release*. 2008; 125: 193-209.
178. Sastry SV, Nyshadham JR and Fix JA. Recent technological advances in oral drug delivery - a review. *Pharmaceutical science & technology today*. 2000; 3: 138-45.
179. Kim MS, Kim SK, Kim SH, Hyun H, Khang G and Lee HB. In vivo osteogenic differentiation of rat bone marrow stromal cells in thermosensitive MPEG-PCL diblock copolymer gels. *Tissue Eng*. 2006; 12: 2863-73.
180. Wang SG and Bo Q. Polycaprolactone–poly (ethylene glycol) block copolymer, I: synthesis and degradability in vitro. *Polym Advan Technol*. 1993; 4: 363-6.
181. Fu SZ, Ni PY, Wang BY, et al. Injectable and thermo-sensitive PEG-PCL-PEG copolymer/collagen/n-HA hydrogel composite for guided bone regeneration. *Biomaterials*. 2012; 33: 4801-9.
182. Jiang CP, Chen YY, Hsieh MF and Lee HM. Solid freeform fabrication and in-vitro response of osteoblast cells of mPEG-PCL-mPEG bone scaffolds. *Biomed Microdevices*. 2013; 15: 369-79.
183. Wen YH, Gallego MR, Nielsen LF, et al. Biodegradable nanocomposite microparticles as drug delivering injectable cell scaffolds. *J Control Release*. 2011; 156: 11-20.
184. Dong YC and Feng SS. Methoxy poly(ethylene glycol)-poly(lactide) (MPEG-PLA) nanoparticles for controlled delivery of anticancer drugs. *Biomaterials*. 2004; 25: 2843-9.
185. Tsuji H and Ikada Y. Blends of aliphatic polyesters .1. Physical properties and morphologies of solution-cast blends from poly(DL-lactide) and poly(epsilon-caprolactone). *J Appl Polym Sci*. 1996; 60: 2367-75.
186. Rosario-Melendez R, Harris CL, Delgado-Rivera R, Yu L and Uhrich KE. PolyMorphine: An innovative biodegradable polymer drug for extended pain relief. *J Control Release*. 2012; 162: 538-44.
187. Wattamwar PP, Hardas SS, Butterfield DA, Anderson KW and Dziubla TD. Tuning of the pro-oxidant and antioxidant activity of trolox through the controlled release from biodegradable poly(trolox ester) polymers. *Journal of Biomedical Materials Research Part A*. 2011; 99A: 184-91.

188. Tang HD, Murphy CJ, Zhang B, et al. Curcumin polymers as anticancer conjugates. *Biomaterials*. 2010; 31: 7139-49.
189. Dziubla TD, Karim A and Muzykantov VR. Polymer nanocarriers protecting active enzyme cargo against proteolysis. *J Control Release*. 2005; 102: 427-39.
190. Ubeaud G, Hagenbach J, Vandenschrieck S, Jung L and Koffel JC. In vitro inhibition of simvastatin metabolism in rat and human liver by naringenin. *Life Sci*. 1999; 65: 1403-12.
191. Vree TB, Dammers E, Ulc I, Horkovics-Kovats S, Ryska M and Merx I. Differences Between Lovastatin and Simvastatin Hydrolysis in Healthy Male and Female Volunteers. *The Scientific World Journal*. 2003; 3: 1332-43.
192. Clark A, Milbrandt TA, Hilt JZ and Puleo DA. Tailoring properties of microsphere-based poly(lactic-co-glycolic acid) scaffolds. *Journal of biomedical materials research Part A*. 2014; 102: 348-57.
193. Perchellet JPH, Perchellet EM, Crow KR, et al. Novel synthetic inhibitors of 3-hydroxy-3-methylglutaryl-coenzyme A (HMG-CoA) reductase activity that inhibit tumor cell proliferation and are structurally unrelated to existing statins. *Int J Mol Med*. 2009; 24: 633-43.
194. Roberts CK, Liang KH, Barnard RJ, Kim CH and Vaziri ND. HMG-CoA reductase, cholesterol 7 alpha-hydroxylase, LDL receptor, SR-B1, and ACAT in diet-induced syndrome X. *Kidney Int*. 2004; 66: 1503-11.
195. Baskaran G, Salvamani S, Ahmad SA, Shaharuddin NA, Pattiram PD and Shukor MY. HMG-CoA reductase inhibitory activity and phytochemical investigation of *Basella alba* leaf extract as a treatment for hypercholesterolemia. *Drug design, development and therapy*. 2015; 9: 509-17.
196. Tsuji H and Ikada Y. Blends of aliphatic polyesters. II. Hydrolysis of solution-cast blends from poly(L-lactide) and poly(ϵ -caprolactone) in phosphate-buffered solution. *Journal of applied polymer science*. 1998; 67: 405-15.
197. Song C, Guo Z, Ma Q, et al. Simvastatin induces osteoblastic differentiation and inhibits adipocytic differentiation in mouse bone marrow stromal cells. *Biochemical and biophysical research communications*. 2003; 308: 458-62.
198. Maeda T, Kawane T and Horiuchi N. Statins augment vascular endothelial growth factor expression in osteoblastic cells via inhibition of protein prenylation. *Endocrinology*. 2003; 144: 681-92.
199. Tracy MA, Ward KL, Firouzabadian L, et al. Factors affecting the degradation rate of poly(lactide-co-glycolide) microspheres in vivo and in vitro. *Biomaterials*. 1999; 20: 1057-62.
200. Pasanen MK, Neuvonen M, Neuvonen PJ and Niemi M. SLCO1B1 polymorphism markedly affects the pharmacokinetics of simvastatin acid. *Pharmacogenet Genomics*. 2006; 16: 873-9.
201. Horgan DJ, Stoops JK, Webb EC and Zerner B. Carboxylesterases (EC 3.1.1). A large-scale purification of pig liver carboxylesterase. *Biochemistry*. 1969; 8: 2000-6.
202. Thomas S, Grohens Y, Jyotishkumar P and eds. Characterization of polymer blends: miscibility, morphology and interfaces. John Wiley & Sons, 2014.
203. Misch CE, Qu Z and Bidez MW. Mechanical properties of trabecular bone in the human mandible: implications for dental implant treatment planning and surgical placement. *J Oral Maxillofac Surg*. 1999; 57: 700-6; discussion 6-8.
204. Cowin SC. Wolff's law of trabecular architecture at remodeling equilibrium. *Journal of Biomechanical Engineering*. 1986; 108: 83-8.
205. Evans SL and Gregson PJ. Composite technology in load-bearing orthopaedic implants. *Biomaterials*. 1998; 19: 1329-42.
206. Na YH, He Y, Shuai X, Kikkawa Y, Doi Y and Inoue Y. Compatibilization effect of poly(ϵ -caprolactone)-*b*-poly(ethylene glycol) block copolymers and phase morphology

- analysis in immiscible poly(lactide)/poly(epsilon-caprolactone) blends. *Biomacromolecules*. 2002; 3: 1179-86.
207. Kulinski Z, Piorkowska E, Gadzinowska K and Stasiak M. Plasticization of poly(L-lactide) with poly(propylene glycol). *Biomacromolecules*. 2006; 7: 2128-35.
208. Wu T, He Y, Fan Z, Wei J and Li S. Investigations on the morphology and melt crystallization of poly (L- lactide)- poly (ethylene glycol) diblock copolymers. *Polymer Engineering & Science*. 2008; 48: 425-33.
209. Mohanty AK, Jana U, Manna PK and Mohanta GP. Synthesis and evaluation of MePEG-PCL diblock copolymers: surface properties and controlled release behavior. *Prog Biomater*. 2015; 4: 89-100.
210. Wilke RA, Ramsey LB, Johnson SG, et al. The clinical pharmacogenomics implementation consortium: CPIC guideline for SLCO1B1 and simvastatin-induced myopathy. *Clinical pharmacology and therapeutics*. 2012; 92: 112-7.
211. Cheng HY, Rogers JD, Sweany AE, et al. Influence of Age and Gender on the Plasma Profiles of 3-Hydroxy-3-Methylglutaryl-Coenzyme a (Hmg-Coa) Reductase Inhibitory Activity Following Multiple Doses of Lovastatin and Simvastatin. *Pharmaceut Res*. 1992; 9: 1629-33.
212. Gonyeau MJ. Statins and osteoporosis: A clinical review. *Pharmacotherapy*. 2005; 25: 228-43.
213. Krauth D, Anglemeyer A, Philipps R and Bero L. Nonindustry-Sponsored Preclinical Studies on Statins Yield Greater Efficacy Estimates Than Industry-Sponsored Studies: A Meta-Analysis. *Plos Biol*. 2014; 12.
214. Aitken M, Berndt ER and Cutler DM. Prescription Drug Spending Trends In The United States: Looking Beyond The Turning Point. *Health Affair*. 2009; 28: W151-W60.
215. Davignon J and Mabile L. Mechanisms of action of statins and their pleiotropic effects. *Ann Endocrinol*. 2001; 62: 101.
216. Liao JK and Laufs U. Pleiotropic effects of statins. *Annual review of pharmacology and toxicology*. 2005; 45: 89-118.
217. Kureishi Y, Luo Z, Shiojima I, et al. The HMG-CoA reductase inhibitor simvastatin activates the protein kinase Akt and promotes angiogenesis in normocholesterolemic animals. *Nature medicine*. 2000; 6: 1004-10.
218. Leung BP, Sattar N, Crilly A, et al. A novel anti-inflammatory role for simvastatin in inflammatory arthritis. *Journal of immunology*. 2003; 170: 1524-30.
219. Chen PY, Sun JS, Tsuang YH, Chen MH, Weng PW and Lin FH. Simvastatin promotes osteoblast viability and differentiation via Ras/Smad/Erk/BMP-2 signaling pathway. *Nutrition research*. 2010; 30: 191-9.
220. Sugiyama M, Kodama T, Konishi K, Abe K, Asami S and Oikawa S. Compactin and simvastatin, but not pravastatin, induce bone morphogenetic protein-2 in human osteosarcoma cells. *Biochemical and biophysical research communications*. 2000; 271: 688-92.
221. Park JB. Use of simvastatin in bone regeneration. *Med Oral Patol Oral Cir Bucal*. 2009; 14: 485-8.
222. Uzzan B, Cohen R, Nicolas P, Cucherat M and Perret GY. Effects of statins on bone mineral density: a meta-analysis of clinical studies. *Bone*. 2007; 40: 1581-7.
223. Rogers MJ. Statins: lower lipids and better bones? *Nature medicine*. 2000; 6: 21-3.
224. Wattamwar PP, Mo YQ, Wan R, Palli R, Zhang QW and Dziubla TD. Antioxidant Activity of Degradable Polymer Poly(trolox ester) to Suppress Oxidative Stress Injury in the Cells. *Adv Funct Mater*. 2010; 20: 147-54.
225. Baba TT, Nemoto TK, Miyazaki T and Oida S. Simvastatin suppresses the differentiation of C2C12 myoblast cells via a Rac pathway. *Journal of muscle research and cell motility*. 2008; 29: 127-34.

226. Katagiri T, Yamaguchi A, Komaki M, et al. Bone Morphogenetic Protein-2 Converts the Differentiation Pathway of C2C12 Myoblasts into the Osteoblast Lineage. *Journal of Cell Biology*. 1994; 127: 1755-66.
227. Ogasawara T, Kawaguchi H, Jinno S, et al. Bone Morphogenetic Protein 2-Induced Osteoblast Differentiation Requires Smad-Mediated Down-Regulation of Cdk6. *Molecular and cellular biology*. 2004; 24: 6560-8.
228. Takeda K, Ichijo H, Fujii M, et al. Identification of a novel bone morphogenetic protein-responsive gene that may function as a noncoding RNA. *Journal of Biological Chemistry*. 1998; 273: 17079-85.
229. Fan J, Guo M, Im CS, et al. Enhanced Mandibular Bone Repair by Combined Treatment of Bone Morphogenetic Protein 2 and Small-Molecule Phenamil. *Tissue engineering Part A*. 2017; 23: 195-207.
230. Fan J, Im CS, Cui ZK, et al. Delivery of Phenamil Enhances BMP-2-Induced Osteogenic Differentiation of Adipose-Derived Stem Cells and Bone Formation in Calvarial Defects. *Tissue engineering Part A*. 2015; 21: 2053-65.
231. Jeon JH, Piegras WT, Lin YL, Thomas MV and Puleo DA. Localized intermittent delivery of simvastatin hydroxyacid stimulates bone formation in rats. *J Periodontol*. 2008; 79: 1457-64.

Vita

EDUCATION

University of Kentucky, Lexington, KY

Doctor of Philosophy in Biomedical Engineering, 2017

Cumulative GPA: 3.51 / 4.00

University of Tennessee, Knoxville, TN

Bachelor of Science in Biomedical Engineering, 2009

Cumulative GPA: 3.58 / 4.00

EXPERIENCE

Wright Medical Group N.V., Memphis, TN, 2017 - present

- Sterility Assurance Engineer

University of Kentucky, Lexington, KY, 2010-2017

- Graduate Research Assistant
- **Lab:** Regenerative Biomaterials
- **Advisor:** Dr. David Puleo, Dept. of Biomedical Engineering
- **Co-Advisor:** Dr. Thomas Dziubla, Dept. of Chemical and Materials Engineering

University of Tennessee, Knoxville, TN, 2007-2008

- Undergraduate Research Assistant, Center for Musculoskeletal Research
- Math Tutorial Center Tutor

PUBLICATIONS

- Asafo-Adjei, T. A., Dziubla, T. D., and Puleo, D. A. (2014). Synthesis and characterization of a poly (ethylene glycol)-poly (simvastatin) diblock copolymer. *RSC Advances*, 4(102), 58287-58298.
- Asafo-Adjei, T. A., Chen, A. J., Najarzadeh, A., and Puleo, D. A. (2016). "Advances in Controlled Drug Delivery for Treatment of Osteoporosis." *Current Osteoporosis Reports* (2016):1-13.
- Asafo-Adjei, T. A., Dziubla, T. D., and Puleo, D. A. (2017). "Tuning Properties of Poly(ethylene glycol)-blockpoly(simvastatin) Copolymers Synthesized via Triazabicyclodecene." *Reactive and Functional Polymers* - accepted for publication

CONFERENCE PRESENTATIONS

- TA Asafo-Adjei, TD Dziubla and DA Puleo, "Characterization of Poly(simvastatin) Copolymers and Blends," World Biomaterials Congress, Montreal, Canada, May 17-22, 2016 - poster presentation

- TA Asafo-Adjei, TD Dziubla and DA Puleo, “Characterization of Poly(simvastatin) Copolymers and Blends,” Center for Clinical and Translational Science (CCTS) Annual Spring Conference, Lexington, KY, April 21st, 2016 - poster presentation
- TA Asafo-Adjei, TD Dziubla and DA Puleo, “Characterization of Poly(simvastatin) Copolymers and Blends,” Biomaterials Day, University of Memphis, Memphis, TN, March 18th, 2016 - oral presentation
- TA Asafo-Adjei, TD Dziubla and DA Puleo, “Degradation of Poly(simvastatin) Copolymers and Blends,” Biomedical Engineering Society (BMES) Annual Meeting, Tampa, FL, Oct. 7-10, 2015 - poster presentation
- TA Asafo-Adjei, TD Dziubla and DA Puleo, “Synthesis and Characterization of a Simvastatin Polyprodrug,” Center for Clinical and Translational Science (CCTS) Annual Spring Conference, Lexington, KY, March 25rd, 2015 - poster presentation
- TA Asafo-Adjei, TD Dziubla and DA Puleo, “Synthesis and Characterization of a Simvastatin Polyprodrug,” Biomaterials Day, Vanderbilt University, Nashville, TN, March 23rd, 2015 - poster presentation
- TA Asafo-Adjei, TD Dziubla and DA Puleo, “Synthesis and Characterization of a Simvastatin Polyprodrug for Potential Tissue Regeneration Applications,” Tissue Engineering and Regenerative Medicine International Society (TERMIS) Annual Meeting, Washington, D.C., Dec. 13-16, 2014 - poster presentation
- TA Asafo-Adjei, TD Dziubla and DA Puleo, “Synthesis and Characterization of a Simvastatin Polyprodrug,” Biomaterials Day, University of Kentucky, Lexington, KY, Sept. 27th, 2014 - poster presentation
- S Ramineni, M Brown, B Orellana, N Anderson, P Fisher, T Asafo-Adjei, D Puleo, T Brown, “Fundamentals of Controlled Release Systems with Hydrogel as an Example,” Education Challenge, Society for Biomaterials (SFB) Annual Meeting, Denver, CO, April 16-19, 2014 - group poster presentation
- TA Asafo-Adjei, TD Dziubla and DA Puleo, “Evaluating Two Methods of Ring-Opening Polymerization for Synthesizing a Degradable, Polymeric Simvastatin Prodrug,” Society for Biomaterials (SFB) Annual Meeting, Denver, CO, April 16-19, 2014 - poster presentation
- TA Asafo-Adjei, TD Dziubla and DA Puleo, “Analysis of Molecular Weight Growth and Degradation of a Simvastatin Polymeric Prodrug,” Society for

Biomaterials (SFB) Annual Meeting, Boston, MA, April 10-13, 2013 - poster presentation

- TA Asafo-Adjei, TD Dziubla, and DA Puleo, "A Comparative Analysis of Synthesis Techniques for the Formation of an Amphiphilic Polymeric Prodrug for Extended Simvastatin Release," Biomedical Engineering Society (BMES) Annual Meeting, Atlanta, GA, Oct. 24-27, 2012 - poster presentation
- TA Asafo-Adjei, TD Dziubla, and DA Puleo, "Synthesis and Characterization of a Bioactive Polymeric Prodrug for Bone Regeneration," Biomaterials Day, University of Kentucky, Lexington, KY, Sept. 22nd, 2012 - poster presentation
- TA Asafo-Adjei, TD Dziubla, and DA Puleo, "Synthesis and Characterization of a Bioactive Polymeric Prodrug for Bone Regeneration", Biomaterials Day, Purdue University, West Lafayette, IN, Oct. 29th, 2011 - poster presentation

AFFILIATED SOCIETIES

TERMIS, Tissue Engineering and Regenerative Medicine International Society, member, 2014- present

SFB, Society for Biomaterials, member, 2011 - present

- President, UK-Chapter, Lexington, KY, 2016
- Secretary, UK-Chapter, Lexington, KY, 2013 - 2014

BMES, Biomedical Engineering Society, member, 2011 - present

- Secretary, UK-Chapter, Lexington, KY, 2011 – 2013

AAAS, American Association for the Advancement of Science, member, 2011 - present

BGPSA, Black Graduate and Professional Students Association, 2010 - present

Tau Beta Pi, alpha UTK chapter member, 2007 – 2009

NSBE, National Society of Black Engineers, member, 2005 - present

HONORS AND AWARDS

University of Kentucky, Lexington, KY, 2010-2016

- NSF – Integrative Graduate and Educational Research Trainee (IGERT) Fellowship
- Graduate Certificate of Bioactive Interfaces and Devices
- 2nd place poster - Biomaterials Day, Vanderbilt University, March 23rd, 2015
- 1st place (group)- Education Challenge, Society for Biomaterials (SFB) Annual Meeting, April 16-19, 2014
- 1st place poster - Biomaterials Day, University of Kentucky, Sept. 27th, 2014
- 2nd place poster - Biomaterials Day, Purdue University, Oct. 29th, 2011

University of Tennessee – Knoxville, TN, 2005-2009

- University Scholarship
- TN Lottery HOPE Scholarship

- African American Achievers Scholarship
- NSBE Board of Corporate Affiliates (BCA) scholarship recipient, 2007

COMMITTEE APPOINTMENTS

College of Engineering, University of Kentucky, Lexington, KY, Spring 2016

- Graduate Student Representative – Diversity and Inclusion committee